

ANALYSIS OF THE MAJOR GRAVITY AND MAGNETIC
ANOMALIES CENTRED ABOUT BATHGATE, CENTRAL
SCOTLAND

by

MIA MOHAMMED AMZAD HOSSAIN

Thesis submitted in fulfilment of the degree of
Master of Science (by research) in the Faculty
of Science, Geology Department, University of
Glasgow.

October 1976

ProQuest Number: 13804096

All rights reserved

INFORMATION TO ALL USERS

The quality of this reproduction is dependent upon the quality of the copy submitted.

In the unlikely event that the author did not send a complete manuscript and there are missing pages, these will be noted. Also, if material had to be removed, a note will indicate the deletion.



ProQuest 13804096

Published by ProQuest LLC (2018). Copyright of the Dissertation is held by the Author.

All rights reserved.

This work is protected against unauthorized copying under Title 17, United States Code
Microform Edition © ProQuest LLC.

ProQuest LLC.
789 East Eisenhower Parkway
P.O. Box 1346
Ann Arbor, MI 48106 – 1346

CONTENTS

	<u>Page</u>
SUMMARY	ix
CHAPTER 1:	
<u>INTRODUCTION</u>	1
1.1 INTRODUCTION	1
1.2 THE GEOLOGY OF THE AREA	2
1.3 PREVIOUS GEOPHYSICAL WORK	14
CHAPTER 2:	
<u>THE GRAVITY AND AEROMAGNETIC SURVEYS IN CENTRAL SCOTLAND</u>	19
2.1 GRAVITY SURVEYS	19
2.1.1 Sources of data	19
2.1.2 Reduction of gravity data	21
2.2 DESCRIPTION OF AEROMAGNETIC MAP	27
CHAPTER 3:	
<u>BASIS OF CALCULATION OF GRAVITY AND MAGNETIC ANOMALIES</u>	29
3.1 CALCULATION OF GRAVITATIONAL POTENTIAL FIELDS	29
3.2 CALCULATION OF MAGNETIC POTENTIAL FIELDS	33
3.3 OUTLINE OF PROGRAM	36
CHAPTER 4:	
<u>QUALITATIVE ANALYSIS OF GRAVITY ANOMALIES</u>	41
4.1 ROCK DENSITIES OF THE REGION	41
4.2 DESCRIPTION OF BOUGUER ANOMALY MAP	42
4.2.1 Bathgate High and geological Models	43

CONTENTS (Contd)

	<u>Page</u>	
4.3	STRIPING OF GRAVITY EFFECTS OF ROCKS ABOVE HURLET LIMESTONE	50
4.3.1	Thickness Map of Carboniferous Sediments between Hurlet Limestone and datum (Newlyn O.D.)	51
4.3.2	Calculation of gravity effect of the sediments from Map 2	52
4.4	COMMENTS ON THE BOUGUER ANOMALIES WHEN CORRECTED FOR THE EFFECTS OF SUPRA HURLET SEDIMENTS	54
CHAPTER 5	<u>QUALITATIVE ANALYSIS OF MAGNETIC ANOMALIES</u>	56
5.1	DESCRIPTION OF AEROMAGNETIC MAP, GEOLOGICAL MODELS FOR THE BATHGATE HIGH AND MAGNETISATION OF ROCKS OF THE REGION	56
CHAPTER 6	<u>QUANTITATIVE ANALYSIS OF THE GRAVITY AND MAGNETIC ANOMALIES</u>	60
6.1	MODEL 1	60
6.1.1	Magnetic	60
6.1.2	Pseudo-gravity	74
6.2	MODEL 2	74
6.2.1	Magnetic	74
6.2.2	Pseudo-gravity	92
6.3	COMPONENTS OF THE BOUGUER FIELD CORRECTED FOR THE EFFECTS OF SUPRA HURLET SEDIMENTS	92

CONTENTS (Contd)

	<u>Page</u>	
CHAPTER 7	CONCLUSIONS	97
REFERENCES		99
APPENDIX 1	Terrain Correction Program	103
APPENDIX 2	Program for the calculation of gravity and/or magnetic potential fields.	114

LIST OF FIGURES	Page
1. Location of the Sources of data and Rashihill Bore hole	20
2. An elementary volume element and the co-ordinate system	30
3. A vertical line element and the co-ordinate system	30
4. A vertical thin sheet and the co-ordinate system	30
5. A right rectangular prism and the co-ordinate system	32
5a. When the point of observation $P(0,0,0)$ lies outside the prism but in the same plane	32
5b. When the point of observation $P(0,0,0)$ lies inside the prism but in the plane	32
6. A vertical thin sheet and co-ordinate system (Magnetic case)	34
7. A right-rectangular prism and co-ordinate system (Magnetic case)	34
8. Specification of body dimension and calculation points for the program used in Potential fields (gravity/magnetic) calculations	38
9. Lava layer of constant thickness	44
10. Lava layer of variable thickness not exceeding Carboniferous structural relief	44
11. Six sub-areas showing the division of the sedimentary basins of Map 2.	53
12. Location of the strip dimension and profile with respect to National Grid for Model 1	61

LIST OF FIGURES

Page

13-17	Show observed magnetic anomalies against calculated anomalies along five N-S profiles and thickness of the Model 1 under each profile	63-73
18	Shows contours of pseudogravity anomaly calculated from magnetic anomaly	75
19	East-West profile [295.670 to 305.670] across the Bathgate Hills where sills and lavas have North-South dipping and assumed base level (main Bathgate anomaly) represented by smooth curve	77
20-24	Show observed magnetic anomalies and anomalies re-calculated from model 1 at a depth increased by 2.0 Km along five North-South profiles	79-84
25	Location of strip dimension and profile with respect to National Grid for Model 2	85
26-30	Show observed magnetic anomalies smoothed by upward continuation (i.e. recalculated from Model 1 at a depth increased by 2.0 Km) against anomalies calculated along five North-South profiles and thickness of the Model 2 under profiles 3 and 4	86-91
31	Shows observed Bouguer anomaly corrected for the effects of Carboniferous sediments - (1), addition of Regional anomaly and calculated pseudogravity anomaly (from magnetic anomaly)-(2) and the residual between (1) and (2) along S.E.-N.W. orientations - (3)	93
32	Arrangement of 16 squares in a block	106

ACKNOWLEDGEMENTS

I wish to thank Professor T. Neville George with whose permission the present project was started and also Professor B.E. Leake for allowing me to complete it.

My grateful thanks to Dr. A.C. McLean for suggesting the problem, for his continued guidance and help at various stages of the work, and for many helpful suggestions while critically reading the manuscript, and to Dr. D.W. Powell for his constant guidance and advice throughout the course of the present work and for writing the program for calculating the potential fields (gravity and/or magnetic).

I am grateful to I.G.S. for the loan of the gravity survey data of the Central Midland Valley of Scotland, to Dr. Bullerwell for sending their regional gravity map of Scotland, and to the Department of Geology, University of Glasgow for access to the gravity survey data lodged with the department by Qureshi and Cotton.

I wish to acknowledge my gratitude to Dr. W. Sharp for his help in writing the graph-plotter program and thanks to the technical staff of the Department of Geology of the University of Glasgow, in particular Messrs. R. Morrison, G. Gordon, R. Cumberland and Mrs. Brown for their willing assistance at various stages of the present work.

I wish to record my gratitude to the British Council for awarding me a Commonwealth Academic Staff Award and to the University of Rajshahi, Bangladesh for granting me study leave during the tenure of the present work.

SUMMARY:

A Bouguer anomaly map and ^{an} aeromagnetic map (Map 1 and 5) are presented for the central part of the Midland Valley of Scotland as a basis for a combined interpretation of a prominent anomaly centred near Bathgate. The gravity data are compiled from surveys carried out by I.G.S., Cotton, Qureshi, and Bullerwell and Phemister. The aeromagnetic map is part of the Great Britain and Northern Ireland, sheet 11 (scale 1:250,000) published by I.G.S.

On the basis of qualitative analysis and geological argument, two limiting case models for the main anomaly are proposed for qualitative investigation. Model 1 consists of Carboniferous lavas in continuity with an intrusion of identical geophysical properties as the magnetic source. Model 2, however, attributes the whole magnetic anomaly, after some smoothing by upward continuation, to a deep intrusion.

The Bouguer anomaly Map is corrected for the effect of known basins of Carboniferous sediments above the lavas filling the basins with material of Lower Old Red Sandstone density. The principal remaining components of the gravity field are considered by combining the pseudo-gravity anomalies, calculated from magnetic anomalies and scaled to + 10 mgal for two density contrasts (+0.11 g/cm³ for shallow model and +0.45 g/cm³ for deeper model), with the regional gravity anomaly, projected from Western Midland Valley of Scotland. This is done after adjusting for a base level shift of 15 mgal which may arise from a

CHAPTER 1

INTRODUCTION

1.1 INTRODUCTION

The regional gravity survey of Scotland by Bullerwell and Phemister (personal communication) was a pioneer effort, which though it has not been published formally, has, through the generosity of the authors, been available in planning and interpreting later surveys. Within the Midland Valley graben, it shows a pronounced gravity high, centred near Bathgate in the West Lothians, and roughly oval in plan, with longer axis trending east-west. The east-west diameter is about 30 Km, and the north-south about 20 Km. The change in Bouguer anomaly value from the margins to the centre is approximately 8 mgal. Later semi-detailed surveys in the Lothians by the Applied Geophysics Unit of Institute of Geological Sciences have confirmed, and defined, this anomaly more fully. During the same period, researchers from the University of Glasgow have carried out gravity work in the Western part of the Midland Valley, including a semi-detailed survey of the region west of Stirling by Qureshi (1969-70), and a detailed survey of the Campsie volcanic area by Cotton (1968), both of which are relevant to the analysis of the high. The geological source of this gravity anomaly is obscure, as it bears no simple and obvious relationships to outcrops. The IGS Aeromagnetic Map Sheet 18 (Bullerwell

1968) shows a near-circular high of amplitude 500 nT in the same region, which may be correlated with the gravity anomaly and which may add considerably to the constraints on its possible geological meaning.

Using the sources mentioned, above, a gravity map has been compiled for the area of the Midland Valley lying between latitudes $56^{\circ}11.8'$ and $55^{\circ}39'$, and longitudes $4^{\circ}15.8'$ and $3^{\circ}7.8'$, that is between Callander to the north-west, Leslie to the north-east, Hamilton to the south-west, and Peebles to the south-east. The high lies at its centre, and the map extends to cover a wide zone apparently clear of it. The corresponding area of the aeromagnetic map is reproduced. Using these data and the known geology - from surface mapping, mining, a few deep bore-holes, and seismic-reflection results in one locality - an analysis and comparison are made of the gravity and magnetic anomalies in an attempt to define the possible geological source.

1.2 THE GEOLOGY OF THE AREA (See Map 6)

The Midland Valley graben The Midland Valley graben is bounded by the Highland Boundary Fault on the north-west, and the Southern Upland Fault on the south-east. It is about 80 Km wide, and stretches for more than 200 Km across Scotland, and probably for the same distance again into Ireland. A block of thick Old Red Sandstone and Carboniferous sediments and lavas is dropped down by as much as 6 Km between metamorphosed Dalradian rocks of the Highlands, and Lower Palaeozoic greywackes of the Southern

Uplands. Its geology has been investigated extensively by IGS, by University geologists, and by geologists of the National Coal Board and other industrial concerns. Systematic accounts are available in the memoirs of IGS (Macgregor and Macgregor, 1948).

Classic accounts of its structural and stratigraphic evolution (that pre-date the theory of plate tectonics) are given by Kennedy (1958) and George (1960). Since plate tectonics, new labels (if not a totally new significance) have been attached to the serpentine bodies associated with the boundary faults, and the region of the graben is interpreted by some (e.g. Gunn 1973) as being distinguished originally, as a structural unit, when Lower Palaeozoic plates collided and created suture lines.

The Upper Palaeozoic Stratigraphy of the central area of the graben.

(a) The Lower Old Red Sandstone

Outcrops of Lower Old Red Sandstone are few within the area of analysis (Map 1) and these are at extreme fringes - the Pentlands in the south-east. Just beyond this central region of the graben, there are outcrops near Distinkhorn in eastern Ayrshire and in Perthshire. Thicknesses (sediments and lavas) at these localities are as follows:-

Pentland

600 m Lower Old Red Sandstone interbedded with conglomerate and grits in south-west and thins to north-

east. At north-east end lava flows and tuffs over 1500 m thick, almost uninterrupted by sedimentary intercalations. (Mykura 1960).

Distinkhorn in Eastern Ayrshire

Feldspathic Sandstone of Lower Sediment group 600 m (Richey, Anderson and Macgregor 1930).

Central Perthshire

dominantly volcanic materials - greatest known thickness.

Sandstone	212 m	Strathmore group
Sandstone	575 m	} Garvock group
Conglomerates of mixed		
Volcanic and Highland materials	750 m	
Conglomerates of basic volcanic material	900 m	} Arbuthnott group
Lavas	450 m	
Conglomerates of mixed volcanic and Highland materials	150 m	} Crawton group
Lavas	420 m	
Conglomerates of - basic volcanic material	180 m	} Dunnottar group
mixed volcanic and Highland materials	60 m	
Lavas	60 m	

After Allan (1940, p.185)

Only a tentative generalised reconstruction of Lower Old Red Sandstone original thicknesses may be inferred from

these data and it is pure speculation to suggest what the present thicknesses may be, after the results of post-Lower ORS movements and erosion. The following generalisations are relevant -

(i) In the major outcrop to the south-east of the Highland Boundary Fault there is a marked decrease of thickness from the north-eastern end at Stonehaven (5750 m) to the Loch Lomond area (2400-3600 m) (Qureshi, 1969-70).

(ii) Observed thicknesses are greatest in this region close to Highland Boundary Fault and probably decrease towards the centre of the graben.

(iii) Post Lower Old Red Sandstone movements affecting the present thickness are predominantly along lines trending north-east-south-west. There are sudden changes across major faults, for example the Highland Boundary Fault at Balmaha (1080 m to zero under the Upper ORS on the north-west side), and the Straiton Fault in South Ayrshire (300 m to zero under the Upper ORS on the north-west side). Pre-Upper ORS folds near Muirkirk also have a control on changes of residual thicknesses. It should be noted that these acute changes are greatest near the margins of the graben where 'Middle ORS' movements are most pronounced. Lower ORS volcanicity is widespread within the graben, and thick (Ochil Hill 1969 m; Carrick Hills, South Ayrshire between 330 and 500 m; Tinto area, south Lanarkshire 390 m) sequences of andesitic and basaltic lavas and tuffs occur in many areas. In the latter area outcrops suggest that the development of lavas is characteristic of each NE-SW Fault block. There are few vents exposed in relation

to the quantity of extrusives. Intrusive rocks occur at Distinkhorn and also South Lanarkshire and are mainly of granodioritic type.

(b) The Upper Old Red Sandstone

The major unconformity in the Upper Palaeozoic rocks of the Midland Valley occurs between Upper and Lower Old Red Sandstone and the development of the Upper Old Red Sandstone is broadly similar to that of the Lower Carboniferous strata, with the same structures and movements controlling development of both. Outcrops within the area of the Map 1 are limited to the fringes, and give little evidence on which to base a general distribution of Upper Old Red Sandstone under the Carboniferous strata.

To the south at the southern extremity of the central coalfield, Upper Old Red Sandstone (and part of the Lower Carboniferous succession) are locally absent, and rest directly on Lower Old Red Sandstone. The area of uplift apparently (in Lower Carboniferous times) appears to trend north-south, and coincides with the "Lanark Line" (Hall, 1971). This is a zone of structural change trending north-south. To the west the major folds affecting Upper Carboniferous rocks trend north-west - south-east, and to the east they trend NNE-SSW.

(c) The Calciferous Sandstone Sediments

The Calciferous Sandstone Measures vary more in thickness from place to place than any other Carboniferous subdivisions. This is due mainly to the great thickness of lavas which broke up the area of deposition into several

basins, (Francis, in Craig (ed) 1965, p.311). There is a major change of this type, from west to east across the area (Map 1). Representative thicknesses of the sediments around the area are as follows:-

West and Central area (Midland Valley)

Maximum thicknesses of

Sediments (lavas 600 m - 900 m)

Upper Sedimentary Group	300 m	near Paisley
Lower Sedimentary Group	60 m	at Strathblane

West Lothian and Midlothian

A dominantly sedimentary sequence - greatest known thickness.

Upper Oil Shale Group	840 m	(West Calder)
Lower Oil Shale Group	1400 m	(Edinburgh)

thinning westward.

Cement Stone Group	1110 m	(Dalmahoy Syncline)
--------------------	--------	------------------------

(d) The Lower Carboniferous extrusive rocks

There are three main lava-fields of Lower Carboniferous age within the Midland Valley, (i) the Clyde Plateau, (ii) Midlothian, (iii) East Lothian and Fife.

(i) The Clyde Plateau Lavas outcrop along the western fringe of Map 1, with extensive outcrops in the Campsie Hills and in the Strathaven Hills to the south. A complete sequence from base to top is not exposed in these areas, but a maximum thickness of 900 m of basaltic lavas

(Tomkiewf, 1937) has been estimated to be present. A more recent investigation (Hall, 1971) combining the results of Rashiehill bore-hole, which failed to reach the base of the lavas, with a local seismic-reflection survey indicates that 470 m are present there, just west of the N-S axis of the central coalfield syncline.

The lavas of the Clyde Plateau thin markedly to the south and south west. Near the S.W. corner of Map 1 there is a dramatic change of thickness across the E.N.E.-W.S.W. trending Inchgotrick Fault, and only two flows are present on the southern side. Further west, near the Ayrshire coast, there is a gradual and persistent decrease of thickness from the Glasgow region to the extreme tip of the lava outcrop at Ardrossan.

(ii) In West Lothian and Midlothian volcanicity is sporadic, and lavas are interbedded with sedimentary layers within the lower part of the Calciferous Sandstone Measures. Lavas and tuffs form about 60 m of this part of the sequence. Above them in the Oil Shale Groups, the Arthurs Seat Volcanic Rocks are 300 m thick near Edinburgh.

(iii) In southern Fife, more than 400 m of Calciferous Sandstone Series lavas are present (base unseen). They form part of an extensive lava field (the "Forth Volcanic Group" of Francis, in Craig, 1965) that extends under the Forth to link with the thick (600 m) lava pile of East Lothian. This field lies at the eastern margin of Map 1.

(e) The Scottish Carboniferous Limestone Measures

These consist predominantly of sequences of shales, limestones, sandstones and thin coals. They are divisible into

Upper Limestone Group

Limestone-coal Group

Lower Limestone Group.

Overall, Limestones are more frequent in the Lower and Upper Groups. Shales predominate in the Limestone Coal Group, except in West Lothian where much of the Lower Limestone Group is volcanic.

(i) Lower Limestone Group: In general, outcrops indicate an overall increase of thickness eastwards across the Midland Valley, from zero in Western Ayrshire to over 250 m in East Fife. The thickness within the area of Map 1 is of the order 200 m. An isopach map has been made by Goodlet (1957) and is reproduced in Craig (1965 p.321).

(ii) Limestone-Coal Group: This also increases in thickness eastwards from the Ayrshire shelf, from about 90 m in southern Ayrshire to about 300 m within the area of Map 1. Second order changes of thicknesses are correlated with development of major "Hercynian" folds and faults.

(iii) Upper Limestone Group: This group shows a similar pattern of variation across faults, with, in general, lesser thicknesses in the west. The greatest thickness within the Midland Valley is 600 m in the northern part of the Central Coalfield Basin at Clackmannan (north-

central part of Map 1).

Neither details of thickness variations within the Scottish Carboniferous Limestone Measures nor of the Carboniferous formations above them are discussed here, as they are incorporated in the process of stripping of the gravity effects of supra-Hurlet Limestone sediments at that stage of analysis (pp 50).

(f) The Passage Group ("Scottish Millstone Grit")

The Passage Group crops out as a fringe around extensive areas of Coal Measures in Midland Valley. It consists mainly of sandstones. Volcanic rocks occur around the Firth of Clyde and Ayrshire region but are not present within the area of Map 1. There is considerable variation of thickness controlled by developing NE-SW trending structures, especially within the area of Map 1. The maximum thickness of 350 m occurs in the middle of the Central Basin, near Clackmannan.

(g) The Scottish Coal Measures

They are traditionally sub-divided into:-

(i) Barren Red Measures (Upper Coal Measures)

(ii) Productive Measures (Middle and Lower Coal Measures)

They outcrop extensively within the area of Map 1. The Productive Measures consist largely of 47% Shale, 47% Sandstone and only 6% coal.

The variations of thickness are controlled by NW-SE folds and faults (rather than the NE-SW lines of the Lower Carboniferous), and the N-S trending Central Basin was developing as a depositional trough during this period.

In the central coalfield, maximum thicknesses are about 450 to 500 m.

The Barren Red (Upper Coal) Measures consist mainly of red sandstones with some clay rocks. About 200 m of weathered basaltic lavas are present above these in Ayrshire, but not within the area of Map 1.

A maximum thickness of 375 m of sediments is present in Ayrshire, but under 300 m are present in the West Central Coalfield (on the western fringe of the map), and even less further east.

Permo-Carboniferous intrusions

There are several episodes of igneous activity within the Midland Valley graben in Upper Palaeozoic and later times, (see Table 1). The centres of activity change with time, for example Lower Carboniferous vulcanicity in the Clyde Region is predominantly of Calciferous Sandstone Series age, but the lavas in the Lothians are mainly of Scottish Carboniferous Limestone Series age. Intrusions are associated with all the lavas, but dykes are mainly of Calciferous Sandstone, Permo-Carboniferous or Lower Tertiary age. The latter are restricted to central Ayrshire, and intrusions outcropping within the area studied are almost exclusively of Permo-Carboniferous age, with the principal exceptions being north-west - south-east orientated Tertiary dykes in the south-western part of the Central Coalfield.

The common rock-type of these hypabyssal intrusions is quartz-dolerite. The dykes have a general west-east trends/

Table 1.

Igneous activity in the Midland Valley of Scotland

TERTIARY

There is extensive vulcanicity of Tertiary age along the Western Scotland, but within the Central Midland Valley igneous activity is restricted to a few N.W.-S.E. trending dykes radiating from the Mull centre.

UPPER PALAEOZOIC

Late Carboniferous and early Permian ("Borcovician") rocks:-

Igneous rocks of this age include thick dolerite sills in much of the Midland Valley, E-W trending dykes, and lavas and tuffs with associated volcanic necks and plugs in central Ayrshire. The lavas have been shown to be late Carboniferous in age (Mykura, 1960).

Passage Beds ("Scottish Millstone Grit"):-

Lavas occur in Arran, Ayrshire and Kintyre with the centre of igneous activity roughly east of Arran (250 m maximum thickness).

Scottish Carboniferous Limestone Series:-

Local lavas at Bathgate and Linlithgow.

Calciferous Sandstone Series:-

Thick lava pile in the Western Midland Valley, with associated volcanic plugs, dykes and sills.

Old Red Sandstone:

Upper:- No igneous activity.

Lower:- Lavas in Ochil hill, with volcanic necks, dykes, sills and stocks of calc-alkaline types.

LOWER PALAEOZOIC

Silurian:- No known igneous activity.

Ordovician:

Arenig:- Spilitic lavas and tuffs.

trends and several stretch continuously across the area analysed for distances as great as 80 Km. The Campsie dyke runs from the Firth of Clyde to the Firth of Forth. The thickness varies from 20 m to 50 m. The dykes are parallel to an important set of east-west, normal faults and inferentially were produced during the same episode of north-south regional tension in late-carboniferous ("Borcovician") times.

In some localities the dykes are seen to be feeders to thick quartz-dolerite sills, which are mineralogically similar. Thicknesses characteristically range between 25 and 90 metres, but borings have shown as much as 180 m in some places (Robertson and Haldane, 1937). Mining has shown that the level of sill intrusion changes in a "step-and-stair" structure, and a sill in East Fife jumps level progressively from Old Red Sandstone to Middle Coal Measures (Knox 1954).

The structure of the central area of the graben

The centre of the area (Map 1) is occupied by the large open fold of the eastern Central Coalfield, trending NNE-SSW. There is evidence of its development during Carboniferous times (Francis, 1956). Near the axial region of the graben, the folds to the east of the Central Coalfield are mainly of this NNE-SSW trend including the major syncline that preserves Coal Measures to the south of Edinburgh (on the eastern fringe of the area). The NNE-SSW folds in the Calciferous Sandstone strata of West Lothian are of much smaller amplitude and wave-length than

those of coal basins. To the west, the major folds trend north-west - south-east, including the western part of the Central Coalfield. Near the margins of the graben, the folding is predominantly along north-east - south-west axes.

In the marginal zones of the graben the major faults trend N.E.-S.W., and a few members of this set are also present near the axis. Within the area studied the most prominent group of normal faults trend east-west veering to E.N.E.-W.S.W. direction in the west of the area. There are two complementary sets throwing in opposite directions by amounts up to 500 m.

They are dynamically related to the major east-west dykes. In the south-east of the area, a group of north-west - south-east faults trends parallel to the major fold axis of that part of the Central Coalfield. The relationship - offsetting and trailing between these faults and members of the east-west set (Anderson, 1951) shows that they are younger. They were inferred (MacGregor & Macgregor, 1948) to be Tertiary in age, and the product of the same regional tension active during Tertiary dyke emplacement, but more recent evidence (Smythe et al 1972) suggests that faults of this trend were active in Triassic times, and have histories of movement since then.

1.3 PREVIOUS GEOPHYSICAL RESEARCH

The gravity surveys by Bullerwell and Phemister (personal communication) and by officers of the IGS (personal communication) have been referred to earlier

(p. 1). Technical detail and acknowledgement of permission to refer to these results are given elsewhere (p. 19, vii). So far, however, little geological interpretation has been made, and there are no published conclusions that bear on the problems tackled in this thesis. The conclusions that do so, come largely from other authors working from Glasgow - viz.

1) Cotton in his Ph.D. thesis (1968) reached the following tentative conclusions about the variation in thickness of the lavas in the north-western part of the area. The maximum thickness of lavas in the Campsie Hills area is 250 m at North Third; to the south in Strathblane it is 750 m; and from there it thins southwards to about 500 m at Kessington. These results are based on gravity anomalies, some magnetics, and a known surface geology, and should be treated with corresponding caution. Cotton inferred that thick lava sequence in Strathblane may be related to piling up of extrusives around the vents of the western Campsies.

2) Park (1961) inferred from the results of a detailed magnetic survey that 300 m of lavas are present at the Dusk Water Fault, near Dalry, north Ayrshire.

3) Hall (1971) made a limited seismic-reflection survey at the site of Rashiehill bore, and after identifying a prominent reflection as the base of lavas, reached the conclusion that their thickness at Rashiehill is 470 m. The results from this area indicate eastward thinning of all the stratigraphic units present above the lavas. The

top and base of the lavas are inferred to converge at 15 to 20 degrees, and if this were so, and the thinning persists, the lavas would thin to zero within 1.5 Km to the east.

4) Hall (1974) determined variations of thickness of the Clyde Plateau Lavas in North Ayrshire and Renfrewshire from a seismic-reflection survey. He concluded that they form a pile (probably original) along a north-west - south-east line along the main outcrop in North Ayrshire-Renfrewshire, and thin away from the outcrop. The maximum thickness is about 900 m. This seismic study largely supercedes earlier gravity work in north Ayrshire by McLean (1966) and Inamdar (personal communication).

5) McLean and Qureshi (1966) in a first attempt to describe and explain the regional gravity in the Western part of the Midland Valley graben, identified a broad high culminating near the axial zone, with steep gradients into the bordering Highlands and Southern Uplands. Later surveys in the Southern Uplands (El-Batroukh, personal communication) and of the Firth of Clyde region (McLean and Wren, personal communication) confirm and extend this pattern. Allowance for the low density sediments infilling the graben, accentuate the gravity high. McLean and Qureshi (1966) favoured crustal thinning of about 5 Km (with the absence of the thick Lower Palaeozoic geosynclinal sequences of turbidites of the Southern Uplands and southern Highlands) as the most probable geological explanation, as in accord with some aspects of

the known geology.

Later results from the Oslo graben and comparable crustal structures appear to be in accord with their view, but the very recent results from the LISPB (Lithospheric Seismic Profile in Britain) experiment (Bumford et al. 1976) suggest that in the eastern part of the Midland Valley (the seismic refraction line passes through Edinburgh) no significant thinning from Southern Uplands into Midland Valley occurs.

6) Gunn (1973) using existing data, particularly the aeromagnetics, suggested that the Midland Valley is a "remnant of the proto-Atlantic ocean", with Highland Boundary Fault and Southern Uplands Fault marking the position of diverging Benioff zones. Sediments eroded from the flanking continental areas of the Highlands and Southern Uplands rest directly on oceanic crust. The limited evidence on which this rests is barely adequate to define a geophysical model, and the geological conclusion is asserted rather than proven.

7) The aeromagnetic anomaly at Bathgate has been studied by Powell (1970) and Gunn (1975), and both have made estimates of depth to the magnetic source. On the premise that the gravity and magnetic highs originate from the same geological body, Powell suggested that the body is probably composed of relatively dense, and magnetic, Lewisian rocks of granulite facies. The magnetic source could be a body 16 Km in diameter at a depth of 4.8 Km (that is below the base of the Old Red Sandstone).

Gunn's estimate of the depth to the causative body is 9.9 Km (below the survey level of +0.3 Km above ground level).

The difference hinges, according to Gunn, on the greater emphasis placed by Powell on steep gradient between [290.670] and [290.680]. If this is treated as resulting from the structure of the same body, Powell's value is closer to reality. Gunn's neglect of it is, however, conditioned by awareness of 12 Km of Lower Old Red Sandstone in the Strathmore region (Armstrong & Paterson, 1970) which makes his figure geologically "reasonable". This geological premise to his argument is, however, open to question, as the Lower Old Red Sandstone varies greatly in thickness, and is everywhere in the Midland Valley thinner than at Strathmore.

CHAPTER 2

THE GRAVITY AND AEROMAGNETIC SURVEYS IN CENTRAL SCOTLAND

2.1 GRAVITY SURVEYS

2.1.1 Sources of data

The area for which the Bouguer anomalies map has been drawn in the present investigation lies between latitudes $56^{\circ}11.8'$ and $55^{\circ}39'$ and longitudes $4^{\circ}15.8'$ and $3^{\circ}7.8'$ and is flanked by Callander on the north-west, Leslie on the north-east, Hamilton on the south-west and Peebles on the south-east. Within it about 1650 gravity stations are distributed over a total area of 3200 Km^2 to give an average of 0.5 stations per square Km.

The data in producing the map 1 are from the following sources and their locations are shown in Fig. 1.

Data for about 1350 stations covering an area of approximately 2500 Km^2 (see Fig. 1) are borrowed from the Applied Geophysics Unit, I.G.S. (personal communication).

154 stations come from Qureshi's survey (1969-70) and 112 from Cotton's survey (1968). These cover a total area of 600 Km^2 in the Bouguer anomaly map (Map 1). They are in Stirlingshire and are included to extend the Bouguer anomaly map over the outcrop of Clyde Plateau lavas that form the Campsie Hills. These surveys are tied to the I.G.S. base station network.

15 stations in Clackmannanshire near Alloa and 14 stations in Lanarkshire in the Motherwell-Wishaw area are

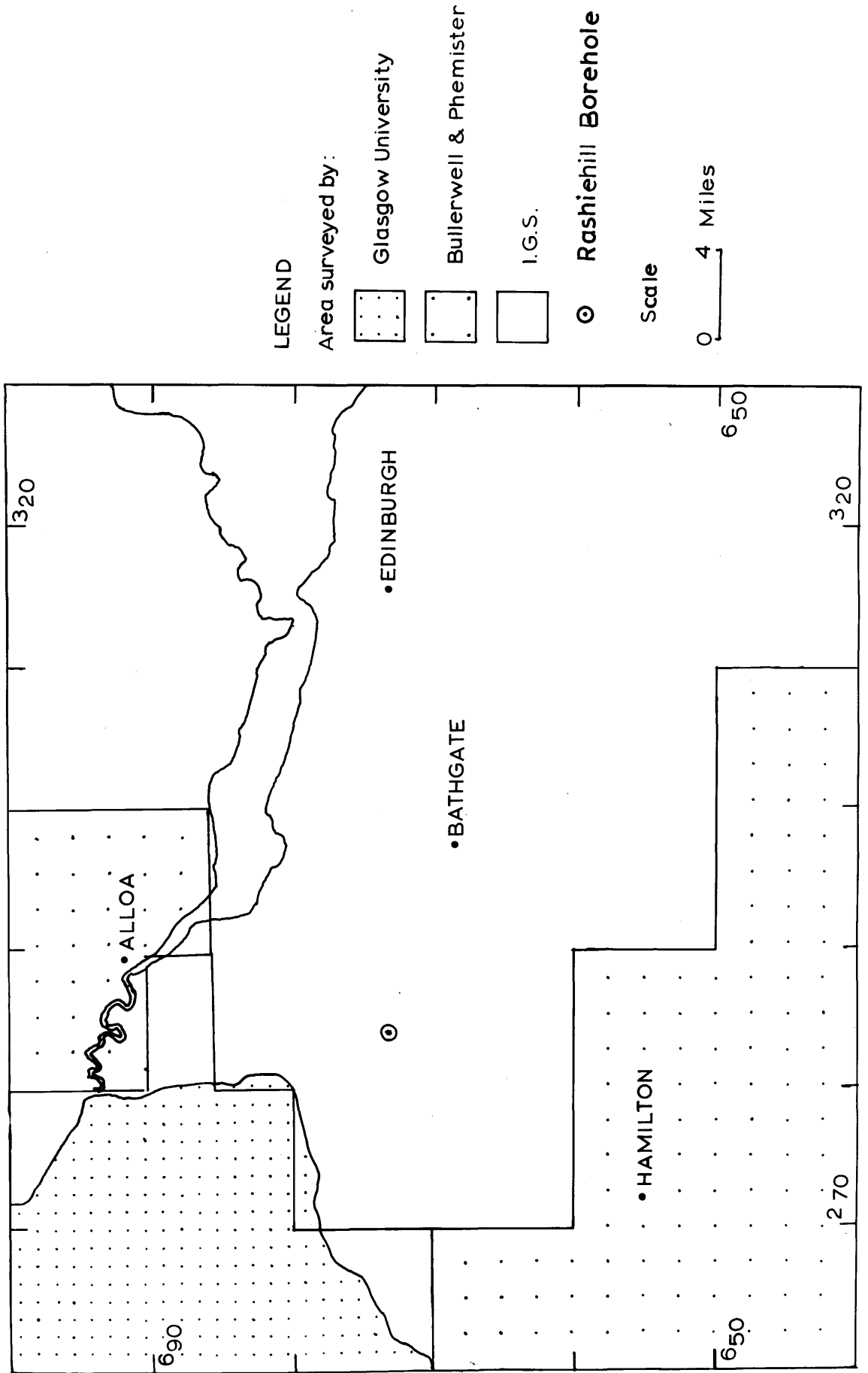


Fig. 1 Location of the sources of data and Rashiehill Bore hole

from Bullerwell and Phemister's survey (personal communication). These have been included to fill gaps in the station coverage. The station density in these areas is very low.

These stations from Bullerwell's Bouguer anomaly map of Southern Scotland are not tied directly to the other stations.

The following base stations were used by the I.G.S. They are related to Pendulum House, Cambridge where value of gravity has been taken to be 981265.0 mgal. The difference in observed gravity (mgal) between each base station and Pendulum House Cambridge is shown in Table 3.

2.1.2 Reduction of gravity data

Changes in elevation and latitude between the points of observation account in part for the differences in observed gravity values at different stations. In order to explain the variation of the observed gravity values due to the density model of interest it is essential to correct the observed gravity value for all these factors.

2.1.2.1 (1) Latitude effect (Theoretical gravity values)

All Bouguer anomaly values shown in Map 1 are corrected using the International Gravity Formula of 1930.

2.1.2.2 Elevation Correction

The Elevation correction consists of Free air plus Bouguer correction: the Free-air part of the elevation correction, made to all stations, is - 0.09406 mgal/ft. The Bouguer correction, which forms the remainder of the elevation correction is usually considered to remove the gravitational/

Table 2 The difference in observed gravity (mgal)
between each base station and Pendulum
House, Cambridge.

<u>Base Station</u>	<u>difference from Cambridge Pendulum House (mgal)</u>
Dennyloanhead	+ 337.20
Airdrie	+ 302.88
Linlithgow	+ 341.58
West Calder	+ 298.58
Kirkliston	+ 334.46
Penicuik	+ 288.82
Dunfermline	+ 321.69
Kirkcaldy	+ 332.92
Edinburgh	+ 316.32
Peebles	+ 271.17
Yetts of Muckart	+ 317.09
Kinross	+ 332.34
Leslie	+ 331.49

All these data are lodged with the Department of Geology,
University of Glasgow.

gravitational effect of an infinite slab of rock of uniform thickness and density between the station and datum. It has a value

$$2\pi G\rho h = + 0.01276 \rho h \text{ mgal/ft.}$$

where G is the Gravitational constant

h is the height in ft.

ρ is the density of material of the slab

The rock-formation lying between each station and datum (O.D. Newlyn) are determined from geological maps of I.G.S. The formation densities are taken from McLean (1961), Qureshi (1969-70) and El-Batroukh (personal communication). Rock density varies from 2.41 g/cm^3 to 2.81 g/cm^3 . The density factor is punched in the second tape of the terrain correction data (see p. 107). The same average values of density are used to get both the terrain correction and elevation correction simultaneously, that is in this reduction the 'Bouguer slab' is considered to have a variable rather than a constant density. The reduction attempts to remove from the observed data the gravitational effects of density contrasts lying above the sea level datum as well as applying the conventional Bouguer correction.* The densities used in calculation of the Bouguer corrections are included in Table 3.

The Free-air and Bouguer correction are combined into a single correction in the form

$$g_o = g_h + (0.09406 - 0.01276 \rho)h \text{ mgal}$$

where g_o = gravity corrected to sea level

g_h = observed gravity at height h

i.e./

Table 3 Densities of rocks used in the calculations

Carboniferous Sediments	= 2.54 g/cm ³
Clyde Plateau Lavas	= 2.72 "
Upper Old Red Sandstone	= 2.41 "
Lower Old Red Sandstone Sediments	= 2.61 "
Lower Old Red Sandstone Lavas	= 2.66 "
Ordovician and Silurian greywackes	= 2.71 "
Sills and dykes (Quartz-dolerite)	= 2.90 "
Granite 	= 2.67 "

*
The Bouguer reduction is based on the density of the outcropping rocks on which the station lies. These densities are listed against the stations on the data sheets.

The densities used for both terrain corrections and for modifying the Bouguer slab effect have been specified as averages for each 4 x 4 km square block on the National Grid. These are listed in the print outs from the program.

Both the station data sheets ^{and} / print outs are lodged with the Department of Geology in the University of Glasgow.

i.e. $g_o - g_h = 0.09406 h - 0.01276\rho h$ mgal.

The elevation corrections are determined using the program of Terrain correction described in Appendix 1.

The variable density of the Bouguer slab is introduced as corrections to an infinite slab having the density of rocks immediately under the station. The correction is applied for the same compartments used for the Terrain correction where these have a different density at outcrop from that under the station. Some allowance has been made for the expectation that some outcropping formations, especially sills, do not extend in depth to sea-level. It has been possible to reduce all the data except at the Bullerwell and Phemister stations in this manner.

The Bouguer anomaly values for the stations of Bullerwell and Phemister are read from the Bouguer anomaly map (without Terrain correction - $\frac{1}{4}$ inch to a mile) produced by the authors. The only heights available for these stations were those read from the 1 inch map on which they were replotted. Using terrain correction programme the terrain effect for the Zones G to M have been calculated and added to the observed Bouguer anomaly values read from the authors' map. No modification to the Bouguer corrections are made for the stations surveyed by Bullerwell and Phemister due to uncertainty of the accuracy of height. Consequently the Bouguer anomaly at these stations is not strictly comparable with that at the majority of the stations.

2.1.2.3 Terrain Correction

Terrain corrections for all stations are made using Bott's (1959) method. The original program written in Algol for Elliot 4100 compiler is converted for the Egdon compiler of Glasgow University computer system KDF9.

The area for which the terrain effect is to be calculated is divided into a grid of equal squares taking each 1 Km² National Grid square as a unit. The average height in feet of every square is read either from 2½ inch or 1 inch Ordnance Survey Maps up to 25 Km from the gravity stations in all directions.

The average heights in tens-of-feet and average rock density of kilometer squares arranged in blocks of 16 along with its left-hand corner co-ordinates (see Fig. in appendix 1) and the station co-ordinates and station heights, in tens of feet, arranged according to program, (see appendix 1) are fed to the computer. The computer then calculates the terrain effect for each station by summing the incremental contribution of all squares except the squares whose centres are less than 1 Km from the station.

The terrain effect of the squares rejected by the computer is calculated by the conventional method using a Hammer zone chart and then added to the value given by computer to obtain the total terrain effect. In the present case the effect due to two inner zones (B and C - a circle of radius 53.34 m) which is usually estimated by the observer in the field is not recorded and is neglected.

Terrain corrections are relatively small for most stations, and are appreciable for only a few stations. The maximum correction is 1.3 mgal.

2.1.2.4 Calculation of Bouguer Anomalies

The Bouguer anomalies are calculated as follows

$$\begin{aligned} \text{Bouguer Anomaly} = & \text{Observed gravity} + \\ & \text{Elevation correction (combined free-air} \\ & \text{and Bouguer correction)} + \\ & \text{Terrain correction} - \\ & \text{Theoretical gravity (Latitude correction)} \end{aligned}$$

2.1.2.5 Presentation of the Bouguer Anomalies

The results of the gravity surveys are presented as a map of Bouguer anomalies (Map 1). It is contoured at 1 mgal interval and drawn to a scale of 1 inch - to - 1 mile.

2.2 DESCRIPTION OF THE AEROMAGNETIC MAP

For the interpretation of the sub-circular magnetic 'high' centred at about NT co-ordinate (290,670) referred to by Gunn (1975) as the "Bathgate anomaly" three 1 inch Aeromagnetic maps (sheet 18/Falkirk, sheet 19/Edinburgh, sheet 29/Lanarkshire) and part of the Aeromagnetic map of Great Britain & Northern Ireland (sheet 11 scale 1:250,000) have been used as source of data. All information about these data are given in Map 5. The sheets were compiled in the Geophysics Department of the Geological Survey of Great Britain, in 1968. These sheets cover part of the large area flown between 1959 and 1963 under contract by

Canadian Aero Service Ltd. or by Hunting Surveys Ltd. The separation between East-West flight traverse lines is 2 Km or closer, with North-south tie lines 10 Km or closer. Mean terrain clearance is approximately 300 m.

The contour interval is normally 10 gammas with thicker lines at 50 gammas. Contour values represent total force magnetic anomalies in gammas after subtraction of a regional field. This is described by a linear equation which implies a regional increase in total force of 2.1728 gammas per Km "northwards" and 0.259 gammas per Km "westwards" (National grid directions) over the area of the British Isles.

CHAPTER 3BASIS OF CALCULATION OF GRAVITY AND MAGNETIC FIELD ANOMALIES

3.1 CALCULATION OF GRAVITATIONAL POTENTIAL FIELDS

The vertical component of gravitational attraction due to an elementary volume dx, dy, dz at a distance r from the point of observation $P(0,0,0)$ (Fig. 2) is

$$\Delta g_z = G \cdot \Delta \rho \cdot \frac{z}{r^3} dx \cdot dy \cdot dz \quad \dots (1)$$

where r^2 is $x^2 + y^2 + z^2$,

G is the Gravitational Constant

$\Delta \rho$ is the density contrast

- (Garland, 1965)

Integration of equation (1) with respect to z , from $z = 0$ to $z = Z$ leads to an expression for a vertical line element (Fig. 3)

$$\Delta g_z = G \cdot \Delta \rho \cdot \frac{1}{r^2 + y^2} \cdot dx \cdot dy \quad \dots (2)$$

The integration of equation (2) with respect to y , from $y = 0$ to $y = Y$, leads to an expression for a vertical thin sheet (Fig. 4)

$$\Delta g_z = G \cdot \Delta \rho \cdot \ln \left(\frac{Y + \sqrt{Y^2 + r^2}}{r} \right) dx \quad \dots (3)$$

where r^2 is $x^2 + z^2$.

If the depth to the top of the sheet is $z_1 \gg 0$ and that to the base is z_2 then

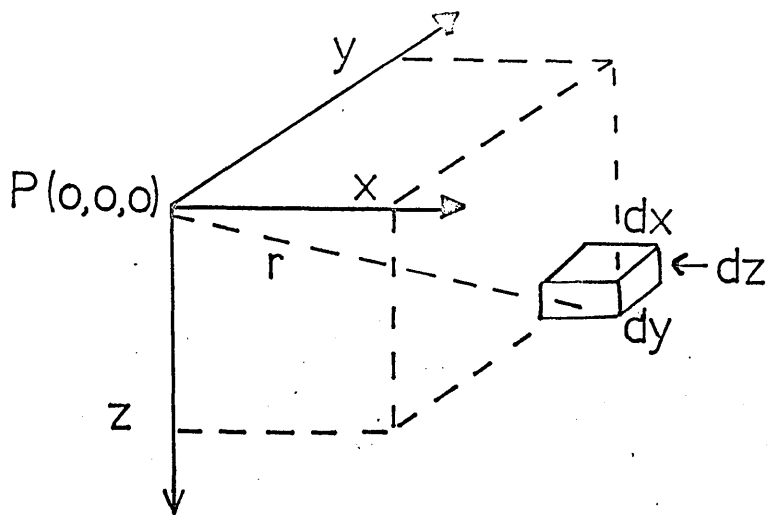


Fig. 2. An elementary volume element and the co-ordinate system

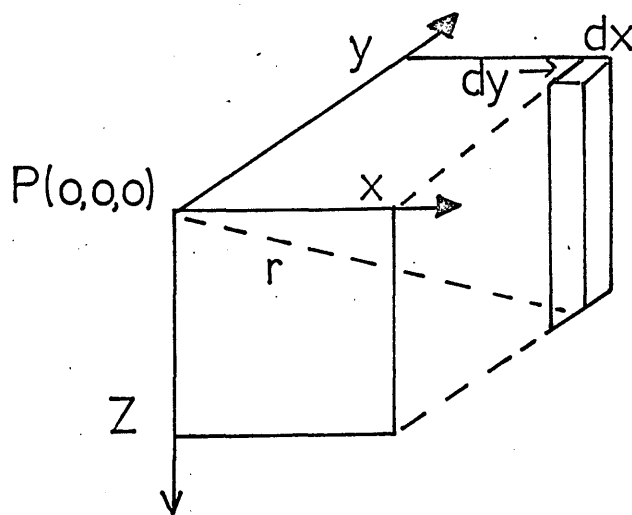


Fig. 3. A vertical line element and the co-ordinate system

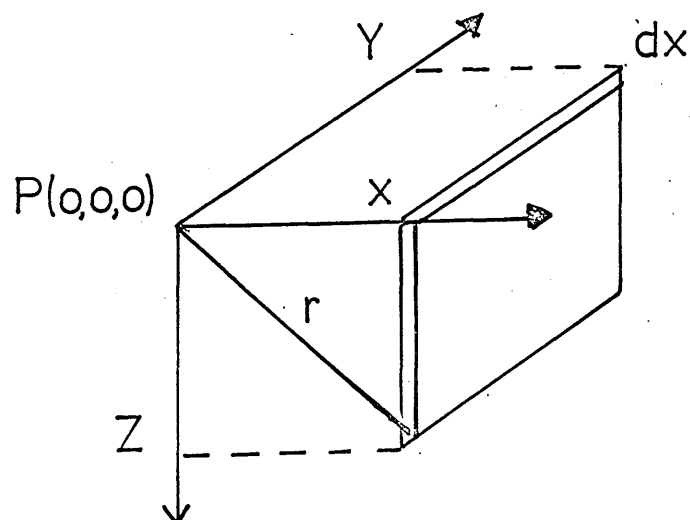


Fig. 4. A vertical thin sheet and the co-ordinate system

$$\Delta g_z = G. \Delta \rho \left[\ln \left(\frac{r_2}{r_1} \right) - \ln \frac{Y + \sqrt{Y^2 + r_2^2}}{Y + \sqrt{Y^2 + r_1^2}} \right] dx \quad \dots (3a)$$

where r_1^2 is $x^2 + z_1^2$

r_2^2 is $x^2 + z_2^2$

If the strike extent is from Y_1 to Y_2 then a double application of (3a) evaluates the gravitational effect at P for any vertical sheet. Equation (3a) is equivalent to that given by Grant and West (1965 p.274) when the angle of dip is 90° and arranged in such a way that (a) the first term within the brackets represents the effect of a sheet with a semi-infinite strike length and (b) the second term within brackets may be considered as its end correction.

Integrating (3) with respect to x from $x = 0$ to $x = X$, the expression for the gravitational effect at the point of observation $P(0,0,0)$ on a corner of a right rectangular prism (Fig. 5) is obtained as follows:-

$$\Delta g_z = G. \Delta \rho \left[X(\ln(r_c(Y + r_a)/X(Y + r_o))) + \right. \\ Y(\ln(r_b(X + r_a)/Y(X + r_o))) + \\ Z(\text{arc tan}(r_c/(r_d^2 - r_e^2)^{\frac{1}{2}}) - \\ \left. \text{arc tan}(Z/X) \right] \quad \dots (4)$$

where G is the Gravitational Constant

$\Delta \rho$ is the density contrast

and $r_o = (X^2 + Y^2 + Z^2)^{\frac{1}{2}}$

$r_a = (X^2 + Y^2)^{\frac{1}{2}}$

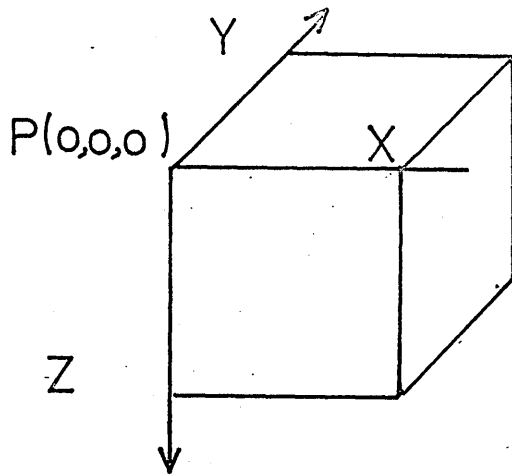


Fig. 5. A right rectangular prism and the co-ordinate system

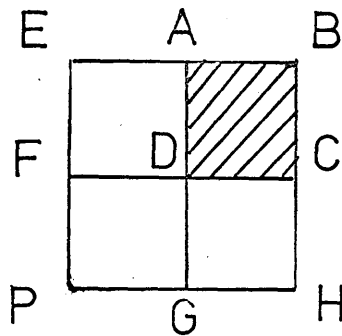


Fig. 5a. When the point of observation $P(0,0,0)$ lies outside the prism but in the same plane

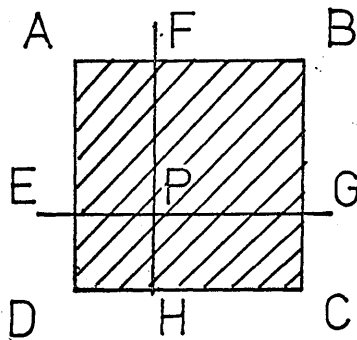


Fig. 5b. When the point of observation $P(0,0,0)$ lies inside the prism but in the same plane.

$$\begin{aligned}
 r_b &= (Y^2 + Z^2)^{\frac{1}{2}} \\
 r_c &= (X^2 + Z^2)^{\frac{1}{2}} \\
 r_d &= (Y + r_o) \times r_b \\
 r_e &= (r_b^2 + Y r_o)
 \end{aligned}$$

... (D. Nagy 1966)

If P (point of observation) lies outside the top area of the prism (Fig. 5a) the effect of the prism in the plane of its top surface is $ABCD_p = PEBH - PEAG - PFCH + PFDG$. But if P lies inside (Fig. 5b)

$$ABCD_p = PFBG + PGCH + PHDE + PFAF$$

If the top of the prism lies below P at z_1 and the base at z_2 , the gravitational attraction due to prism is obtained by applying equation (4) eight times in all.

3.2 CALCULATION OF MAGNETIC POTENTIAL FIELDS

The magnetic field component at P(0,0,0) in the direction of \vec{T} due to an elementary volume dx, dy, dz (Fig. 2) magnetised in a direction \vec{S} with an intensity I_p at a distance r is

$$\Delta I_p = I_p \frac{\partial^2}{\partial s \partial t} \left(\frac{1}{r} \right) dx dy dz \quad \dots (5)$$

where ∂s is an element of length in the direction of \vec{S} , ∂t is an element in the direction of \vec{T} , the total field of earth and

$$r^2 = x^2 + y^2 + z^2$$

Following Bhattacharyya (1964), (5) may be written as

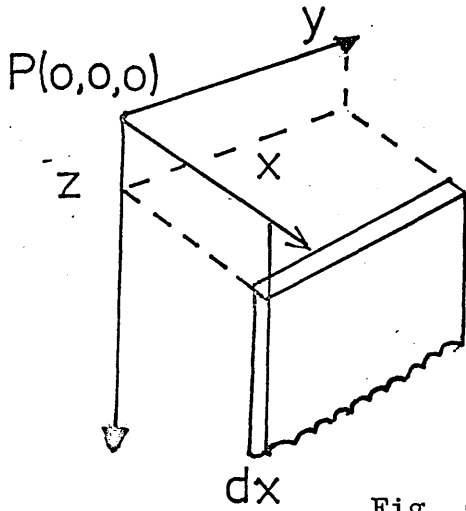


Fig. 6. A vertical thin sheet and co-ordinate system (Magnetic case)

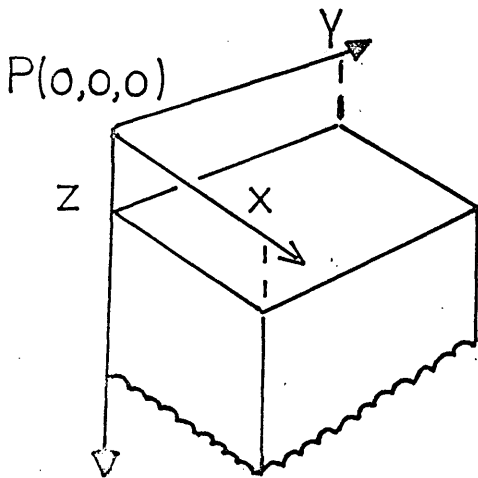


Fig. 7. A right-rectangular prism and co-ordinate system (Magnetic case)

$$\Delta T = I_p \left[\frac{1}{r^3} \cos \theta + \frac{3}{r^5} \left(lLx^2 + mMy^2 + nNz^2 + \alpha_{12}^{xy} + \alpha_{13}^{xz} + \alpha_{23}^{yz} \right) \right] dx dy dz$$

where l , m and n and L , M and N are the direction cosines of the field and magnetisation vectors respectively,

$$\alpha_{12} = Lm + Ml, \quad \alpha_{13} = Ln + Nl \quad \text{and}$$

$$\alpha_{23} = Mn + Nm,$$

and

$\cos \theta = lL + mM + nN$ where the magnetisation vector makes the angle θ with the field direction.

In a similar way to that outlined for the gravity case, integration with respect to z , from Z to infinity, and with respect to y , from 0 to Y , leads to an expression for the field due to a thin vertical sheet (Fig. 6)

$$\begin{aligned} \Delta T = I_p \left[\alpha_{23} \frac{xY}{p^2 r_o} - \alpha_{13} \frac{1}{r_o} - \frac{\alpha_{12}^x}{a^2} \left(1 - \frac{Z}{r_o}\right) \right. \\ \left. - \frac{lL}{a^2} Y \left(1 - \frac{Z}{r_o}\right) + mMY \left\{ \frac{1}{a^2} - \frac{Z}{r_o} \right. \right. \\ \left. \left. \left(\frac{1}{a^2} + \frac{1}{p^2} \right) \right\} + \frac{NnYZ}{p^2 r_o} \right] dx \quad \dots (7) \end{aligned}$$

where $a^2 = x^2 + y^2$, $p^2 = z^2 + x^2$

and $r_o^2 = x^2 + y^2 + z^2$

The magnetic attraction (field) due to a thin sheet having finite depth and strike extents is obtained by applying equation (7) four times.

After the integration of (7) with respect to x from 0 to X , the expression for the effect over one corner of a

right rectangular prism (Fig. 7) may be written as

$$\Delta T = I_p \left[\frac{\alpha_{23}}{2} \ln \left(\frac{r_o - X}{r_o + X} \right) + \frac{\alpha_{13}}{2} \ln \left(\frac{r_o - Y}{r_o + Y} \right) - \alpha_{12} \ln(r_o + Z) \right. \\ \left. - \mu L \arctan \left(\frac{XY}{X^2 + r_o^2 + Z^2} \right) - mM \arctan \left(\frac{XY}{r_o^2 + r_o^2 + Z - X^2} \right) \right. \\ \left. + nN \arctan \left(\frac{XY}{r_o Z} \right) \right] \dots (8)$$

By applying eqn. (8), eight times, the effect of the prism is obtained.

The three term representing the field components parallel to magnetisation components i.e. with coefficients μL , mM and nN have been reduced to two with coefficients $(mM - \mu L)$ and $(nN - mM)$ using the relationship

$$\frac{T_{x,x}}{I_x} + \frac{T_{y,y}}{I_y} + \frac{T_{z,z}}{I_z} = 0$$

(Affleck 1958)

where the first suffix denotes the field component and the second the magnetisation component.

A computer program has been written by Powell (personal communication) using equation (3a) and (7) for the calculation of gravity or magnetic effect of a body. The program has been described in appendix 2. An outline of its utilisation follows.

3.3 OUTLINE OF PROGRAM

In this thesis the fields of less regular bodies than right rectangular prisms have been found by approximating them to a number of thin vertical sheets and summing their effects by repeated use of equations 3a and 7 evaluated by means of a computer program. A single pass

of the calculation routine evaluates the effect of a body with uniform contrast (RO) and shaped such that any vertical line cuts its boundary surface either twice or not at all.

Specification of body and calculation points (see Fig. 8)

In this system the body is subdivided into a number of parallel strips sufficient to represent variations in the Y-direction i.e. the X-Z cross-section specified by top and bottom depths of each sheet i.e. at equal X-increments (KMS) from LXC to HXC, is constant across each strip (LYC to HYC). Only the corners of linear X-Z segments need be input. The thin sheet approximation is maintained to the extent that sheets are automatically subdivided until their widths are no greater than their top depths. (In earlier version, while calculating gravity effect of the sedimentary basins, this was achieved, in part, by modelling with a cuboid (equations 4 or 8) under the shallowest part of the top; this however had limited flexibility in describing the X-Z cross-section).

The X-co-ordinates of the calculation points or stations (Xs) correspond with sheet centres but may extend beyond the model ($X_s < LXC$ or $X_s > HXC$). The stations are arranged on any number of profiles of constant length parallel to X and at any specified Y-positions (PYC).

Adjustment of a model to match an observed anomaly

Subsequent to a calculation and output of the effect of the specified i.e. initial model, the program is designed to adjust depths iteratively towards a reduction in the differences between observed and calculated field values or

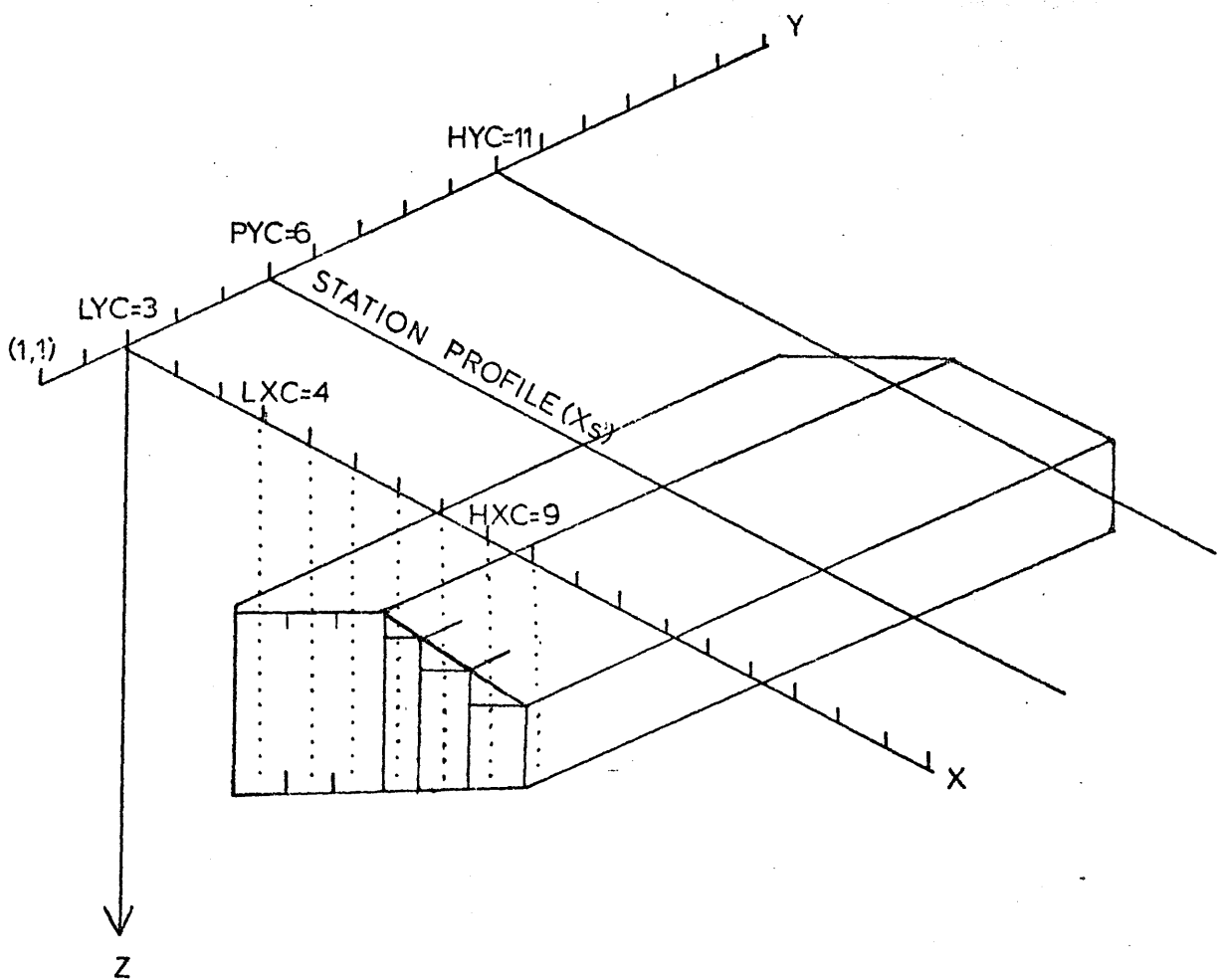


Fig. 8 Specification of body
 dimension and calculation
 points for the program used in Potential
 fields (gravity/magnetic) calculations.

residuals at those stations over sheet elements where the residuals exceed the mean (sum of the absolute values of the residuals during previous iteration/the number of stations over the model).

In the gravity case the amount of adjustment is based on the thickness of a slab which would produce the residual.

The magnetic case is, in general, complicated by an offset of the peak effect with respect to the point of depth adjustment which is itself dependent on the depth as well as the field and magnetisation direction. This offset is estimated for the shallowest part of the body and applied throughout as a constant.

The incidence of the depth adjustment is also controlled through two parameters for each element which, like the depths, need only be input at the corners of linear X-Z segments. The first, varying from zero to one, specifies the proportion of the residual to be used for adjustment (zero for none, one for all). The second distributes the adjustment between the bottom and top surfaces at each point (zero for bottom, one for top, 0.5 for an equal distributions etc.).

The calculations involved in the interpretational sections which follow have been made by various applications of this program. They are

- 1) Direct calculation of the gravity effect of a specified model representing sedimentary basins.

- 2) Calculation and adjustments of depths to fit a model to a given magnetic anomaly. Subsequent calculation

CHAPTER 4

QUALITATIVE ANALYSIS OF GRAVITY ANOMALIES

4.1 ROCK DENSITIES OF THE REGION

No new density determinations have been made as a part of this research. The densities of rock formations used in different calculations are taken from McLean (1961, p.105) and Qureshi (1969-70) and El-Batroukh (personal communication). The values of rock density are given in table 3.

The principal density contrast in the Midland Valley is between Upper Palaeozoic sediments ($2.52 \pm 0.10 \text{ g/cm}^3$) and Lower Palaeozoic rocks (2.72 g/cm^3). Within the Upper Palaeozoic Group there are also important density contrasts between the following formations

1. Carboniferous Sediments
2. Carboniferous Lavas.
3. Lower Old Red Sandstone sediments
4. Lower Old Red Sandstone lavas.

Contrasts of local importance occur around igneous intrusions especially where basic rocks are emplaced.

In the present investigation the density contrasts between Carboniferous sediments and rocks of Lower Old Red Sandstone age; and between Lower Old Red Sediments and Carboniferous lavas, and igneous intrusion of diorite or gabbro are considered.

4.2 DESCRIPTION OF BOUGUER ANOMALY MAP

In the extreme north-west and south-east corners of Map 1 contours trend parallel to the Midland Valley boundary faults, but, contrary to any expectations based on geological outcrops, define gradients (about 1 mgal/Km) away from its axis, that is towards the denser bounding massifs.

McLean and Qureshi (1966) inferred that, when correction is made for the low density cover of Upper Palaeozoic sediments, a regional high culminates at +30 mgal near the centre of the Midland Valley graben in the region just west of Map 1.

Basins filled with Upper Palaeozoic strata within the area of Map 1 are the apparent cause of the contoured minima (for example the coalfield areas - Lanarkshire, oval around [282.655]; Midlothian, elongated in north-east directions from [320.654] to [330.668]; Clackmannan, oval around [295.695] and Cowdenbeath, oval around [316.692]).

Pronounced flanking gravity highs are seen

- 1) along the Old Red Sandstone outcrop at the core of the Pentlands [316.660] to [329.676].
- 2) along the axis of the Carboniferous lava outcrop running from [262.660] to beyond the Map in Renfrewshire.
- 3) along the Carboniferous lava outcrop around Campsie Fells [265.683] and
- 4) in the centre of the Midland Valley around Bathgate [295.674]. This is the anomaly with which this thesis is primarily concerned and which culminates, surprisingly, over the central Coalfield syncline. Relative to the Bouguer minima over the deeper Carboniferous basins this anomaly has an amplitude of about 23 mgals.

4.2.1 Bathgate High and Geological Models

- (1) A possible source - the effect of structure on and thickness variations in the Carboniferous lavas

A simplified density model consisting of Carboniferous sediments (2.54 g/cm^3) resting on Carboniferous lavas (2.72 g/cm^3) and on rocks of Lower Old Red Sandstone age (sediments 2.61 g/cm^3 and lavas 2.66 g/cm^3) is considered first. The effects of the following geological structures are neglected (a) the buried channel of the Forth which is too narrow to affect significantly the stations on which Map 1 is based, (b) the sediments between lavas and Lower Old Red Sandstone which are relatively thin, and (c) the boundary between Lower Old Red Sandstone and Lower Palaeozoic rocks (where a density contrast of $2.72 - 2.63(5) = -0.09(5)$ probably exists) since the thickness of Lower Old Red Sandstone here cannot be deduced with any confidence from the geology. Below the Bouguer datum (mean sea-level) structure developed during and since Carboniferous times has produced a maximum, known, differential relief (i.e. structural depression) of about 1.3 Km between the eastern flank of central coalfield syncline, over the anomaly, on the one hand and Lanarks and Clackmannan basins to the south-west and north of it, on the other. Assuming firstly that the lavas have a uniform thickness between these regions not significantly greater than the structural relief (maximum thickness estimated elsewhere 1 Km), the net positive gravity effect produced by this structure on the sequence would be from the sum of the effects of the slabs involved ($\Delta g = 2\pi G \cdot \Delta \rho \cdot h$).

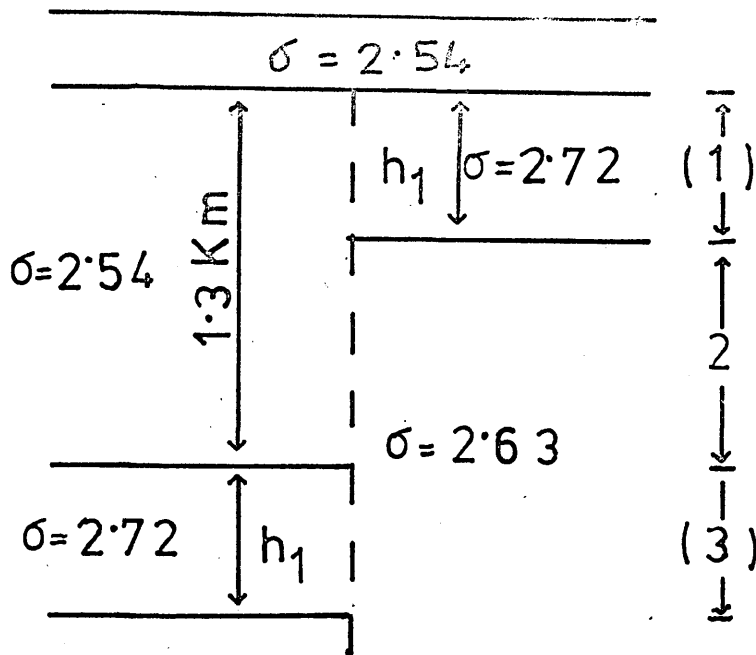


Fig. 9 Lava layer of constant thickness

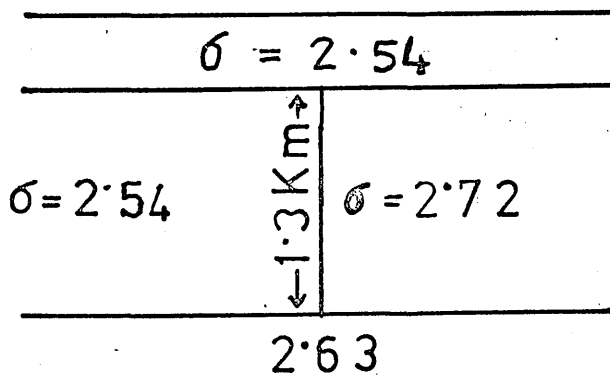


Fig. 10 Lava layer of variable thickness
not exceeding Carboniferous
structural relief

$$\begin{aligned}
 \text{i.e. } \Delta g &= \frac{40 \times (2.72 - 2.54) \times h}{\text{Slab 1}} + \\
 &\quad \frac{40 \times (2.63 - 2.54) \times (1.3 - h)}{\text{Slab 2}} + \\
 &\quad \frac{40 \times (2.63 - 2.72) \times h}{\text{Slab 3}} \\
 &= 40 \times (0.09 \times 1.3) \approx 5 \text{ mgal.}
 \end{aligned}$$

(see Fig. 9)

If however lava thickness varies from zero to no more than 1.3 Km, being thick on structural high then the maximum amplitude is

$$\Delta g \ll 40 \times (2.72 - 2.54) \times 1.3 \ll 10 \text{ mgal}$$

(see Fig.10)

This assumes zero lava thickness under the Carboniferous basins and full 1.3 Km thickness in between the structural high.

As the observed amplitude (23 mgal) is much greater than the larger effect from such a structural model, and since the lavas are known to thin in some places to the south it is impossible to explain the anomaly in this way. A differential thickening of the lavas under Bathgate is the next possibility to evaluate. Cotton (1968) has used such a model to explain Bouguer anomalies around Glasgow.

Hall (1971) has inferred from seismic evidence that there is only 0.5 Km of lavas under Slamannan - that is some 10 Km west of Bathgate. It is therefore concluded that the possible anomaly amplitude due to models of these types is 5 mgals and the maximum no more than 10 mgals. That type of Model allowing thickness variations in the lavas will be

referred to as Model 1.

(2) Intrusive Models

Cotton considers the Campsie gravity high, which has its peak value at Waterhead [2645.6835] to be related to a large basic mass (Table 4 Waterhead model parameters from Cotton) under the lavas. This may have served as a magma chamber during their eruption. A similar model might explain the Bathgate anomaly. Alternatively, if the intrusion were late-Carboniferous in age, it may have fed the late-Carboniferous sills which are distributed above it, within the Carboniferous sediments. This is, perhaps, less likely as some of the sills have been fed by East-West dykes which extend beyond Map 1.

Another possibility is that such an intrusion is comparable with the Distinkhorn granodiorite of Lower Old Red Sandstone age. (This intrusion is situated just beyond the south-west corner of Map 1.) Or, with a more basic diorite of similar age such as are found in the Grampians.

For each of these geological possibilities the density model is essentially the same. The effect of the known Carboniferous sediments on top of the lavas can be separated leaving the remainder of the anomaly to be attributed to some combination of structure on the base of the lavas and an underlying intrusion. As both these effects arise from similar depths and are inseparable the two geological bodies, lavas and intrusion, are investigated as one gravitating mass. For analytical convenience the special case is considered where the top of the intrusion is/

Table 4 Waterhead Model Parameters from Cotton (1968)

Density Models:

for Spheres

$\Delta \rho$ (density contrast ranges from 0.2 to 0.4 g/cm³,
radius ranges from 2.57 Km to 3.19 Km, depth to
the top 3.41 Km.

and

for Frustum

$\Delta \rho$ (density contrast)	=	0.4 g/cm ³
depth to upper surface	=	0.28 Km
" " Lower "	=	3.86 Km
Upper radius	=	0.68 Km
Lower "	=	2.46 Km

and estimated volume of the mass varies from 31.30
to 62.40 cubic Km.

Regional Gravity Field

to the regional gravity field which is assumed to be
a vertical axis of the inclined plane of the field. The
field is assumed to be a vertical axis of the inclined plane of the field.

is in contact with, or intrudes into, the base of the lavas, and both igneous bodies have the same density. Both the lavas and the intrusion may then be treated as a single body with a known top and without cavities, i.e.

geophysically this is simply Model 1 as previously defined. The existence/or not of an intrusion is to be a geological judgement.

(3) A model unrelated to local geology (Model 2)

A much deeper source is also considered which may be thought of as an inhomogeneity, within a crystalline basement of either structural or intrusive origin. Approximate dimension for this model are taken from Gunn's (1975) prismatic block model which satisfies an aeromagnetic anomaly similarly located to the Bathgate gravity high. The main purpose of this analysis was to determine the required density contrast and judge its likelihood against a probable background density. To carry out the calculations for this model it has been assumed that the contribution of the Carboniferous lavas to the anomaly is negligibly small, and that the lava layer is relatively thin under the area of the Bathgate high.

(4) Regional Gravity Field

If the regional gravity high which culminates at the central axis of the Midland Valley in Ayrshire, extends north-eastwards along the graben then the Bathgate high is superimposed upon it. A significant part of the Bathgate high may, therefore, be related to the crustal structure. It is not obvious even after applying a correction for the effects of surrounding Carboniferous sedimentary basins,

how to separate out the local and regional components. A simple projection of the Ayrshire regional parallel to the Midland Valley boundaries (cf fig. 31) leaves negative residuals, everywhere up to - 25 mgals over the Clackmannan and Lanarks Basins, considerably in excess of the amplitude deduced from the known or probable geology (p. 45). A N.N.E. regional gradient is also possible. If this subtracts 15 mgals from the Ayrshire regional then the residuals are small at the N.W. and S.E. limits of the area (Map 1) and positive (up to 10 mgals) over the Bathgate anomaly. These aspects of the Bouguer field are discussed again in Section 6.3.

4.2.1.1 Conclusions on which quantitative interpretational steps are based

Models 1 and 2 are investigated after the Bouguer field has been modified by correction for the effects of Carboniferous sedimentary basins. This correction removes the gravity effect of the low-density sediments in the basins and replaces them with material of Lower Old Red Sandstone density. The resulting anomalies are then considered as the sum of the effects of either

(a) Model 1 (Carboniferous lavas and intrusion with same physical properties and in continuity with lavas) or Model 2 (a deep intrusion with negligible lava anomaly), plus, in both cases, regional components.

A description of the first step (qualitative discussion of gravity model) is given earlier. The second step i.e. resolution of the observed anomalies into local and regional anomalies is approached through a prior

definition of a magnetic model from the magnetic anomalies, then, calculation of the corresponding pseudo-gravity effect as a means to separating local and regional gravity components, on the premise that only the source of the former anomaly is also magnetic. Step 1 is a necessary preliminary to analysis since the density contrast between the Carboniferous sediments and Lower ORS rocks affects only the gravity anomalies. It is then proposed to test the assumption that the magnetised body is also a gravitating one in which the ratio of the appropriate physical contrasts is a constant. In so far as models of types 1 and 2 can be fitted to the magnetic anomaly the test will consist of scaling the pseudogravity anomaly (for a geologically reasonable density contrast), and determining whether the modified Bouguer anomaly can then be approximated by the component sums set out above.

4.3 STRIPPING OF THE GRAVITY EFFECTS OF ROCKS ABOVE HURLET LIMESTONE

To obtain a clearer picture of the anomaly it is desirable to strip the gravity effects of the known sedimentary cover from the Bouguer anomalies. In attempting to define thickness of this cover a compromise must be struck between completeness and certainty. The geology (that is the thickness of the sedimentary pile at a given locality) becomes increasingly uncertain as successively lower horizons are chosen. Mapping supported by geological information from mining and quarrying gives a usable synthesis of stratigraphy and structure as deep as the Calciferous Sandstone Series. For these reasons, the

Hurlet Limestone or its equivalent, a well defined horizon, present over most of the area of Map 1 (except east of Bathgate) is chosen. The gravity effects of all sediments above it are computed assuming that they are to be replaced by strata having the density of Lower Old Red Sandstone age (i.e. average of the density of Lower ORS sediments and lavas $(2.61 + 2.66)/2 = 2.63(5) \text{ g/cm}^3$.

4.3.1 Thickness Map of Carboniferous Sediments between Hurlet Limestone and datum (Newlyn O.D.)

Map 2 shows thickness in feet of sediments between the Hurlet Limestone (or its equivalent horizons) and datum (Newlyn O.D.). The sources of geological information on which this map is based, are the Memoirs and geological (solid) 1 inch maps (sheets 23, 24, 31, 32, 39 and 40) of the area, published by I.G.S. The generalised section, given on each map, of the Carboniferous succession above the Calciferous Sandstone Series is used to get the thickness of the principal Carboniferous rock-formations at that locality.

The depth to the Hurlet Limestone can then be plotted at any locality by subtracting the thickness of strata between the horizon outcropping there and the Hurlet Limestone, with a further adjustment to allow for elevation of the locality above datum. For convenience and speed of working, the horizons chosen were the boundaries between the principal Carboniferous formations. The outcrops are clearly shown on the 1-inch maps used. These values are contoured at an interval of 500 ft (150 m) to produce Map 2.

4.3.2 Calculation of gravity effect of the Sediments from Map 2.

This calculation was carried out with the program outlined in (p. 36). Map 2 was subdivided into six sub-areas for the convenience of computer input and the effect of each was calculated separately. The effects of the five sub-areas have been added together at the contouring stage and that of the sixth (which is isolated) has been contoured separately. Thus from these calculated gravity values expressed in mgal, a gravity anomaly map (Map 3) for the supra-Hurlet sediments is produced.

Five of the subareas have at least one common boundary with another so that divisions of each of these into strips for the program input was in a single orientation in order to ensure continuity of the overall model. This direction is taken to be East-West as it best defines the basin shapes. The widths of the strips range from 0.63 Km to 6 Km and the specified depths (and calculation points) are spaced at 1.27 Km, except in area six in which they are spaced at 0.63 Km. The calculation is carried to a distance at which the effect fell below 0.25 mgal for a density contrast of + 0.1 g/cm³.

Although the actual density contrast between Carboniferous sediments and rocks of Lower ORS age is 0.09(5) g/cm³ but for the convenience of computation + 0.1 g/cm³ as the density contrast between the two has been used since the difference between the two is small.

Fig. (11) shows the boundary of six sub-areas which have been further subdivided into several strips. The calculation points lie along profiles central to each strip

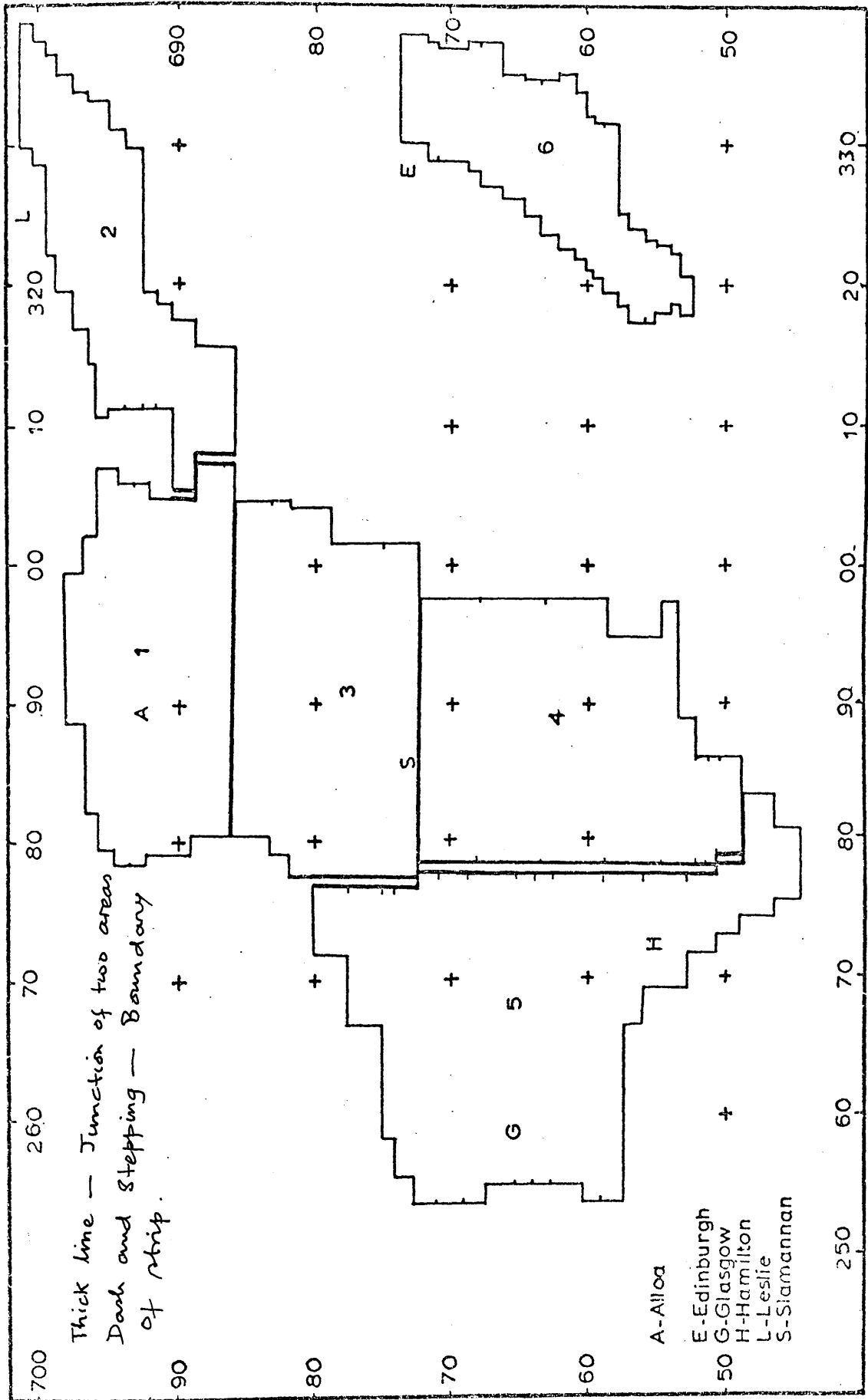


Fig. 11 Six sub-areas showing the division of the sedimentary basins of Map 2.

The contours representing the gravity effect of these basins have been added to the Bouguer anomalies in the sense which makes the latter more positive i.e. replaces the rocks in the basins with denser material. The new values are then contoured to get the Bouguer anomaly map (Map 4) corrected for the sedimentary effect.

This step in analysis and interpretation still bears recognisable traces of known structure on the residual isogals of Map 4, but the certain contribution of a large part of the sedimentary pile has been removed, and constraints on the geological meaning of the gravity anomalies are correspondingly tightened.

4.4 COMMENTS ON THE BOUGUER ANOMALIES WHEN CORRECTED FOR THE EFFECTS OF SUPRA HURLET SEDIMENTS

The correction, made to the observed Bouguer anomalies, for the effect of the sedimentary basins using a density contrast of $+ 0.1 \text{ g/cm}^3$, does not produce any marked change either in shape or location of the gravity 'highs' and 'lows'. Apart from increasing relatively the level of the field over basins, that is reducing the amplitude of the Bathgate high by about 3 mgal, the anomaly is not changed appreciably. However the effect of correction does not eliminate the 'low' but does reduce the amplitude of the Bathgate high. The Bathgate high still remains markedly positive with respect to its surroundings and the thickness of sediments required to replace the 'lows' over the surrounding basin is not geologically possible.

Uncertainty in defining the thickness of the Oil Shale Group precludes a systematic assessment of its

gravitational effects. This may however be estimated crudely if the effect of the maximum known thickness, about 1.5 Km (from the generalised section of sheet 32 (solid geology, Edinburgh), using a density contrast of $\Delta\rho = 0.1 \text{ g/cm}^3$ is calculated. The value obtained, 6.21 mgal, is then added to the anomalies (corrected for supra-Hurlet sediments). This reduces the amplitude of the Bathgate anomaly but the position of its peak remains unaltered.

To conclude, the Bathgate anomaly corrected for the sedimentary basins (Map 4) does not display any new relation with the known geology. The considerations embodied in Model 1 and 2, and the Regional anomaly still apply.

CHAPTER 5QUALITATIVE ANALYSIS OF AEROMAGNETIC ANOMALIES

5.1 DESCRIPTION OF AEROMAGNETIC MAP, GEOLOGICAL MODELS
FOR THE BATHGATE HIGH AND MAGNETISATION OF ROCKS IN
THE REGION

5.1.1 Description of magnetic anomalies and their
relationship to geology

Like the Bouguer gravity, the aeromagnetic Map 5 shows contours parallel to the Midland Valley margins in the extreme North-west and south-east corners. Also like the gravity map, it has a central high culminating near Bathgate [292.670] at 500 nT. This feature, the Bathgate magnetic high, equidimensional in plan (30 x 35 Kms), dominates the map because it is surrounded by smaller anomalies (generally $< \frac{1}{40}$ the area and $< \frac{1}{3}$ the amplitude of it). Only the Campsie anomaly (see below) has a comparable amplitude.

As in the gravity case most of these features, except the Bathgate high itself, can be accounted for, qualitatively in terms of geological outcrops.

1) In the south-east lie non-magnetic Lower Palaeozoic sediments with a band of magnetic Ordovician volcanics shown by the north-east striking anomaly against the Southern Upland Fault.

2) Lavas of Lower Old Red Sandstones and Lower Carboniferous age and associated intrusives together with

post-Carboniferous intrusives (especially sills) cause the host of smaller anomalies mentioned above. The effects of some of these are superimposed on the Bathgate high especially east and north east of its peak. Where they are absent the field over sedimentary basins is smoother and exhibits gradients into the 'lows' complementing the more complex 'highs' over the igneous outcrops, that is, over the Old Red Sandstone in the North-west corner into the linear minimum along the north face of the Campsie lava plateau, and over the Lanark coalfield basin along the north-east facing edge of the Renfrew-Strathaven lava plateau).

Similarly the lack of igneous outcrop reveals the extended gradient on the southern flank of the Bathgate anomaly on Profile 2 (Models 1 and 2) and the minimum associated with the high to the north, along the Forth.

In each of these cases where dipolar features can be recognised they appear to be consistent with induction by the present field.

Even more clearly than in the gravity case the Carboniferous lavas alone seem an inadequate source for the Bathgate anomaly. This is apparent from the following considerations. Upward continuation of the field over the Campsie or Renfrew-Strathaven lavas, to simulate depth of burial, would inevitably attenuate the amplitudes of such short wavelength anomalies to below that at Bathgate (Hall and Dagely, 1970), i.e. the source of the Bathgate 'high' is not simply a deeper equivalent to the lavas at outcrops.

5.1.2 Geological Models for the Bathgate High

It is suggested, therefore, as in the discussion of the Bathgate gravity high, that the most promising model for the magnetic anomaly is, at least in part, an intrusion (Model 1 or 2). Furthermore it is additionally proposed that the same body exhibits both density and magnetisation contrasts with its surroundings. In reaching this conclusion for the gravity, comparison was made with Cotton's (1968) Waterhead model. This comparison does not extend to the magnetic case as no magnetic anomaly is localised at Waterhead.

Since the magnetic anomalies, unlike the gravity, do not indicate any more regional component than the Bathgate anomaly itself it was decided to derive the unknown dimensions of Models 1 and 2 by fitting to the magnetic anomaly. Where, as in Model 2, shallow sources are not part of the model their effects were first reduced by a form of upward continuation (see further under Model 2). Once a model satisfying the magnetic anomaly had been found its pseudo-gravity anomaly was calculated. Finally an attempt was made to simulate the Bouguer anomaly, corrected for the effects of the carboniferous sedimentary basins, by summing the pseudo-gravity (with a suitable density contrast) to a projected regional component.

5.1.3 Magnetisation of igneous rocks in the region

Since Model 1 involves Carboniferous lavas and an intrusion which may be of similar composition data on the intensities of magnetisation of these rocks are of value in testing the model. Cotton (1968) measured the

susceptibility of 20 specimens of fresh lava, each specimen coming from a different flow and selected at random throughout the Campsie and Kilpatrick hills. He found a mean K of 5.0×10^{-3} c.g.s. The polarisation contrast (I) used for Model 1 was derived from this ($I = K \times T$ where T is the Earth's field strength i.e. 3.0×10^{-3} c.g.s.)

Wren (1968) found susceptibilities in the range 10^{-3} to 5×10^{-3} c.g.s., both by measurement and calculation (assuming induction) on anomalies, applicable to Upper Palaeozoic and Tertiary basic intrusions.

Powell (1963) found susceptibilities up to 0.01 for the quartz-dolerites (dykes).

Verification

Many of the models in Section 2 are based on the assumption that the magnetic field is uniform (Fig. 1B). This is certainly not true in the field but the models have been checked in the field and the results are given in Table 1. The most direct test is to compare the calculated magnetic field with the observed field. It is intended to represent a typical field in the area of the lavas where there are no well defined magnetic anomalies. These rocks within the area are of the same age and have a West-West width to about 1000 ft. The magnetic field is quite high but the contribution from the lavas is small.

CHAPTER 6

QUANTITATIVE ANALYSIS OF THE MAGNETIC AND GRAVITY ANOMALIES

6.1 MODEL 1

6.1.1 Magnetic

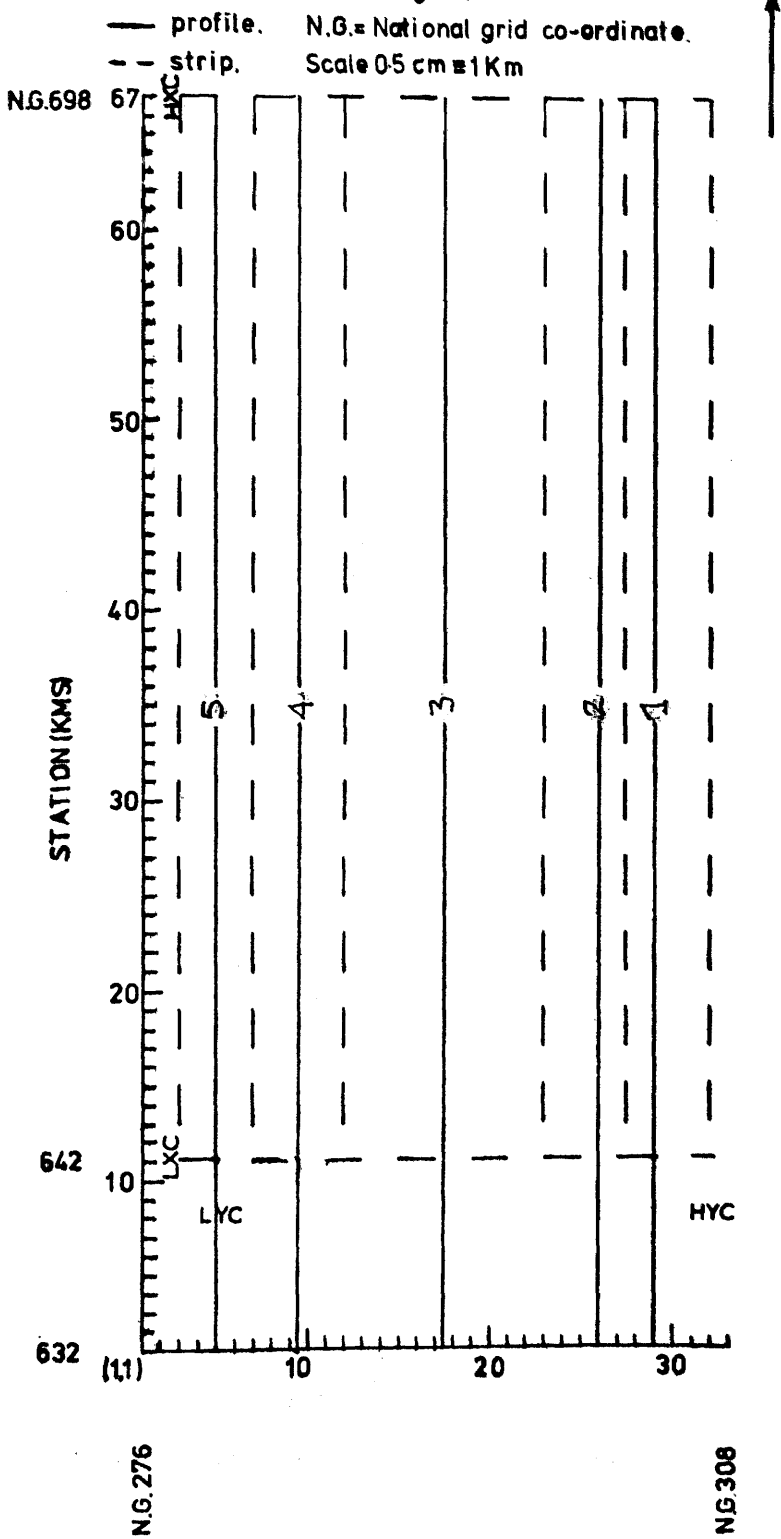
6.1.1.1 Anomaly and profiles

As previously outlined the first interpretational step has been to adjust some dimensions of an inductively magnetised body until its calculated field approximates to the Bathgate aeromagnetic anomaly. For calculations by the program the observed anomaly has been digitised at 1 Km intervals on five north-south profile (Map 5, figs. 12 and 25).

6.1.1.2 Body Specifications

The geometry of the model is described along five north-south strips (fig. 12). Their boundaries, like the profiles positions have been chosen in relation to changes in the east-west direction across the anomaly. Although the model is intended to represent, at least in part, the Carboniferous lavas there are no well defined East-West limits of these rocks within the area i.e. the model has sufficient East-West width to cover the principal sources of the Bathgate high but the Carboniferous lavas may extend beyond it. To the north and south, however, Lower Old Red Sandstone outcrops do limit these lavas, and the model, at the Ochil Fault and, less regularly, near Lanark respectively.

Fig. 12 Location of strip dimension and profile of Model 1 with respect to National grid.



The depths to the top surface of the model are fixed and taken to represent the top of the Carboniferous lavas. These depths were derived from the contours of Map 2 + 0.3 Km flying height (assumed constant above sea level) and extended to the lava outcrop where necessary. (The actual top surface is more complicated, especially in the east where flows at higher stratigraphic levels outcrop in the Bathgate Hills. Also the model takes no account of sills above the lavas. A method of adjustment for this was devised and applied for Model 2 where it is described. Some of the structure on the base of Model 1 is, therefore, in error from these sources). Initial estimates of the depths to the base were found, by trial and error, so that a uniform intensity of 3.0×10^{-3} c.g.s., similar to that measured on lava specimens, could produce the required amplitude (500 nT for the positive peak).

Adjustments of depths to the base by the program were restricted in the south to retain a gradual thinning of the model consistent with some geological evidence there.

6.1.1.3 Results and conclusions

The results of the computer calculations are shown, on the five profiles, in figs. 13-17. Except at some profile limits, where the local sources outside the model may be assumed to contribute to the observed profile, the anomaly residuals are acceptably small.

The main conclusion: Thicknesses on the flanks of the model are within the range (0.5 to 1 Km) established elsewhere for the thickness of Carboniferous lavas but that in the centre (4 to 5 Km) are outside the maximum known thickness /

Figs. 13-17

Show observed magnetic anomalies against calculated anomalies along five N-S profiles and thickness of the Model 1 under each profile.

Thick line - Calculated magnetic anomaly

Thin line - Observed magnetic anomaly

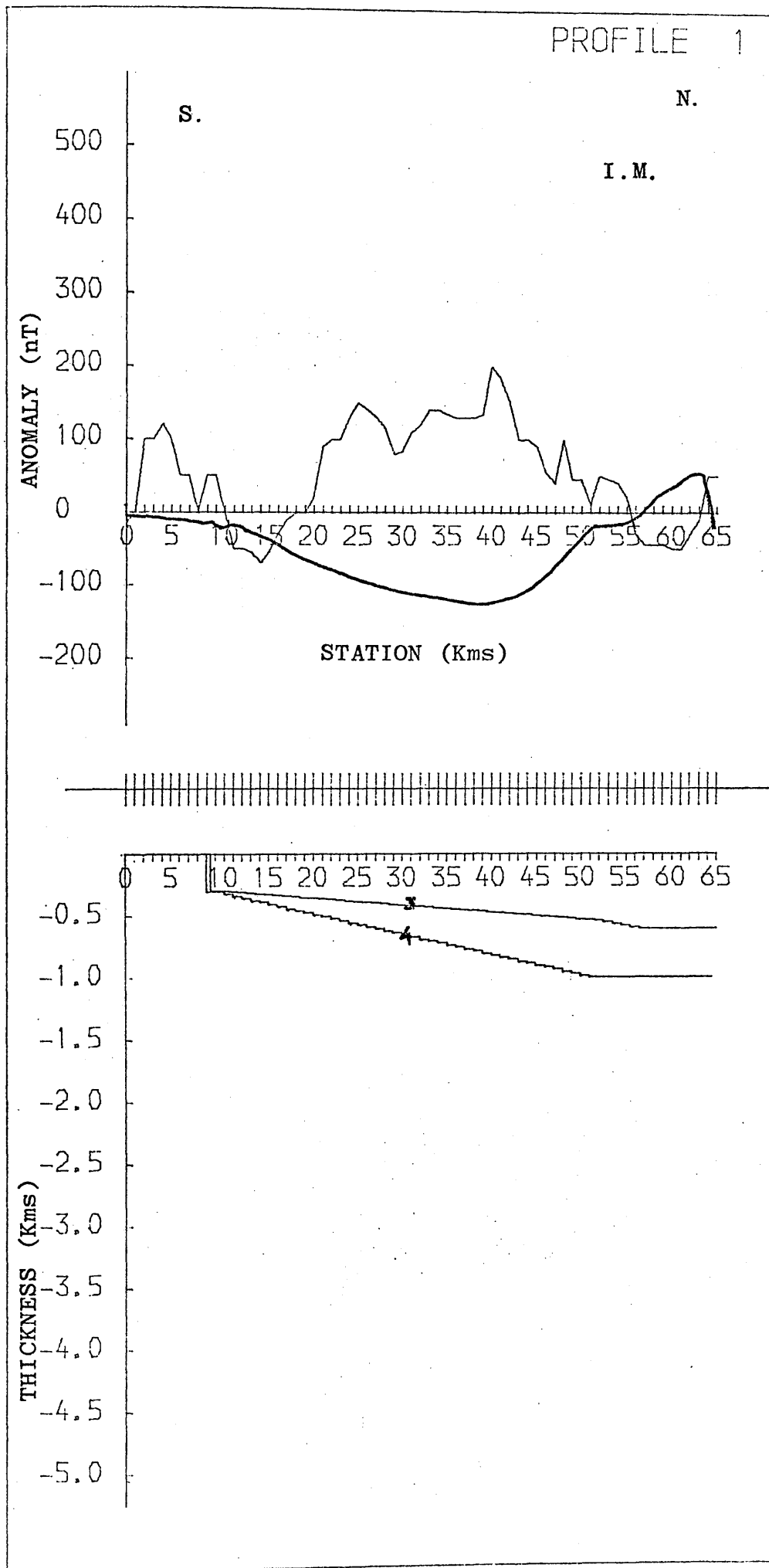
3 - Depth to the top of the model

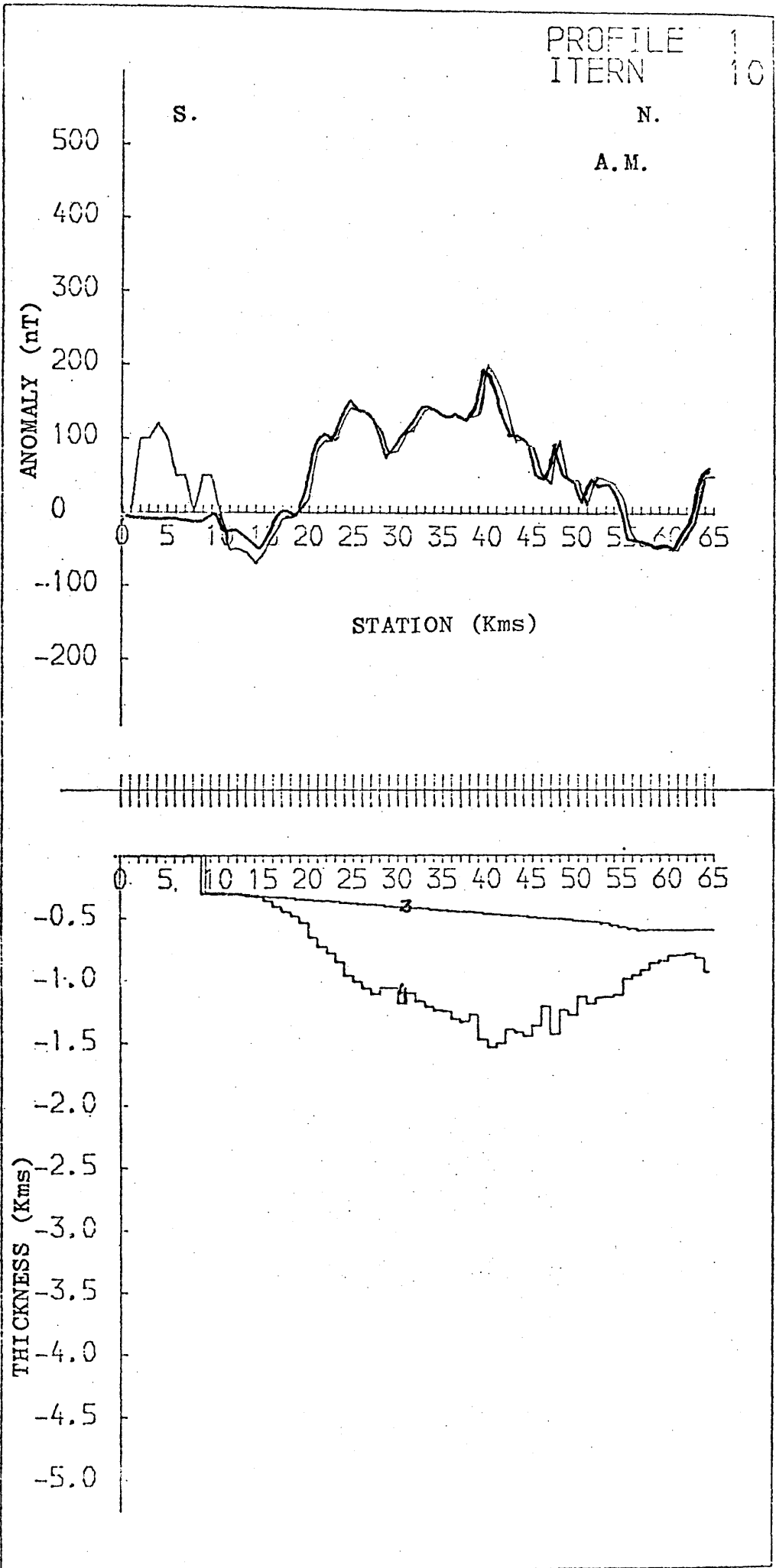
4 - Depth to the bottom of the model

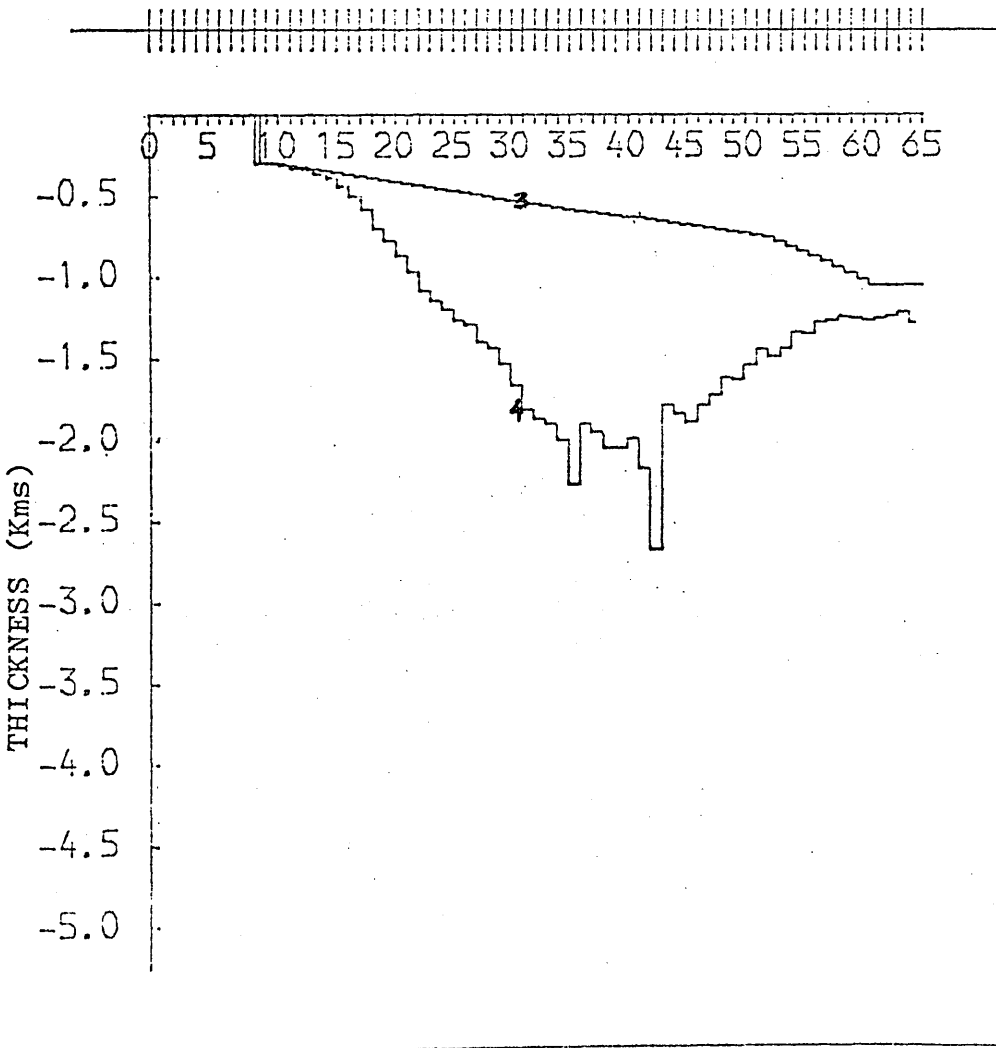
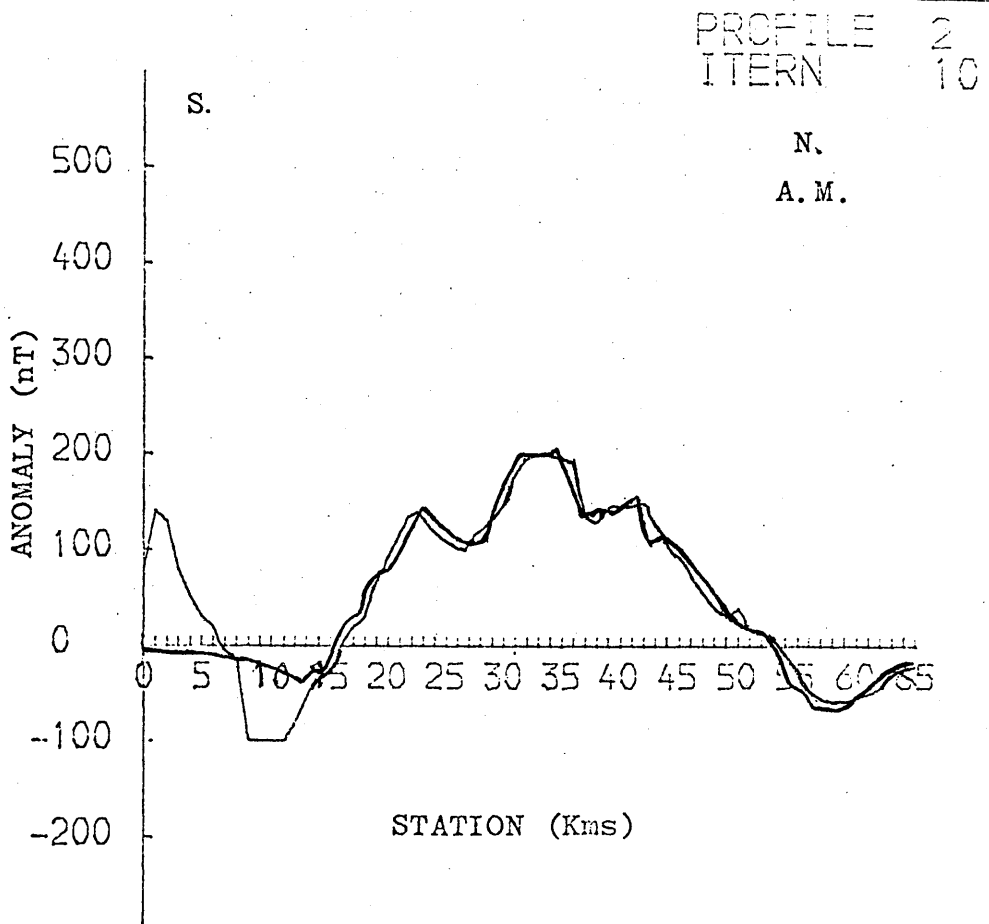
I.M. = Initial Model shows observed anomaly against anomaly calculated corresponding to the thickness of the model supplied to the computer.

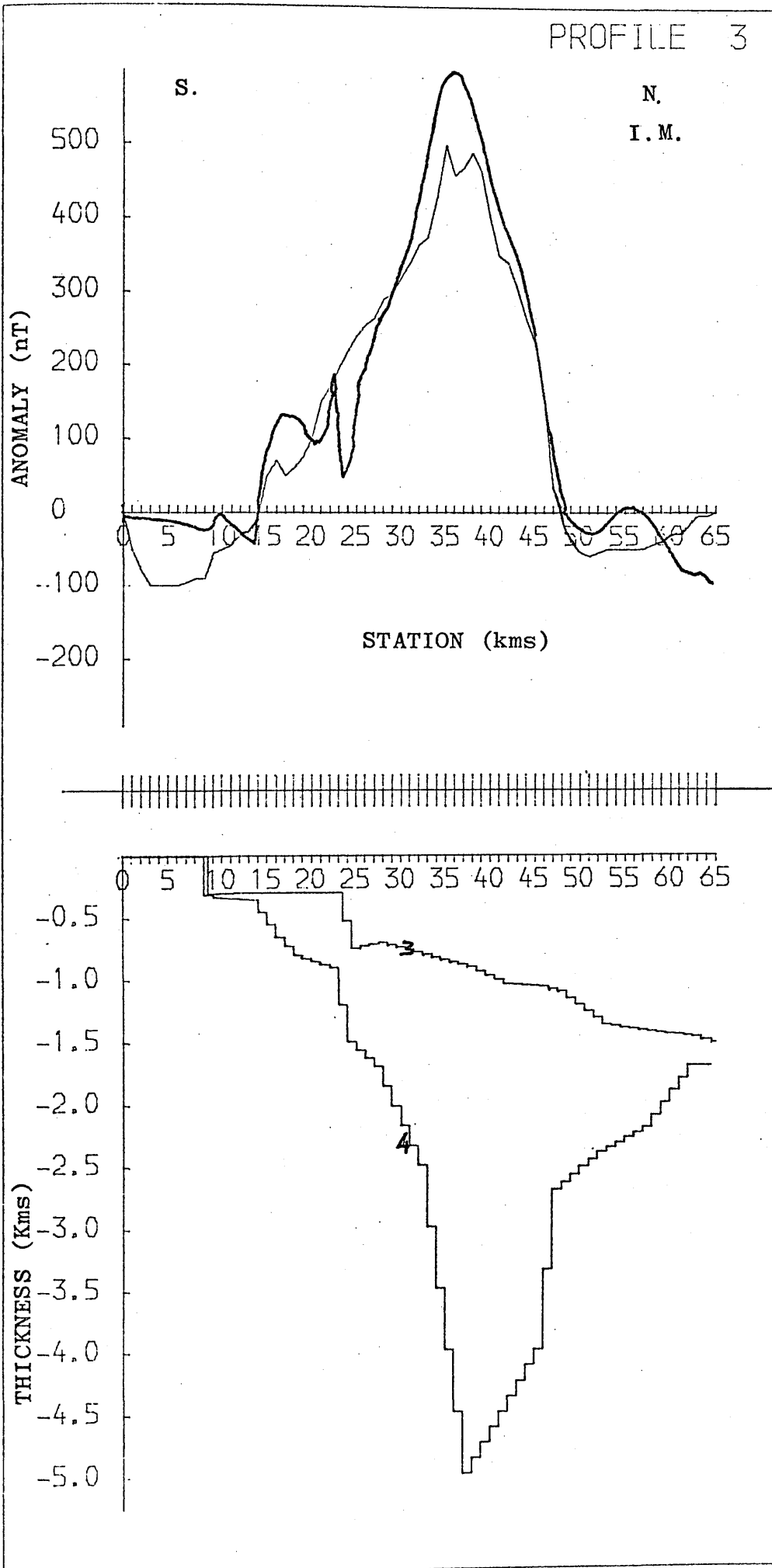
A.M. = Adjusted Model shows observed anomaly and anomaly calculated for the thickness of the model adjusted (from the supplied thickness) by the computer after 10 iterations and the adjusted thickness of model under each profile.

Fig. 13









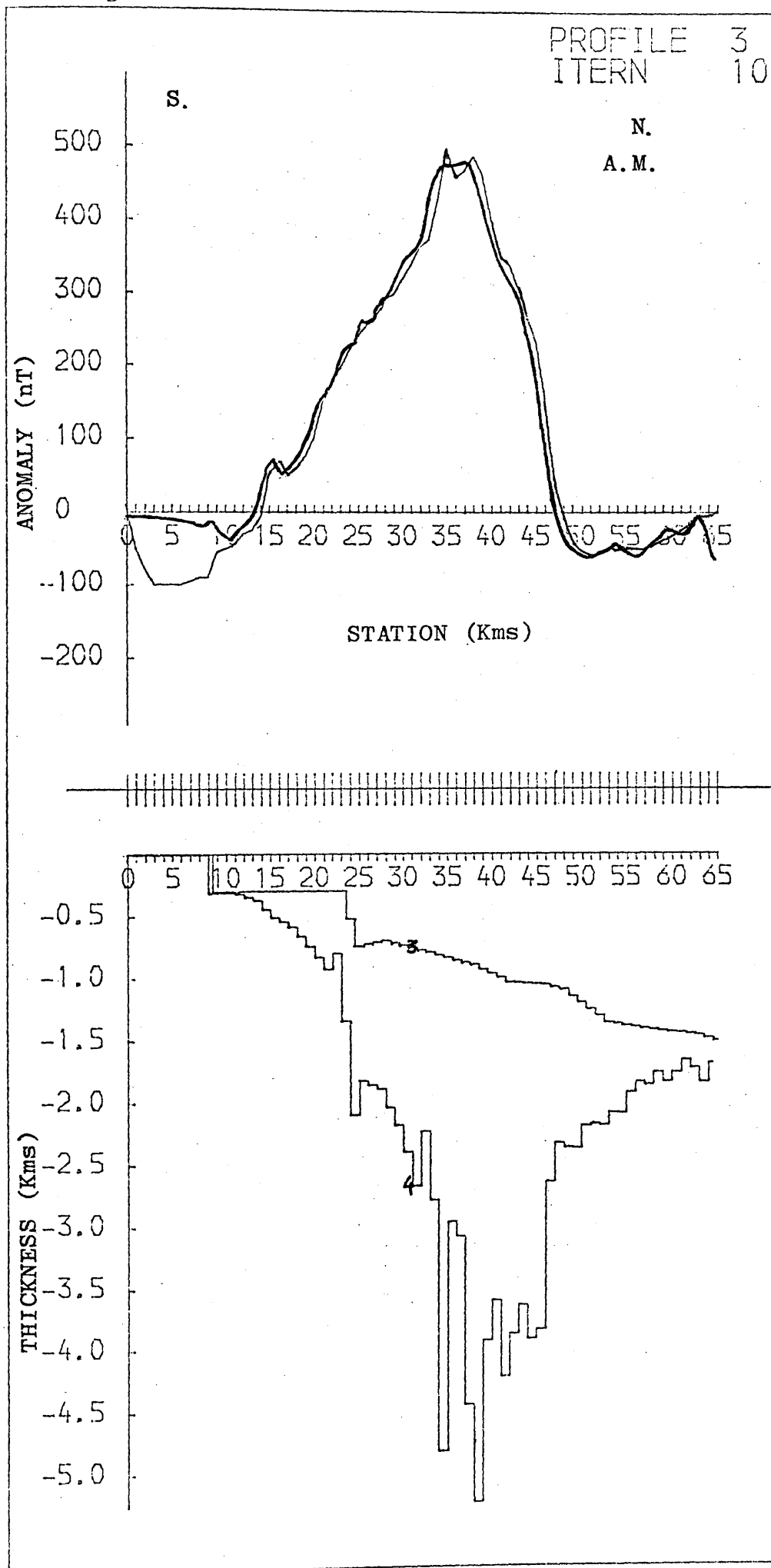


Fig. 16a

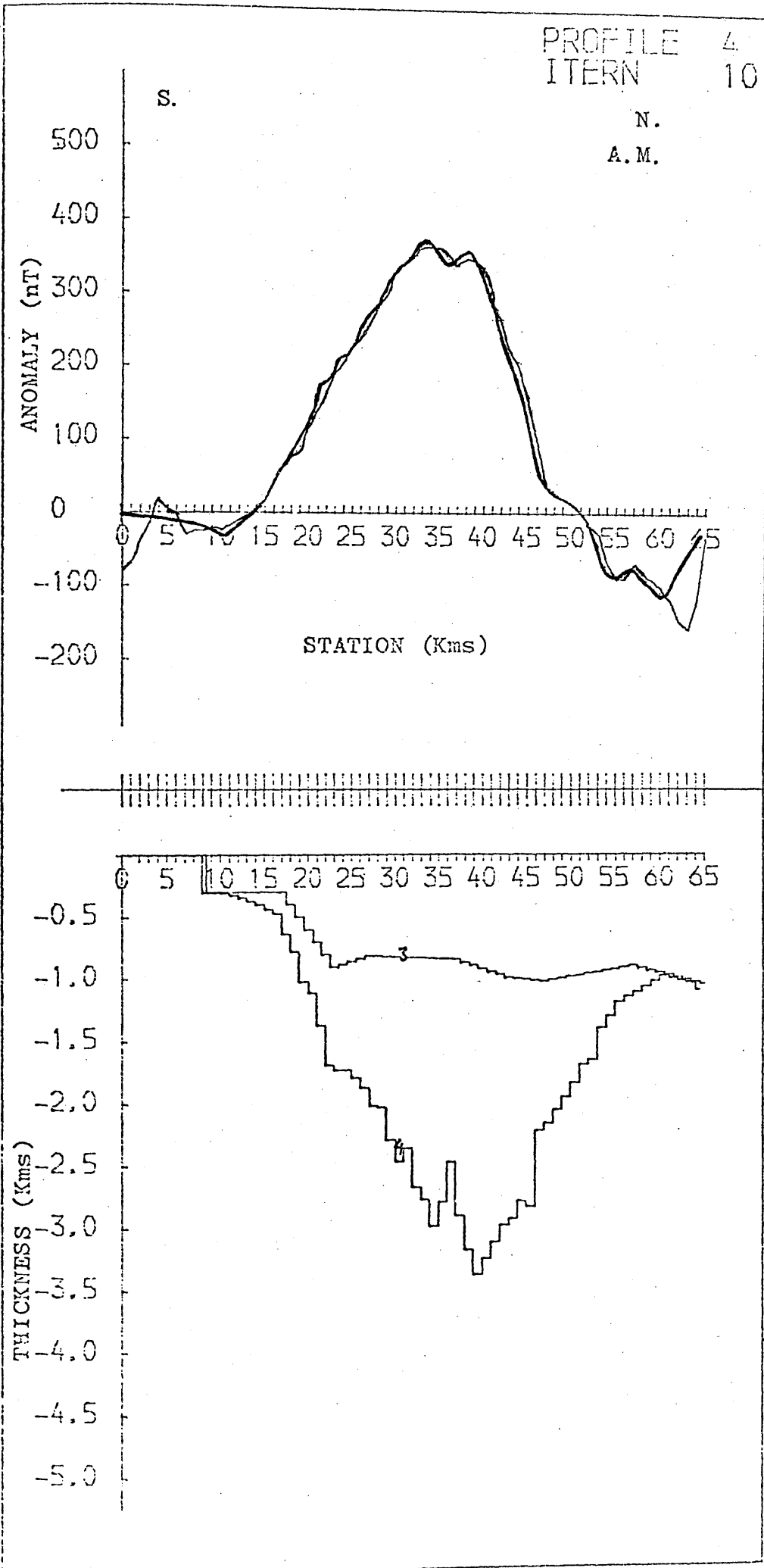


Fig. 17

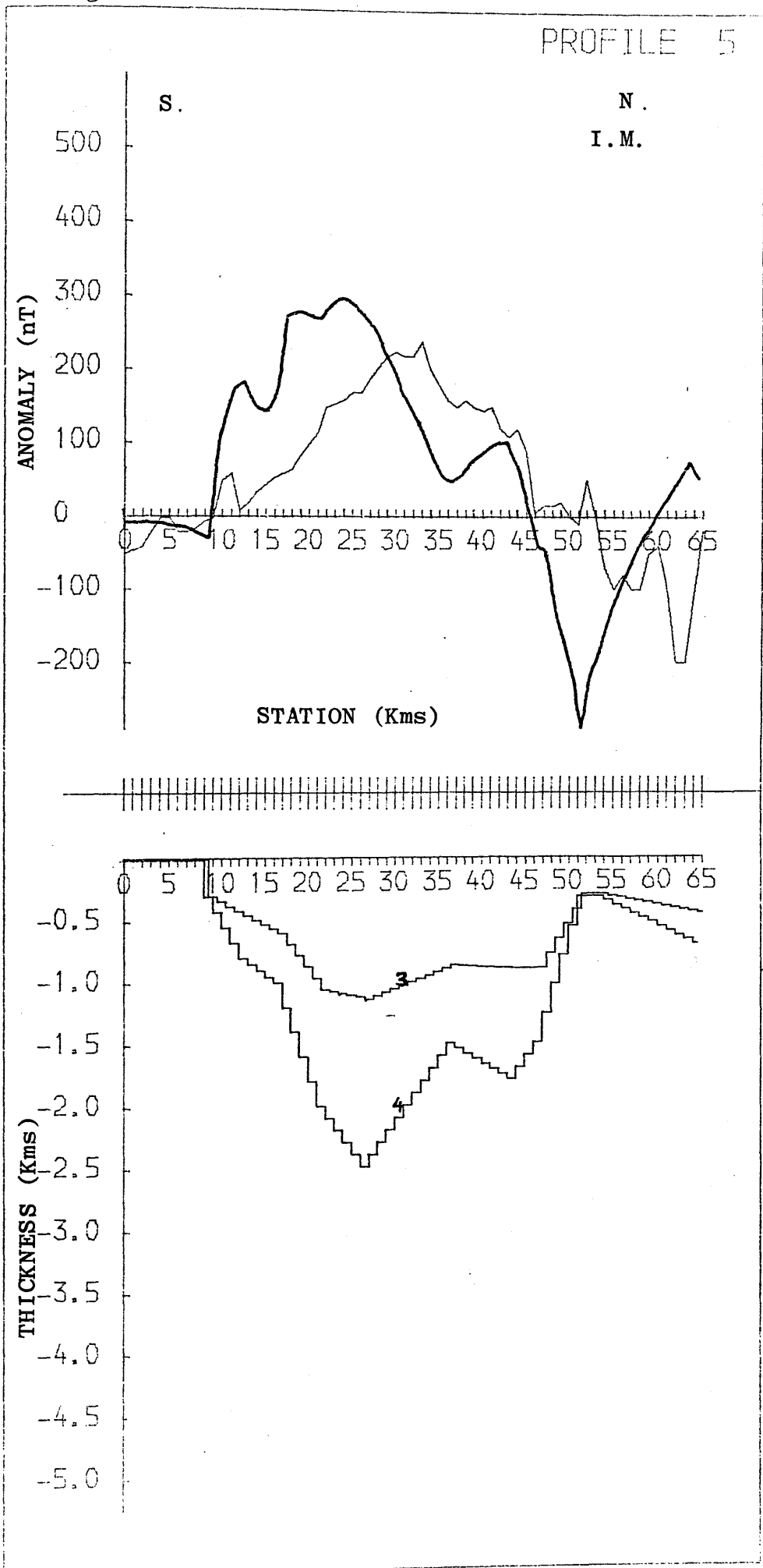
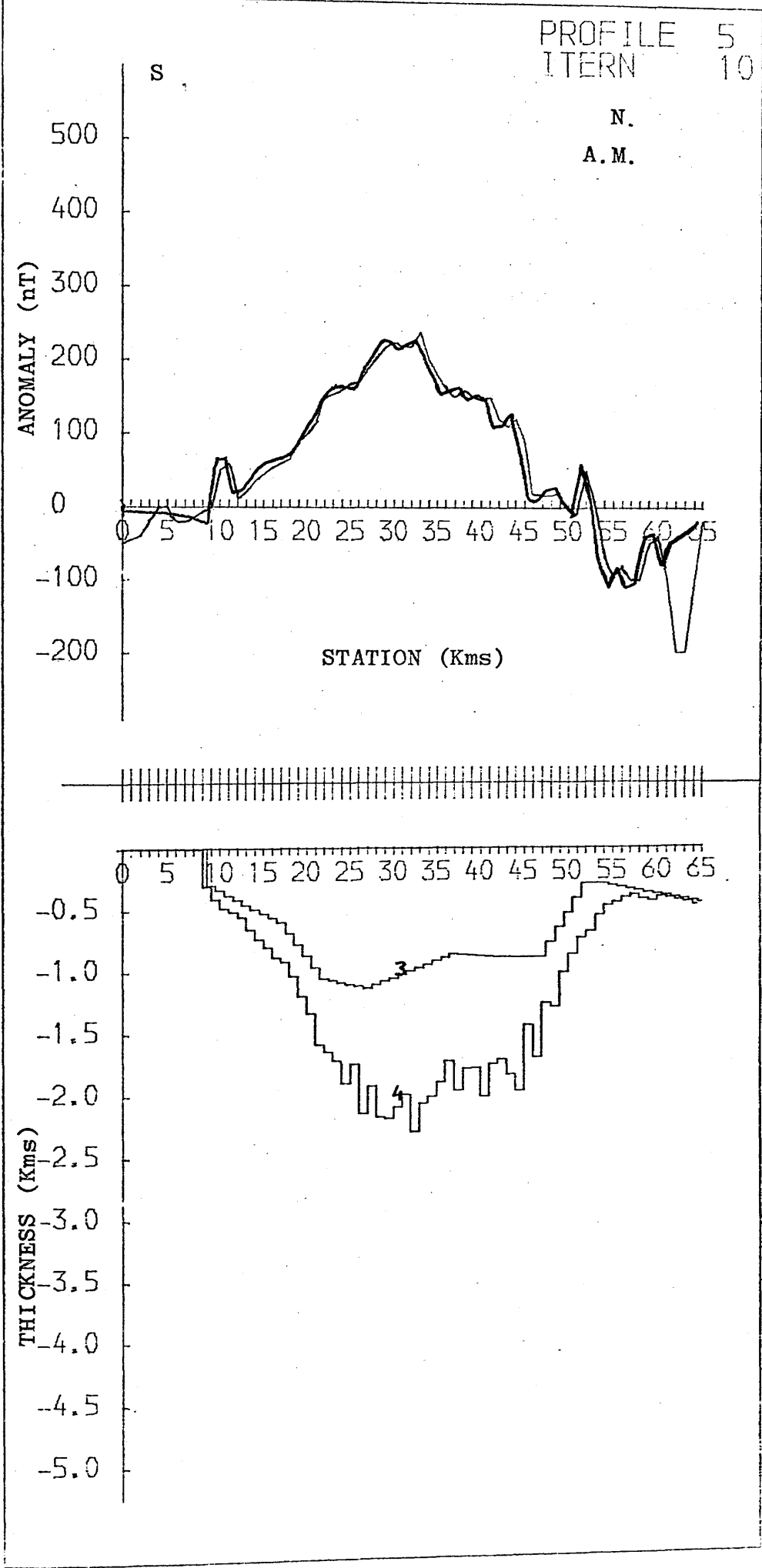


Fig. 17a



thickness of Carboniferous lavas. The excess thickness of the model in the centre bears out the qualitative suggestion that the main source of the anomaly could be an intrusion. An East-West model was also calculated with essentially the same conclusion, that is, maximum model thickness is of the order of 4-5 Km under the peak of the anomaly. Since both the anomaly and the model parameters defined by the known elements of the geology are better described in North-South strips the detailed results, having little significance, are not included in the thesis.

6.1.2 Pseudo gravity

In a second pass of the program, in which the depth to the model was reduced by the flying height (0.3 Km) its gravity effect was calculated. These results, are shown as a contours (fig. 18), scaled for a density contrast of $+ 0.11 \text{ g/cm}^3$, that is, an igneous body density of $2.63 + 0.11 = 2.74 \text{ g/cm}^3$ (density contrast of Waterhead model is more see table 4), appropriate for basalt lavas and intrusive rock of similar composition. The significance of the pseudo-gravity is discussed further, under section 6.3 p. 92.

6.2 MODEL 2 (attributing the whole of magnetic anomaly to an intrusion)

6.2.1 Magnetic

6.2.1.(1) Anomaly and profiles:

The same five north and south profiles were used as a starting point to describe the observed aeromagnetic anomaly. Since the deeper model is a separate entity from the/

the Carboniferous lavas and hypabassal intrusions, their contribution of the lavas and sills to the anomaly should first be removed. This contribution cannot however, be estimated without specifying, independently of the magnetic anomaly, the depth distribution of these rocks. If it is assumed that the main body of lavas under the Bathgate high is relatively uniform, in depth and thickness then they will not produce local anomaly of the same wavelength. Although questionable on geological grounds, it defines a limiting case of some interest. There are, however, short wavelength anomaly features associated with sills and minor lava outcrop close to the main anomaly. The contributions of these localised sources is fairly clear, on detailed East-West profiles across the Bathgate Hills where sills and lavas have north-south outcrop, (Fig. 19) with reference to a smooth but varying base level judged to represent the main anomalies the local features have amplitudes up to 100 nT over distances of 2 Km. On five such profiles the residuals (local anomalies) defined in this way were fitted to inclined tabular models consistent with the geology. For such models (width nearly 2 Km, depth 0.3 Km) the anomaly amplitude is reduced to 10 or 20% at a height of 2 Km, that is, about 7 times the flying height. Generalising from this estimate, it was concluded that upward continuation applied to the north-south profiles would remove from them most of the effects attributable to shallow sources. This operation was carried out by using Model 1. Thus the observed profiles are closely duplicated by the calculated

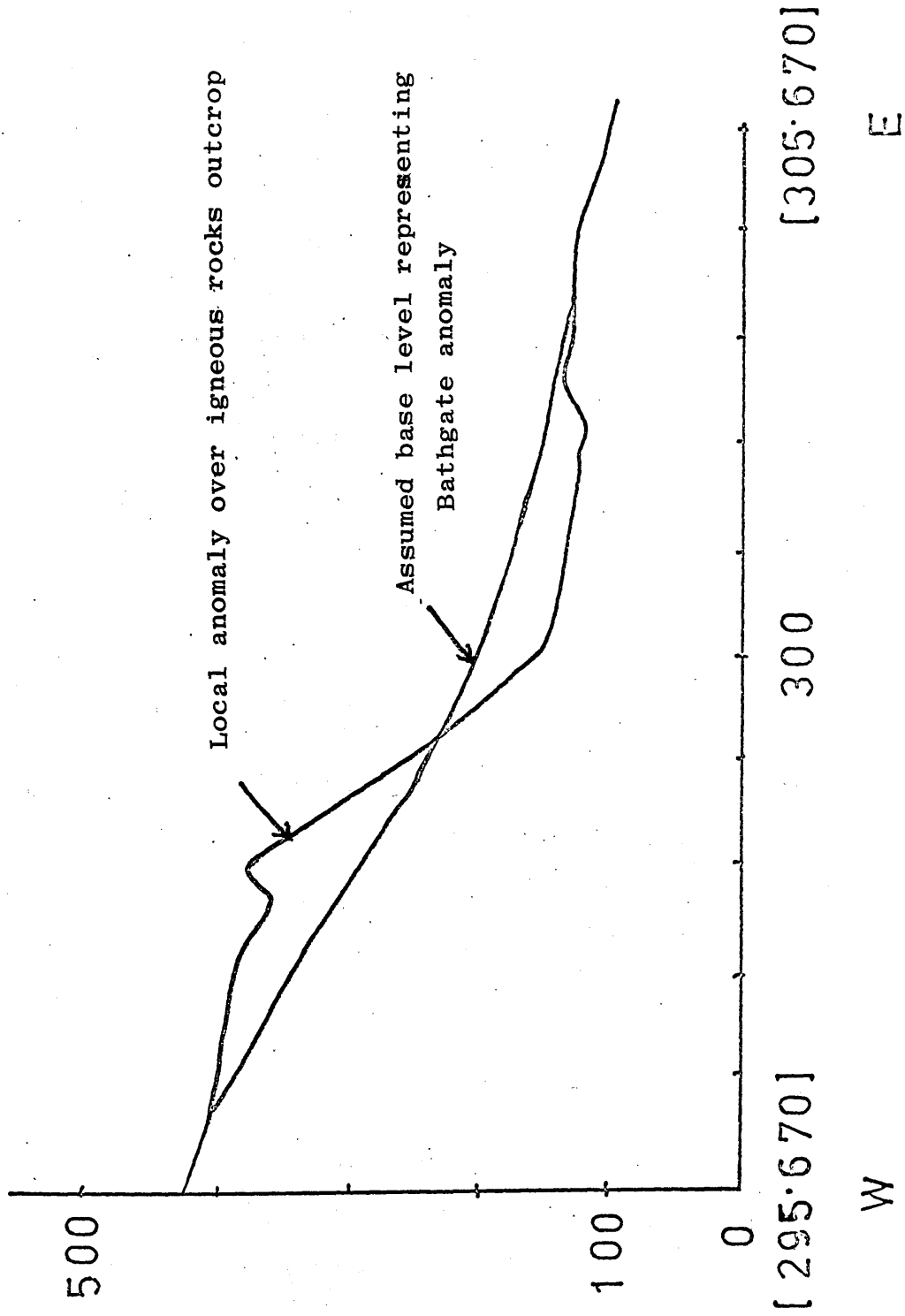


Fig. 19 East-West profile [295.670] to [305.670] across the Bathgate Hills where sills and lavas have North-South dipping and assumed base level (main Bathgate anomaly) represented by smooth curve.

anomaly for Model 1. Recalculation of the anomaly for this model at a depth increased by 2.0 Km provided the smoothed (upward continued) anomalies Figs. (20-24) taken to represent the effect of Model 2.

6.2.1.2 Body Specifications

Gunn (1975) found an inductively magnetised prismatic body, with its top surface at 9.9 Km, base at 23 Km and north-south width 10 Km, gave a calculated anomaly which was a least square best fit (from a range of prisms) to the observed median profile [290.600] to [290.700]. Neither the east-west dimension of the prism nor its polarisation contrast were specified in his paper.

By trial and error adjustment a model in the same depth range represented within a single north-south strip (Fig. 25) was found to give a close fit to the observed median profile (3) and a reasonable fit on the flanking profiles.

6.2.1.3 Results and Conclusions

The results of the calculation are shown in Figs. 26-30. From the initial attempt adjustments were made to (1) strip width, (2) depth to the base and (3) north-south extent of the model. The top surface of the model was taken to be variable whereas base had a constant depth (datum 2.3 Km above ground). None of these dimensions provides a basis for judging whether the model is geologically reasonable or not. A polarisation contrast 1015×10^{-5} cgs (or about 10^{-2} cgs) i.e. more than three times that used for calculation in Model 1 and that implied by/

Figs. 20-24

Show observed magnetic anomalies and anomalies recalculated from model 1 at a depth increased by 2.0 Km (upward continued) along five N-S profiles.

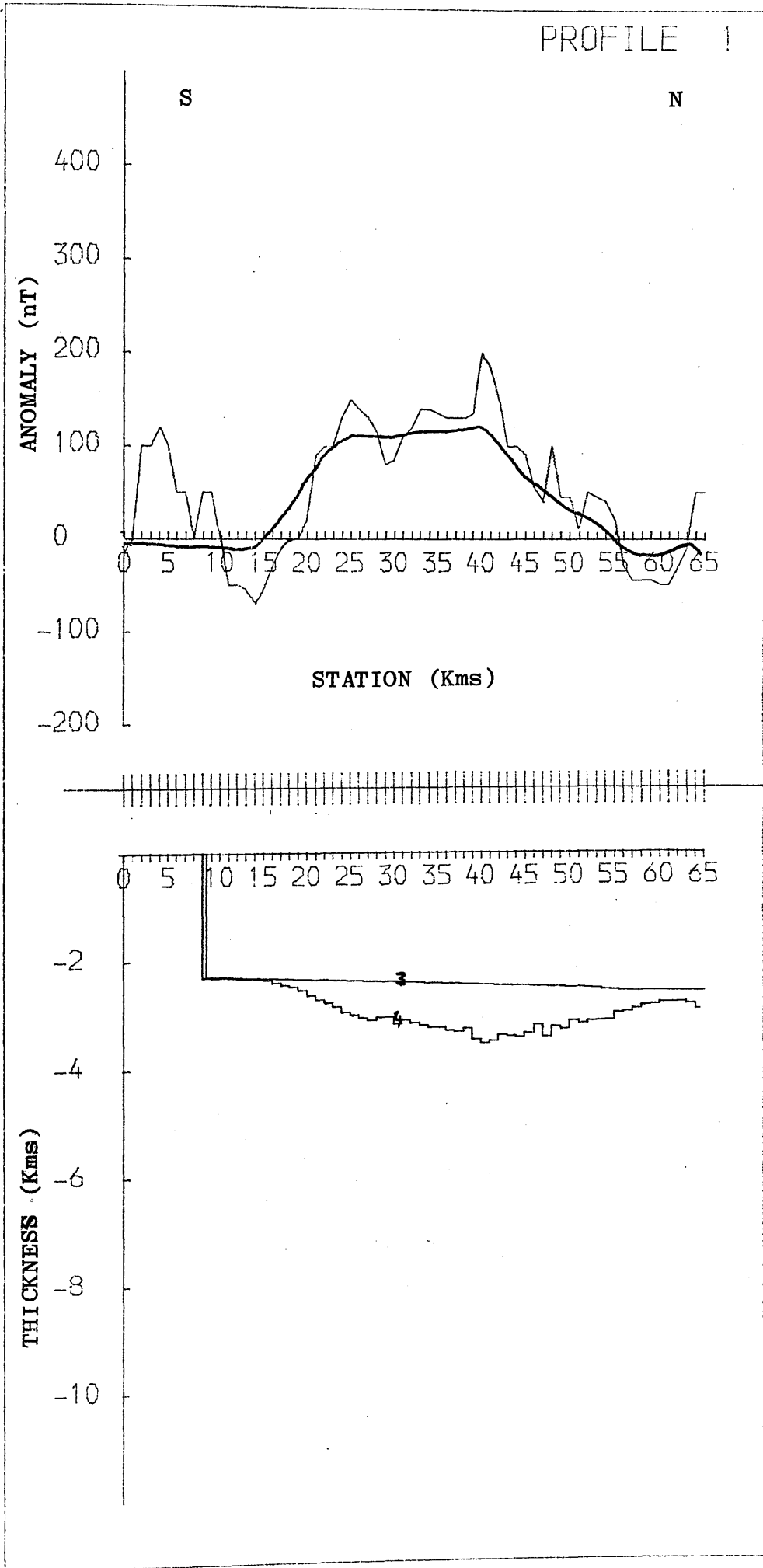
Thin line - Observed magnetic anomaly

Thick line - Anomaly recalculated from model 1 at a depth increased by 2.0 Km.

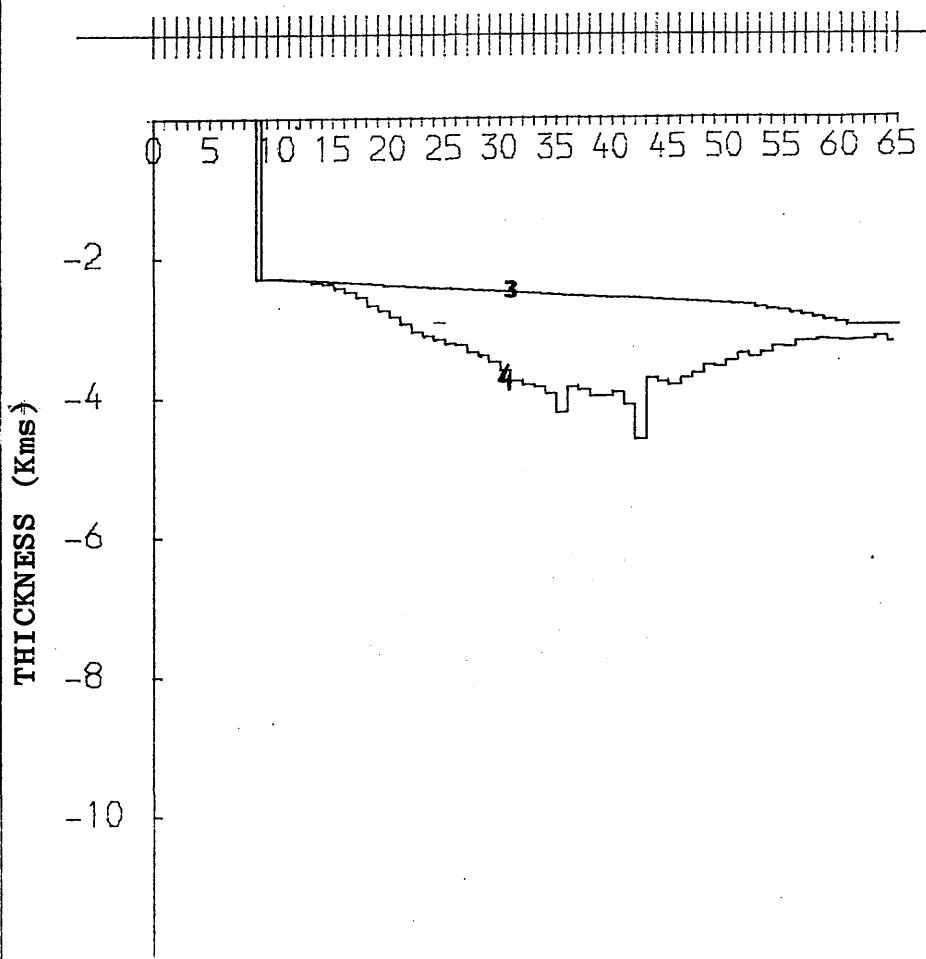
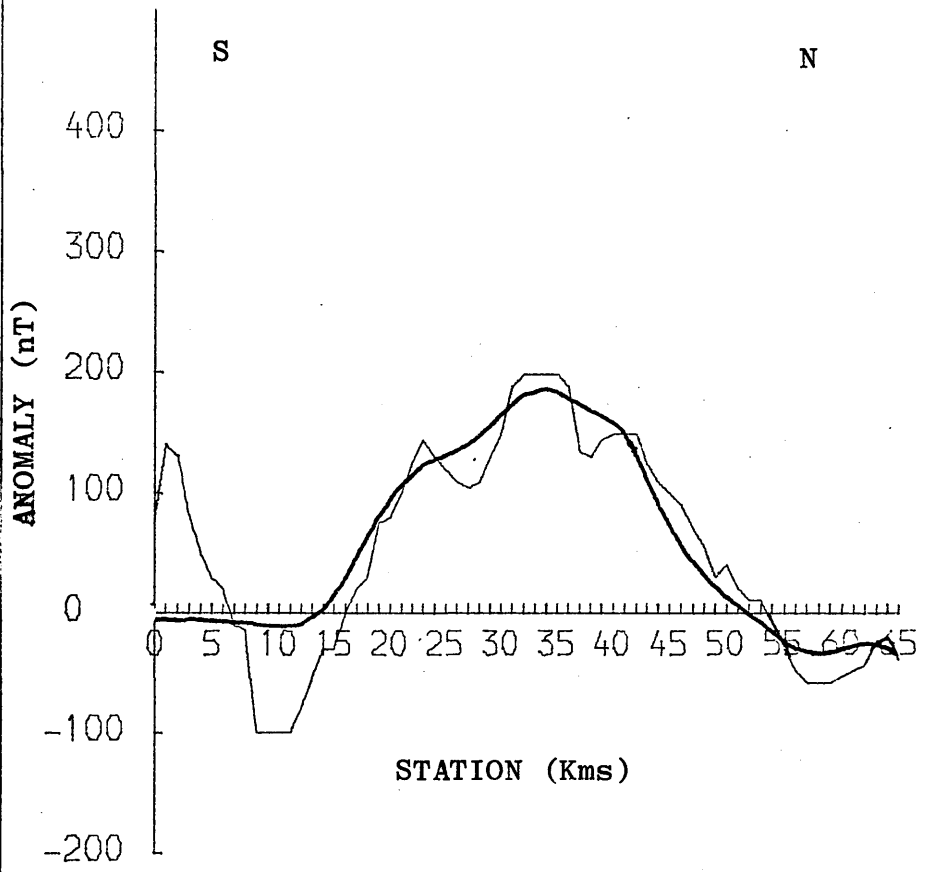
3 - depth to top of model

4 - depth to base of model

Fig. 20



PROFILE 2



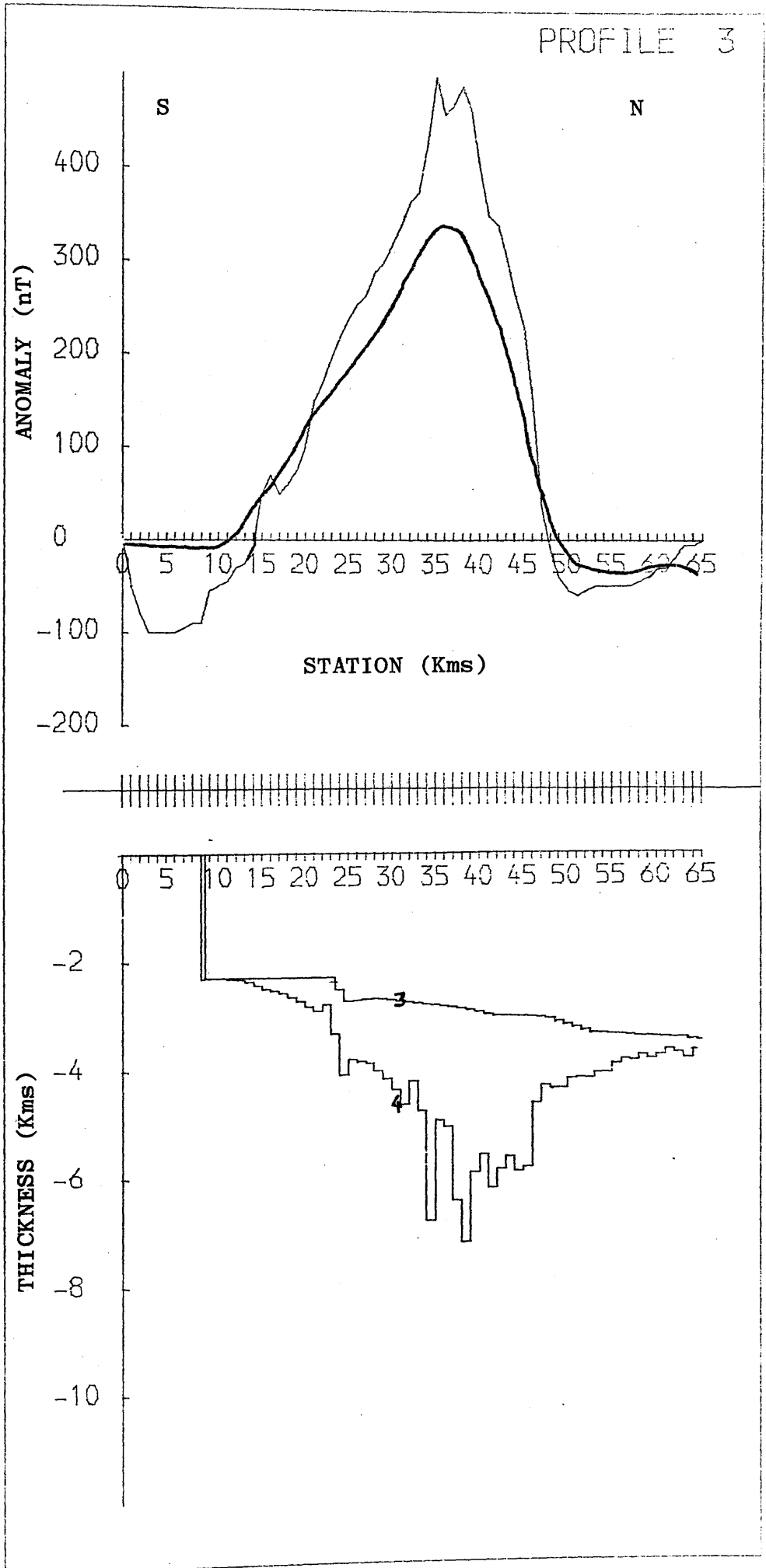
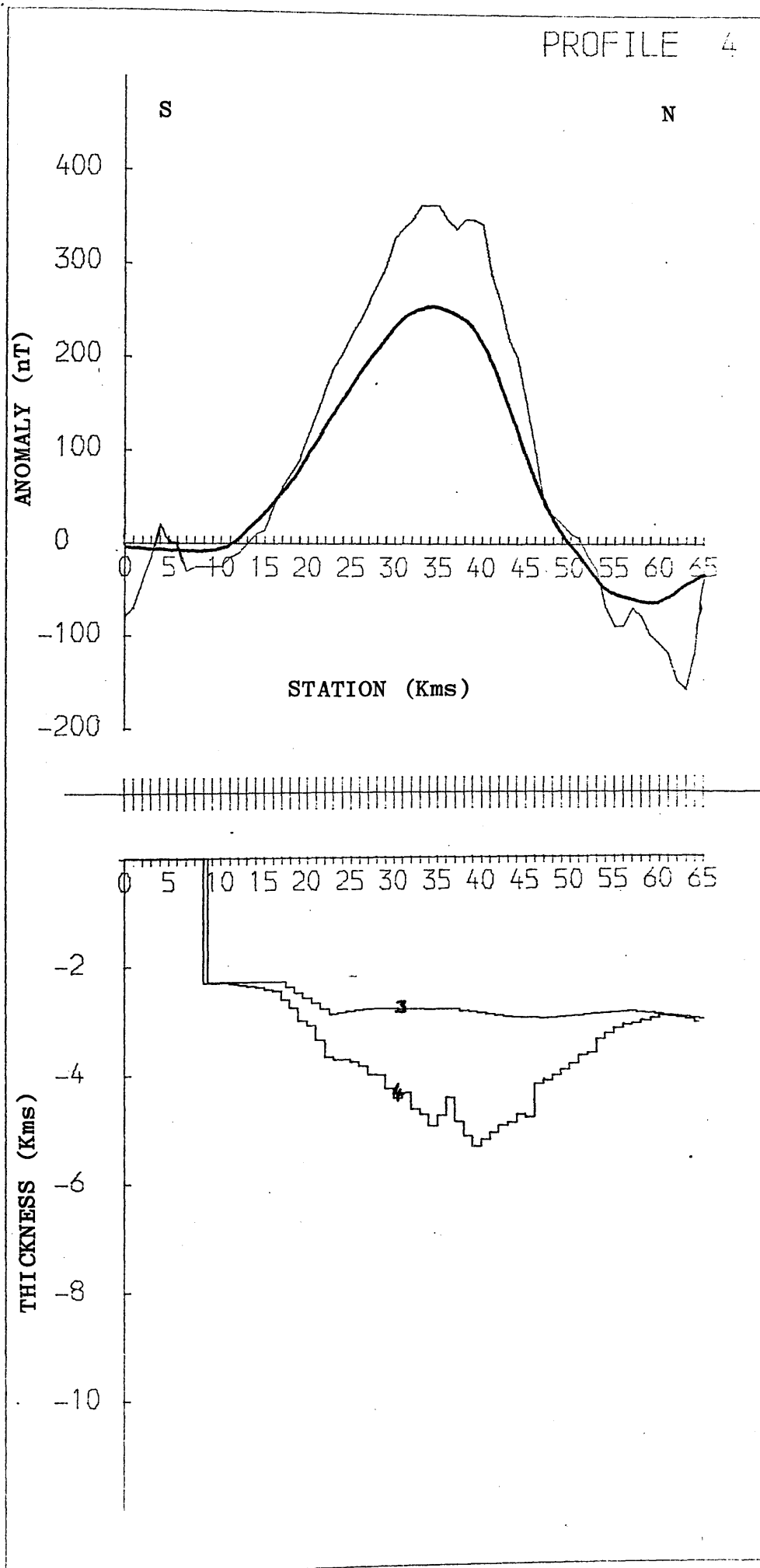


Fig. 23



PROFILE 5

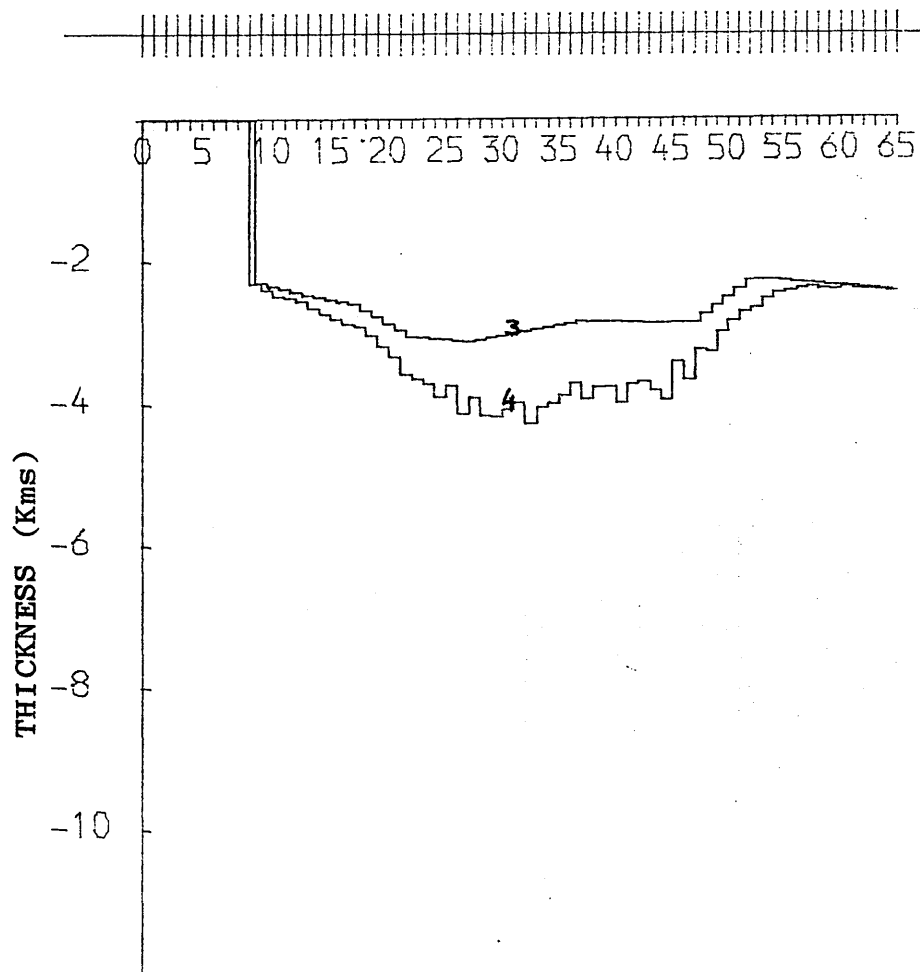
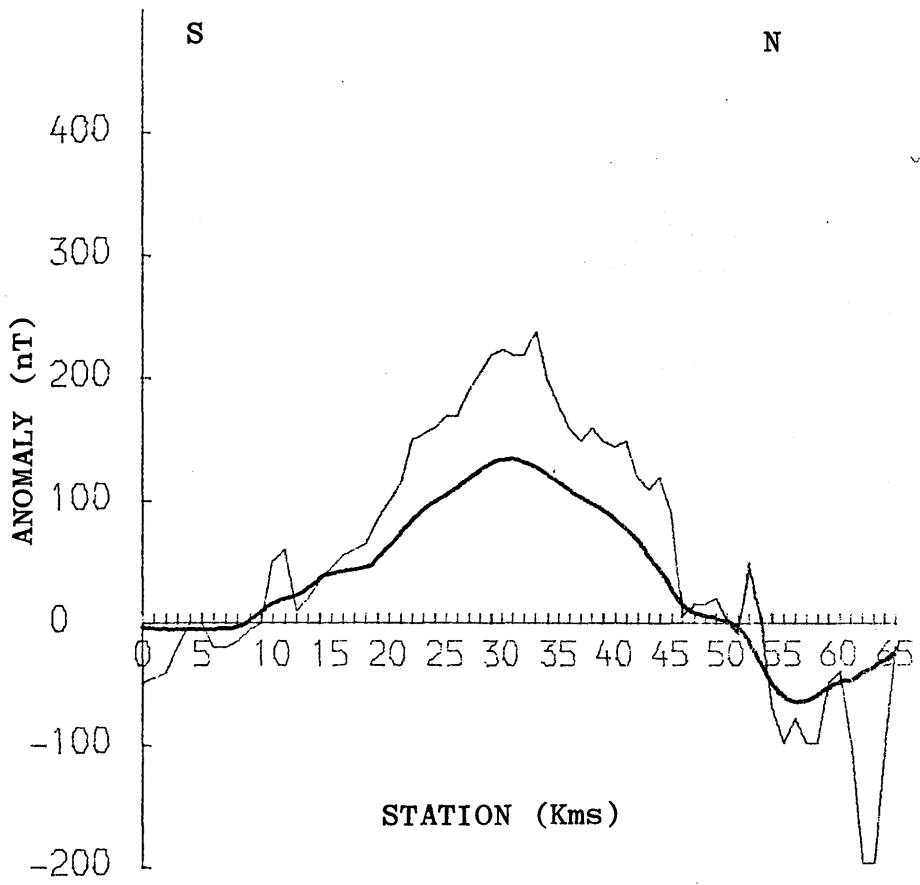
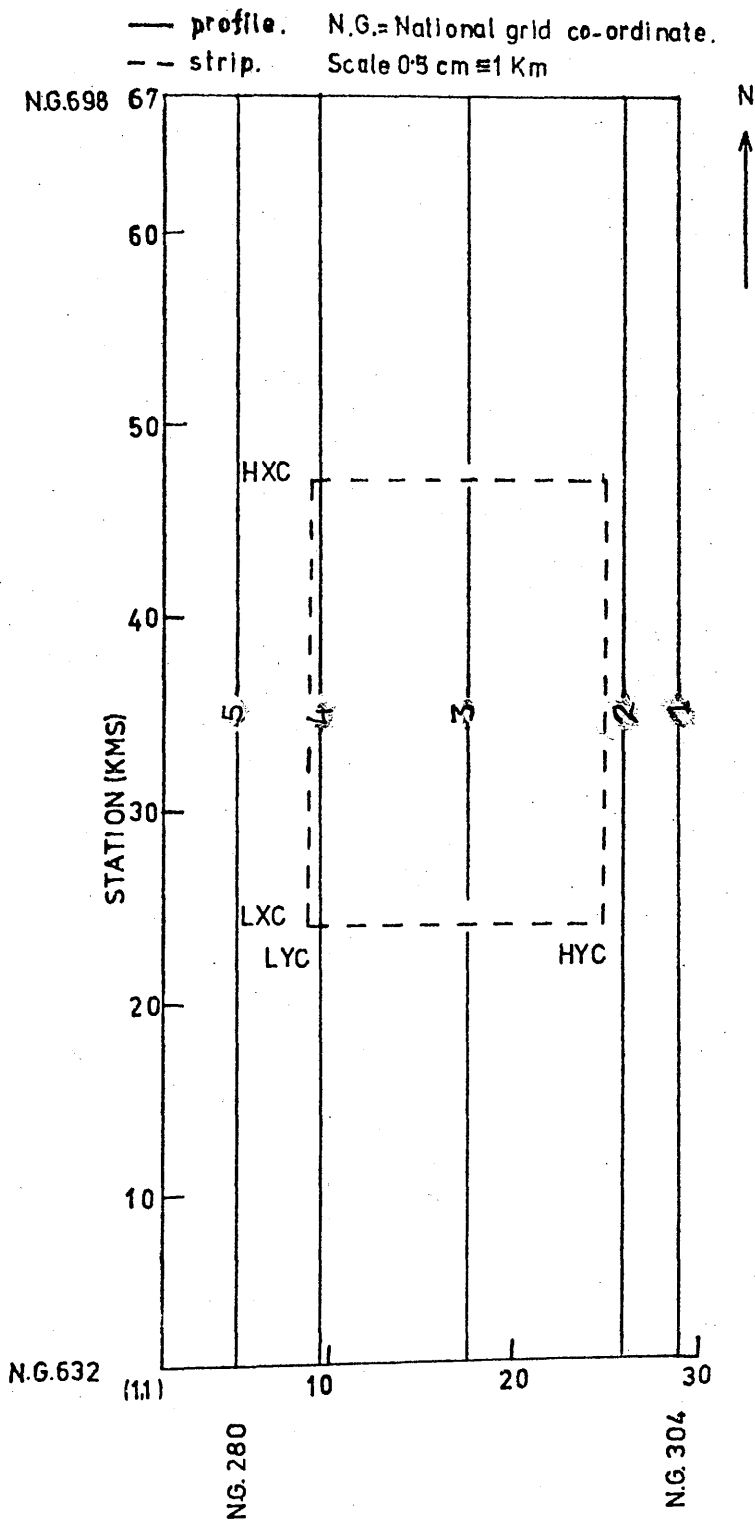


Fig.25 Location of strip dimension and profile with respect to National grid for Model2.

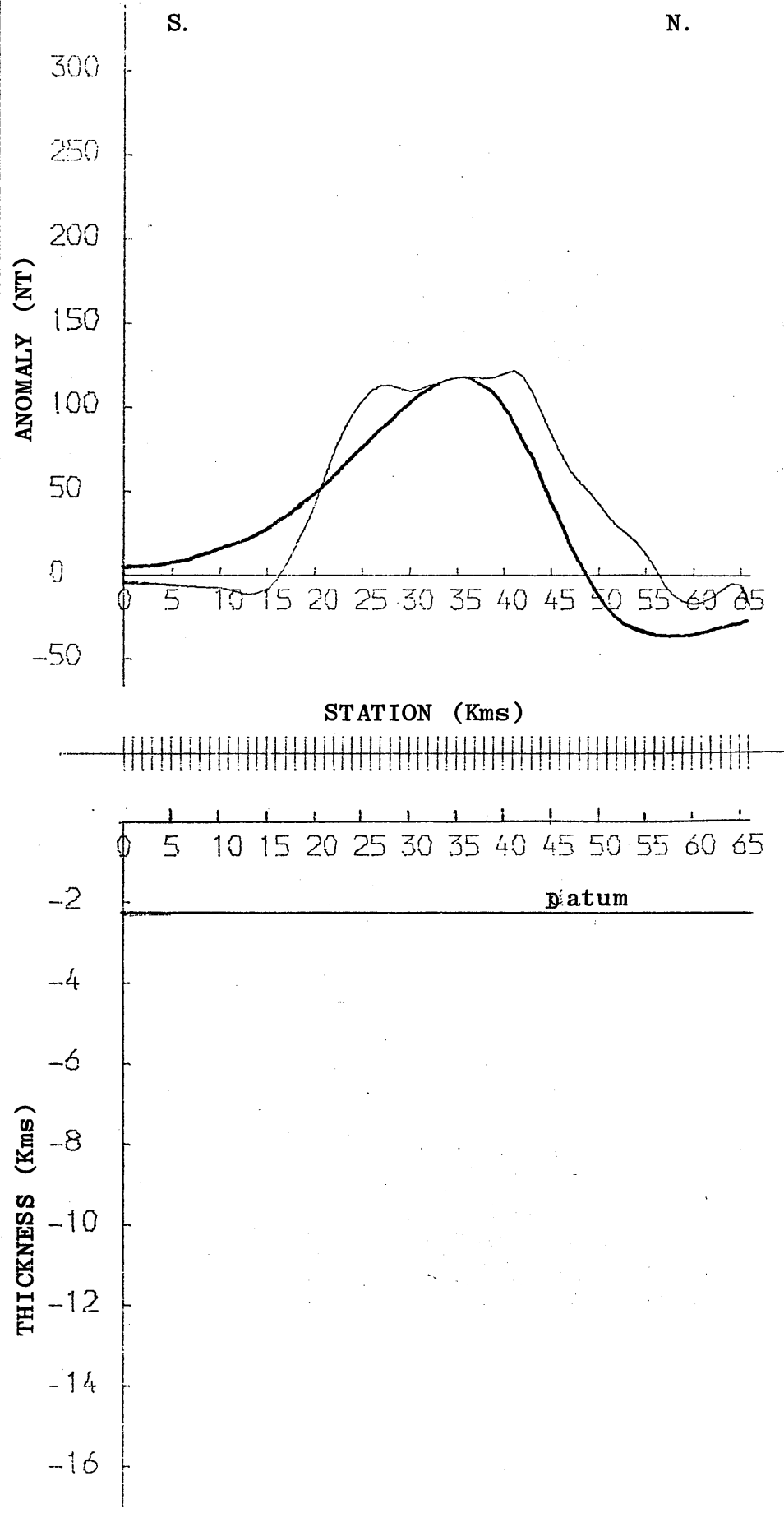


Figs. 26-30

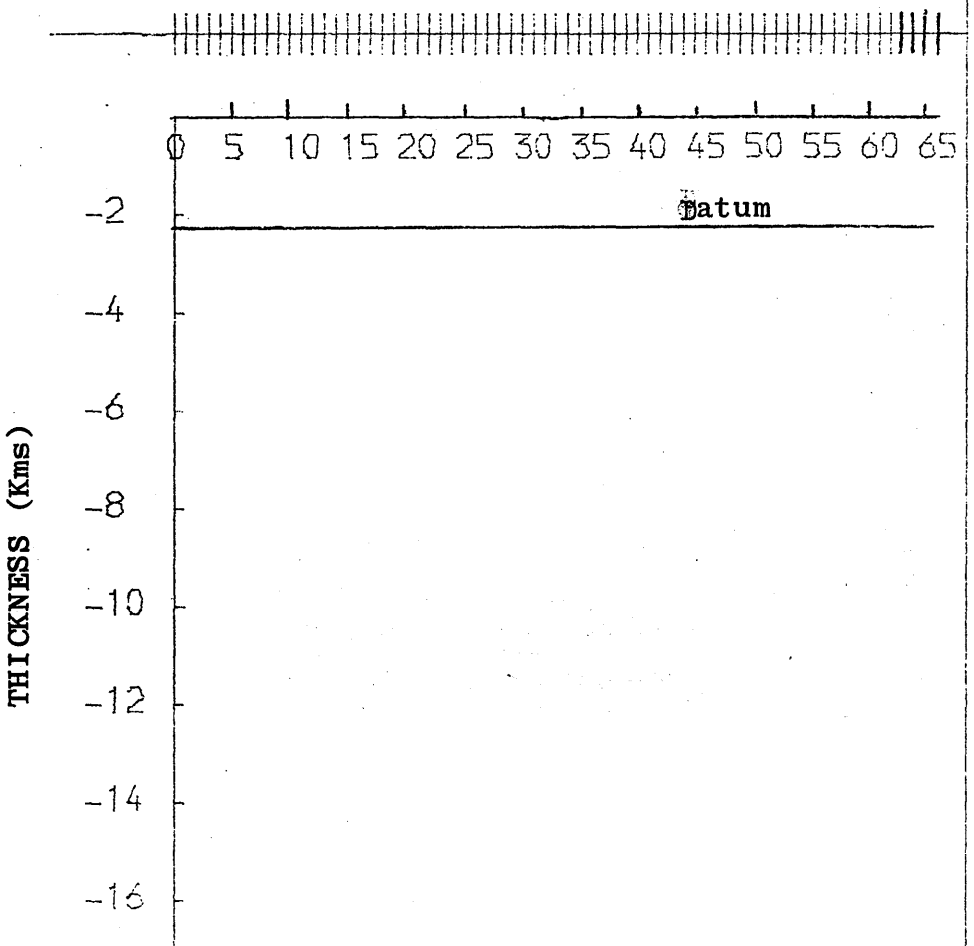
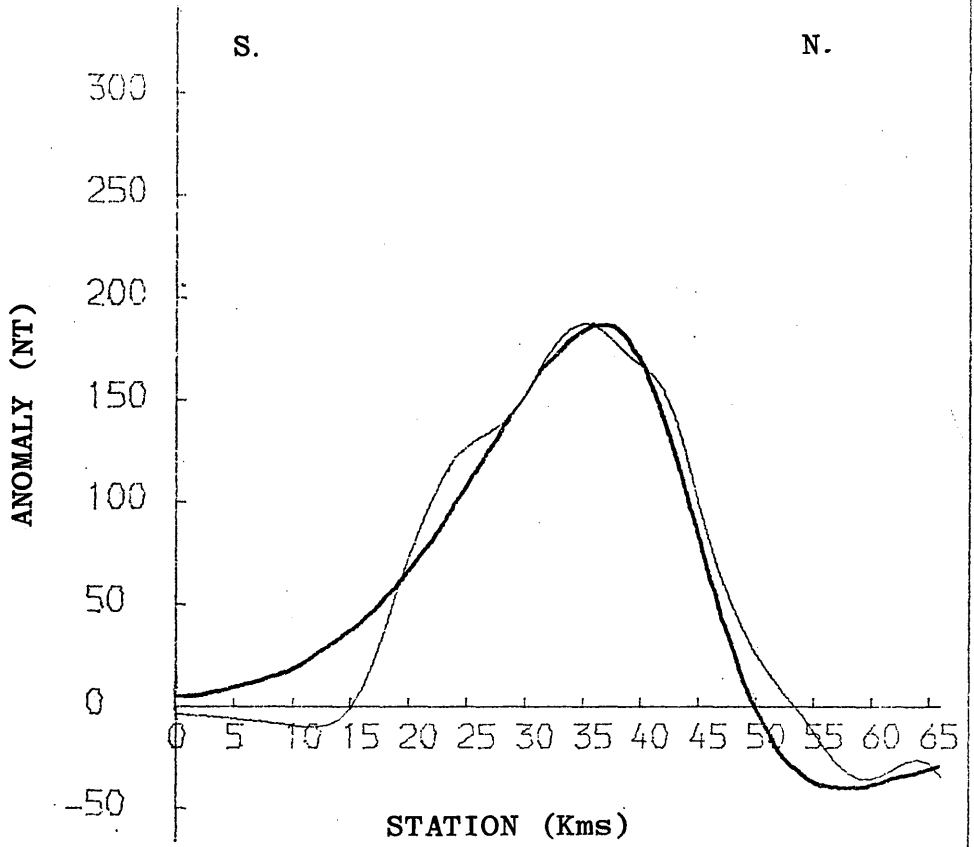
Show observed magnetic anomalies smoothed by upward continuation (i.e. recalculated from Model 1 at a depth increased by 2.0 Km) against anomalies calculated along five north-south profiles and thickness of the Model 2 under profiles 3 and 4.

Thin line - smoothed observed magnetic anomaly
Thick line - calculated magnetic anomaly
3 - Depth to the top of model
4 - Depth to the bottom of model

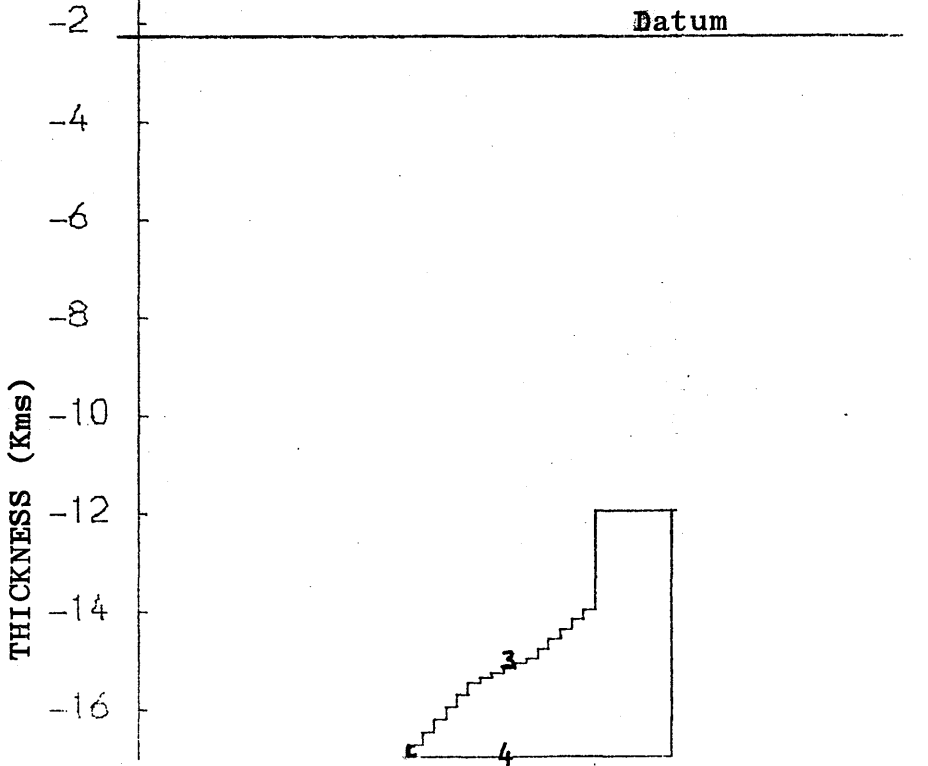
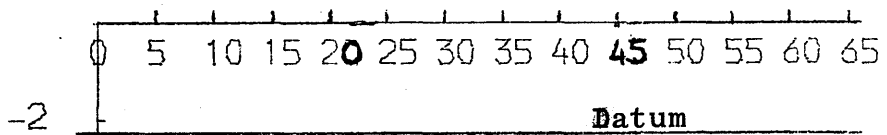
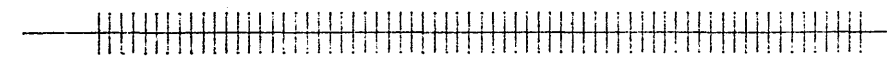
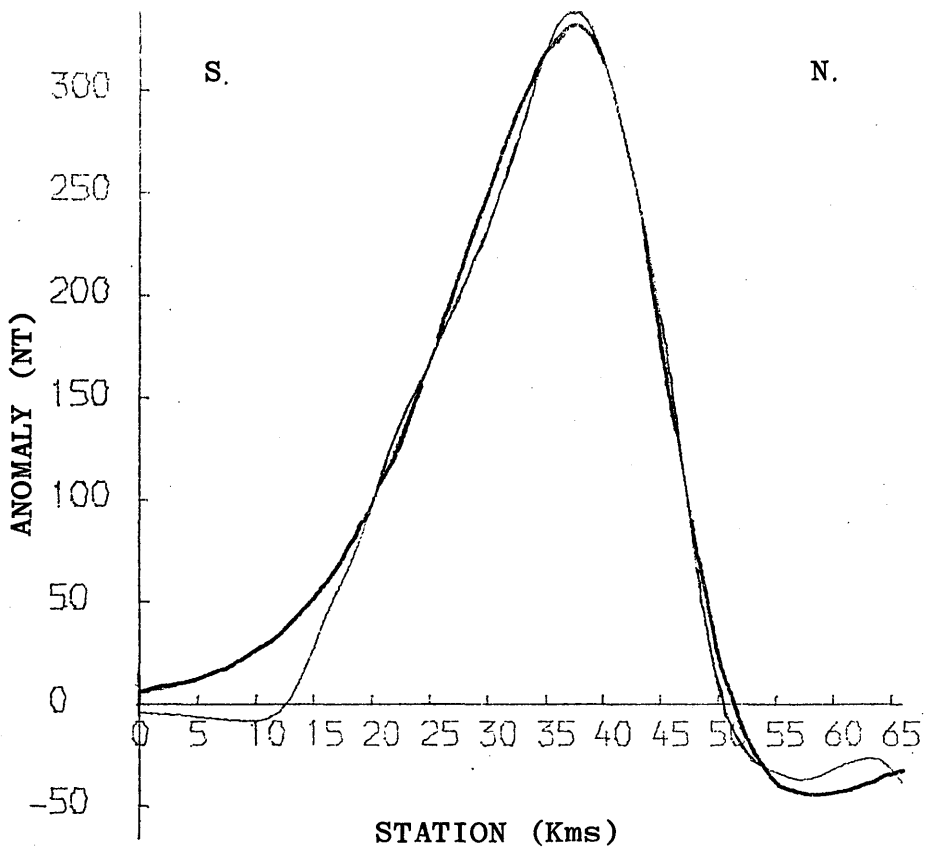
PROFILE 1



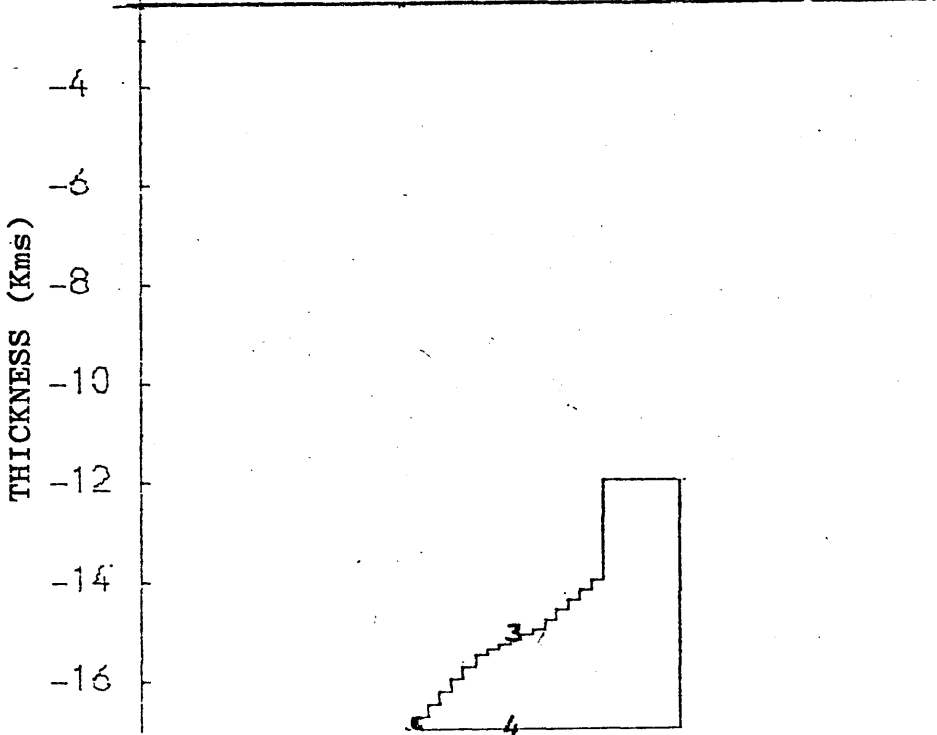
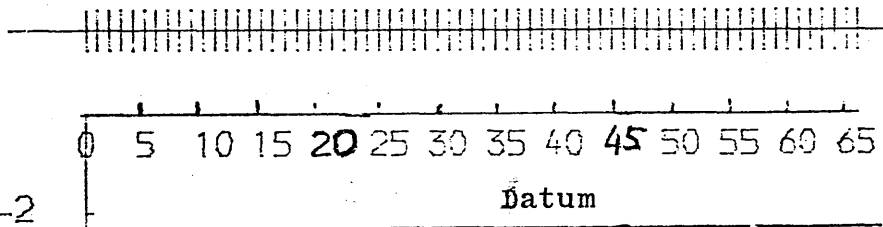
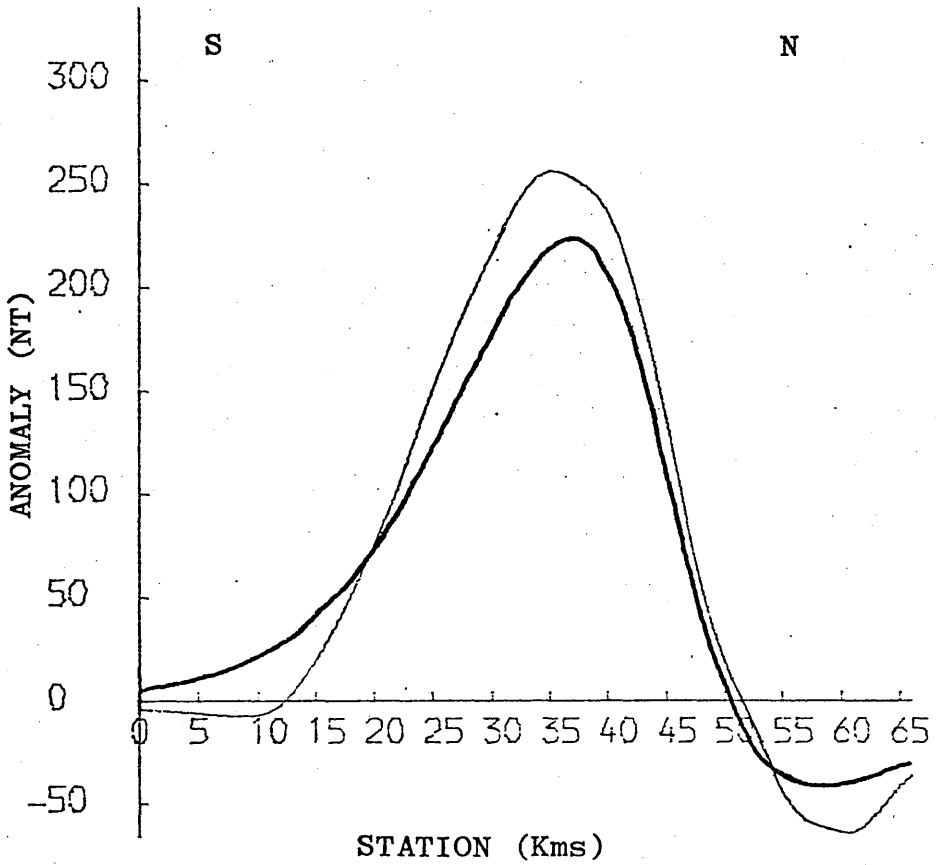
PROFILE 2



PROFILE 3



PROFILE 4



by the susceptibilities of basic intrusions as the outcrop is required to get the optimum fit. However Model 2 is not related to these rocks and a susceptibility of 2×10^{-2} c.g.s. is far from a geological impossibility. The susceptibility of rocks varies with their magnetic contents and according to Balsley and Buddington (1958) a susceptibility of rocks of 2×10^{-2} c.g.s. corresponds to a magnetite content of about 5% i.e. within the range found in basic and ultra-basic rocks.

6.2.2 Pseudo gravity

Since the magnetic anomaly, apart from minor smoothing, is unchanged, so too is the shape of the pseudogravity anomaly derived from it. For the same pseudogravity amplitude as for Model 1, however, a contrast of about $+ 0.45 \text{ g/cm}^3$ is required. If the mean background density of rocks at this depth is no less than 2.8 g/cm^3 then the minimum density of the anomalous body would be 3.25 g/cm^3 - an ultrabasic rock. So far no reason applicable to Model 2 has been given for preferring a solution which takes the pseudo-gravity amplitude to be 10 mgal and a contrast of $+ 0.45 \text{ g/cm}^3$ rather than something less. Such a reason is set out in the following section.

6.3 COMPONENTS OF THE BOUGUER FIELD CORRECTED FOR THE EFFECTS OF SUPRA HURLET SEDIMENTS (Map 4)

Fig. 31 illustrates the similarity along a NNW line between the modified Bouguer anomaly (from Map 4) on the one hand and the sum of the pseudo-gravity anomaly (Model

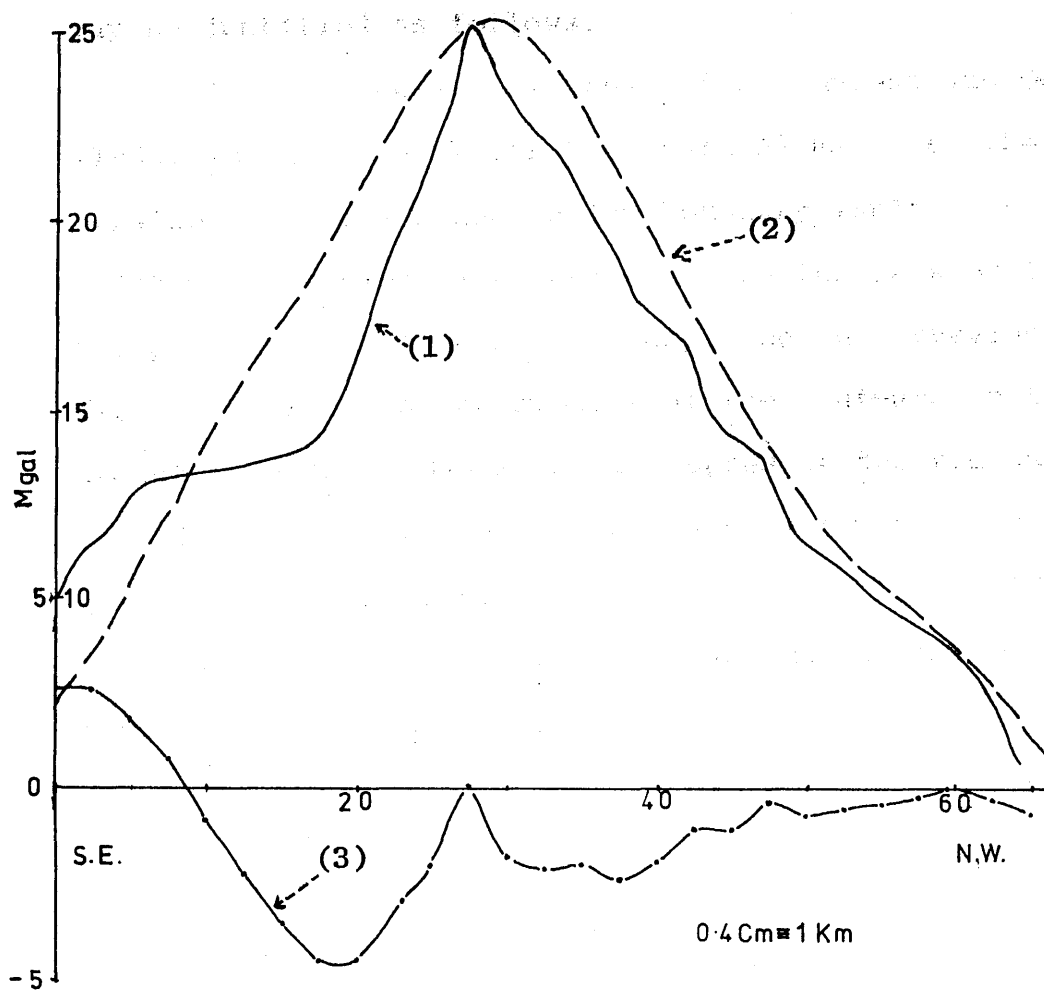


Fig. 31 Shows observed Bouguer anomaly corrected for the effects of Carboniferous sediments-(1), addition of Regional anomaly and calculated pseudogravity anomaly (from magnetic anomaly)-(2) and the residual between (1) and (2) along S.E.-N.W. orientations. - (3)

1 or 2), through its peak, and the regional anomaly projected from Ayrshire/Renfrewshire (Regional A) on the other. In making this comparison the adjustable parameters are (1) the direction of projection of the Regional A, (2) the base level of the Regional A and (3) amplitude of the pseudo-gravity.

The values of these parameters embodied in fig. 31 may be justified as follows.

(1) The direction of projection - McLean and Qureshi (1966) implied that their Regional (A) had a strike parallel to the Midland Valley boundary faults; a direction which would project its peak close to the peak of the Bathgate high. It has been suggested in a previous section (see Qualitative discussion) that the contours in the NW and SE corners of Map 1 (or 4) represent the regional A. Considering only the SE where there is no ORS effect, a gradient of about 1 mgal/Km is seen where the field has a mean value of 9 mgal. From McLean and Qureshi's (1966) equation for Regional A i.e.

$$\ast \quad \Delta g = 30.8 - 0.0135 x^2$$

where x is the offset in Km N40W or S40E from the peak; the gravity gradient is given by

$$\partial (\Delta g)/dx = 0.027 x,$$

so that the SE corner of Maps 1 and 4 should lie at $x = 1/0.027 = 37$ Km from the peak of regional A. As this is the (same as the) offset from the Bathgate high peak it tends to confirm the qualitative suggestion made above. The precise direction of projection in Fig. 31 which minimises residuals is 80° rather than 90° to N40W.

(2) For this offset the absolute value of Regional A in the SE corners of Map 1 and 4 should be

$$\Delta g = 30.8 - 0.0135 \times 37 = 25.8 \text{ mgal}$$

i.e. about 15 mgal greater than observed. Perhaps another regional component (B) at right angles to A, accounts for the base-level shift of this amount applied in Fig. 31.

(3) The amplitude of the pseudo-gravity component (10 mgal) is thus that which when added to the Regional A, peaking at 15 mgal best matches the modified Bouguer anomaly.

It is concluded that the sum of these components (Pseudo-gravity + Regional A + a constant (Regional B?)) is sufficiently similar to the modified Bouguer anomaly along the line of Fig. 31 to justify the choice of the parameters values.

Building on this conclusion it follows that (1) the rock types in Model 1 involve an appropriate density contrast i.e. + 0.11 g/cm³ giving a pseudo-gravity amplitude of 10 mgal.

(2) the density contrast for Model 2 which gives same amplitude of pseudo-gravity for Model 2 is + 0.45 g/cm³ is near the upper limit of geological probability and would be indicative of an ultra-basic body.

(3) Since both Models 1 and 2 are geophysically similar and both are geologically possible there is no firm basis for preferring one against the other.

(4) Negative residuals (about 5 mgal) SE of the Bathgate high (Fig. 31) may be attributed to the effect of Oil Shales in a Carboniferous basin not included in

* There is an error in the coefficients of the equations on p.94

They should read

$$\Delta g = 30.8 - 0.0083x$$

$$\text{and } \partial(\Delta g)/\partial x = 0.016x$$

This invalidates the comparisons made between the field values and gradients in the SE corner of Maps 1 and 4 with the Ayrshire parabolic regional

The following revised considerations are made bearing on the regional and local components of the modified Bouguer anomaly illustrated in Fig. 31 (Curve 1):

1. The Ayrshire data suggest that the regional near the Midland Valley axis has a low gradient (0.1 mgal/km for the first 10 kms). It is assumed, therefore, to have a negligible effect on the slope of the local anomalies in this region which are observed to have gradients over 1 mgal/km. On this basis the psuedo-gravity anomaly is scales, as in Fig. 18, to give the observed gradients near the axis. The psuedo-gravity commonly then has an amplitude of 10 mgals thus setting its base-level at +15 mgals to match the peak observed field value of +25 mgals.

2. This base-level (+15 mgals) (relative to field values in Ayrshire and the Southern Uplands) can be explained in terms of two factors.

- (a) In Ayrshire the regional correction for the O.R.S. is about 7 or 8 mgals near the Midland Valley axis.
- (b) In a ENE direction El-Batroukh estimates a regional component which would give a 6 mgal fall between the Ayrshire profile and Bathgate. (This gradient is in accord with the field values in the SE corner of Maps 1 and 4.)

It follows that if the O.R.S. is similar at Bathgate to Ayrshire, then a 15 mgal base-level for the local psuedo-gravity effect is explicable.

Maps 2 and 3 (1.5 Km at 0.1 g/cm^3 gives about 6 mgal effect).

(5) Other significant residuals may be expected off the line of fig. 31 e.g. over the Clackmannan and Lanarks coalfield basins. Their precise estimation is dependent upon defining Regional B elsewhere than the line of fig. 31. (= - 15 mgals) and the parallel line in Ayrshire/Renfrewshire (McLean and Qureshi's fig. 2, p.275 1966) (= 0 mgals). El-Batroukh (1975) in considering the Western Southern Uplands proposed a regional component in this direction (North-East) which, when projected, gives a difference of -8 mgal i.e. about half that required. It is therefore possible that the -15 mgal base level shift includes a more local gravity component. This and the residuals over the coalfield basins, mentioned above could be considered as the effect of concealed basins of Lower Old Red Sandstone sediments. Time has not been available to follow this proposition further.

CHAPTER 7CONCLUSIONS

1. The shallowest source which is geologically likely (Model 1) for the Bathgate gravity and magnetic anomalies is immediately under the Carboniferous Limestone Series and is about 4.5 Km thick, if its physical properties compare with Carboniferous basalts.

2. As this thickness is five times that deduced anywhere else for these lavas, the model is considered to represent an inverted cone-shaped basic intrusion in continuity with their base.

3. On a NNW profile across the peak gravity anomaly the observed field is essentially reproduced by the sum of

- (i) Carboniferous sedimentary basin effect (up to 4 mgal).
- (ii) Pseudo-gravity effect calculated from the magnetic anomaly and scaled to 10 mgals amplitude.
- (iii) the parabola shaped regional projected parallel to the Midland Valley boundary faults from Ayr/ Renfrewshire ($\Delta g_x = 30.8 - 0.0135 x^2$).
- (iv) A constant of -15 mgal which may be due to a NE regional gradient and/or a component of an O.R.S. basin effect.

4. The pseudo-gravity amplitude corresponds to a density contrast appropriate to a basic intrusion (Model 1).

A deeper body (≈ 10 Km, Model 2) possibly an intrusion into crystalline rocks of the Lower Crust is an

alternative source (cf Gunn 1975). In this case the 10 mgal pseudo-gravity amplitude requires a density contrast of $+ 0.45 \text{ g/cm}^3$ approaching the limit of geological credibility and indicative of an ultra-basic composition.

REFERENCES

- AFFLECK, J. (1958) Interrelationship between magnetic anomaly components: *Geophysics* ,23 pp.738-748.
- ALLAN, D.A. (1940) The geology of the Highland Border from Glen Almond to Glen Artney. *Trans. Roy. Soc. Edinb.* 60, pp.171-193.
- ANDERSON, E.M. (1951) *The dynamics of faulting.* 2nd edition, Edinburgh.
- ARMSTRONG, M. and PATERSON, I.B. (1970) The Lower Old Red Sandstone of the Strathmore Region. *Rep. No. 70/12 Inst. Geol. Sei.*
- BALSLEY, J.R. and BUDDINGTON, A.F. (1958) Iron-titanium oxide minerals, rocks, and aeromagnetic anomalies of the Adirondack area, New York, *Econ. Geol.* 53, pp.777-805.
- BHATTACHARYYA, B.K. (1964) Magnetic anomalies due to prism shaped bodies with arbitrary polarisation. *Geophysics* -, 30, pp.829-851.
- BOTT, M.H.P. (1959) The use of Electronic Digital Computers for the Evaluation of gravimetric Terrain Correction connections. *Geophys. Prospect.*, 7, pp.45-54.
- BULLERWELL, W. (1968) *Aeromagnetic Maps for Great Britain and Northern Ireland.* Geol. Surv. G.B.
- BUMFORD D. et.al.(1976) A lithospheric seismic profile in Britain. *Geophys. J.R. astr. Soc. Vol. 44* part 1, pp.145-160.
- COTTON, W.R. (1968) A geophysical survey of the Campsie and Kilpatrick Hills. Ph.D. thesis (unpublished) University of Glasgow.

- CRAIG, G.Y. (1965) The Geology of Scotland. Oliver and Boyd. Edinburgh and London.
- EL-BATROUKH, S.I. (1975) Geophysical investigations on Loch Doon Granite South-West Scotland. Ph.D. Thesis (unpublished) University of Glasgow.
- FRANCIS, E.H. (1956) The economic geology of the Stirling and Clackmannan Coalfield, Scotland; area north of the River Forth. Coalfield papers Geol. Surv. Gt. Brit. 1.
- GARLAND, G.D. (1965) The Earth's Shape and Gravity. Pergamon Press, N.Y.
- GEORGE, T.N. (1960) The stratigraphical evolution of the Midland Valley of Scotland. Trans. geol. Soc. Glasgow 24, pp.32-107.
- GOODLET, G.A. (1957) Lithological variations in the Lower Limestone Group in the Midland Valley of Scotland. Bull. geol. Surv. U.K. 12. pp.52-65.
- GRANT, F.S. and WEST, G.F. (1965) Interpretation Theory in Applied Geophysics. McGraw Hill.
- GUNN, P.J. (1973) Location of the Proto-Atlantic Suture in the British Isles. Nature, 242, pp.111-112.
- GUNN, P.J. (1975) Interpretation of the Bathgate magnetic anomaly, Midland Valley, Scotland. Scott. J. Geol. 3, pp.263-266.
- HALL, J. (1971) A preliminary seismic survey adjacent to the Rashiehill borehole near Slamannan, Stirlingshire, Scott. J. Geol. 7 (2), 170-174.
- HALL, J. (1974) A seismic reflection survey of the Clyde Plateau Lavas in North Ayrshire and Renfrewshire. Scott. J. Geol. 9 (4), pp.253-279.

- HALL, D.H. and DAGLEY, P. (1970) Regional magnetic anomalies. An analysis of the smoothed Aeromagnetic Map of Great Britain and Northern Ireland. Institute of Geological Sciences Report No. 70/10.
- KENNEDY, W.Q. (1958) The tectonic evolution of the Midland Valley of Scotland. Trans. Geol. Soc. Glasg. 23, pp.110-133.
- KNOX, J. (1954) The economic geology of the Midlothian Coalfields. Mem. Geol. Surv. U.K.
- MACGREGOR, M. and MACGREGOR, A.G. (1948) British Regional Geology: The Midland Valley of Scotland. Mem. Geol. Surv. U.K.
- McLEAN, A.C. (1961) Density measurements of rocks in South-West Scotland. Proc. R. Soc. Edinb. (B), 68, pp.103-111.
- McLEAN, A.C. and QURESHI, I.R. (1966) Regional anomalies in the Western Midland Valley of Scotland. Trans. Roy. Soc. Edinb., 66, pp.267-283.
- MYKURA, W. (1960) The Lower Old Red Sandstone igneous rocks of the Pentland Hills. Bull. Geol. Surv. G.B. 16, pp.131-55.
- NAGY, D. (1966) The gravitational attraction of a right rectangular prism. Geophysics Vol. 31. pt. 2, p.362.
- PARK, R.G. (1961) A vertical-force magnetic survey over part of Dusk Water Fault of North Ayrshire. Trans. Geol. Soc. Glasg. 24, pp.154-168.
- POWELL, D.W. (1963) Significance of differences in magnetisation along certain dolerite dykes. Nature, London, 199, pp.674-6.

- POWELL, D.W. (1970) Magnetised rocks within the Lewisian of Western Scotland and under the Southern Uplands. Scot. J. Geol. 6 355.
- QURESHI, I.R. (1969-70) A gravity survey of a region of the Highland Boundary Fault in Scotland. Q. Jl. Geol. Soc. Lond. 125, 481-502.
- RICHEY, J.E., ANDERSON, E.M. and MACGREGOR, A.G. (1930) The geology of North Ayrshire. Mem. Geol. Surv. U.K.
- ROBERTSON, J. and HALDANE, D. (1937) The economic geology of the Central Coalfield, Area 1. Mem. Geol. Surv. U.K.
- SMYTHE, D.K. et al. (1972) Deep Sedimentary basin below Northern Skye and the Little Minch. Nature (PS), 236, p.87.
- TOMKIEFF, S.I. (1937) Petrochemistry of the Scottish Carboniferous-Permian igneous rocks. Bull. Vulcanol. [2] 1, pp.59-87.
- WREN, A.E. (1968) A magnetic survey of part of the Firth of Clyde Ph.D. Thesis (unpublished) University of Glasgow.

APPENDIX 1

Terrain correction program

Terrain correction program

The program is based on Bott's formula using the approximation (mass of the square is concentrated at the centre uniformly along a vertical line attaining the average height)

$$\Delta g = \frac{GPA}{2} \times \frac{h^2}{r(r^2 - p^2)} \quad \dots (1)$$

for the calculation of gravity effect (Δg) at a station due to a segment of a hollow vertical cylinder where the inner and outer radii is given by $r \pm p$. Δg is in mgal .

r = distance from station to centre of the square,

A = area of square,

p = half-width of the square, ρ = density of rocks,

h = height difference from station to centre of square, and

G = Gravitational const.

Equation (1) has been reduced to

$$\Delta g = \frac{0.3096 \times B(n + 19) \times Y}{(J-P) \times 10000} \quad \dots (2)$$

in the present computer program

where

$B(n + 19)$ is an array for density, P represents rp^2 where

r is the distance from station to centre of square and p^2

is the square of half width of square, J represents r^3

where r is as before and Y is equivalent to h^2 in eqn. (1).

Again the eqn (2) reduces to

$$\Delta g = 0.00309 \times 2.69 \times \frac{h^2}{r(r^2 - \frac{1}{4}) \times 100} \quad \dots (3)$$

when the computer parameters of eqn (2) are transferred to an expression for calculating the terrain correction due to a single Km.sq.

Where 2.69 is the density measured in gm/cc, h and r are measured in tens of feet and in Km respectively and are as mentioned in equation (1)

$$\frac{0.3096}{10000} \text{ is equivalent to } \frac{GA}{2 \times 107649.61}$$

Where 107649.61 is a unit conversion factor and G and A are as defined in eqn.(1). The area A and p^2 (square of the half width of square) are multiplied by 4 (for 4 squares) and by 16 (for 16 squares). This program has been changed in order to calculate the modification of the Bouguer correction due to any difference between the specific gravity of a compartment and that under the station. The calculation is based on the formula

$$\begin{aligned} \Delta g &= 2\pi G \rho_{\text{stn}} h_{\text{stn}} \\ &+ \frac{GA}{2} \times \frac{h^2}{r(r^2 - p^2)} (\rho_c - \rho_{\text{stn}}) \quad \dots \quad (4) \end{aligned}$$

where $(\rho_c - \rho_{\text{stn}})$ replaces ρ of Bott's formula.

Equation (4) has been reduced to

$$\Delta g = J \times GY \times Z_{BC} + Z_B \quad \dots \quad (5)$$

in the computer program.

Where GY is (station height)² x Area,

ρ_c is specific gravity of the compartment,

Z_{BC} is the difference between the specific gravity of the compartment and the specific gravity under the station.

ρ_{stn} is the specific gravity under the station and the rests are as before.

The calculation is carried out under the following assumption that

$$1) \quad J = \frac{0.3096}{(J-P) \times 1000} \quad \text{when } z_c > 0 \quad \text{and } z_c = J - P.$$

otherwise $J = 0$

$$2) \quad P \text{ (half width of the square) is not } < 0.25.$$

The program ignores the squares whose centres lie within a distance less than 1 Km from the station as small (r) (Bott, 1959) introduces large error into the calculation. The contribution of those squares can be estimated either by using a terrain correction program for the inner zone or by using a Hammer Zone chart.

Listing of the program is included in order to record the modifications which have been incorporated to allow for the density differences between compartments within the Bouguer slab.

Arrangements and preparation of input data, the description of the parameters and the procedures of the program are given in the following section.

Arrangements and preparation of input data:

The average heights in ten-feet of Km squares have been read from Ordnance Survey map (1 inch to one mile) up to 25 Km from each station and are arranged in blocks of 16 (Fig. 32). The location of each block is specified by the National grid co-ordinates of its S.W. corner. There are two tapes for the input data.

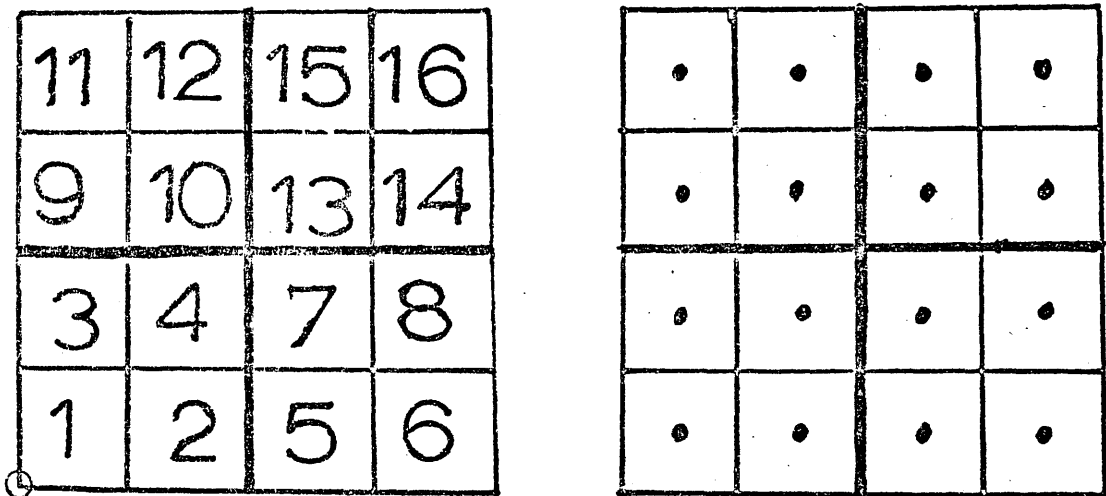


Fig. 32.- Arrangement of 16 squares in a block.

Tape 1:

Blocks x 19

- 1) Each block consists of values of X & Y (co-ordinates of S.W. corner of the block),
- 2) 16 heights in 10 feet unit,
- 3) average density of the block
i.e. X, Y, h, ... h₁₆, Z. Data are separated by space.

Tape 2:

- 1) No. g gravity stations
- 2) Station number
- 3) & 4) co-ordinates of the station in 100 m units
- 5) Height of the gravity stations in 10 feet units,
- 6) Density of the rock under the stations in gm/cc.
Data from (2) to (6) are punched in one line until the total number of stations are finished and are separated by semi colon (;),
- 7) £ card → → → → (Halt code) is punched at the end.

In the present case paper tape has been used for preparing the data.

Description of the parameters:

The parameters used in the program are:-

Real parameters:

- E & F - gravity station co-ordinates in 100 meters.
- G - Station heights in 10 ft. units
- J - Distance between station and centre of square.
- X₁, X₂ - Co-ordinates of a block eastern and northern which are changed by the program from the left hand corner to the centre of the square.

- Y - Means gravity contribution of terrain correction from a square in procedure G, but it represents the square of height difference between station and the square in other procedures.
- G2 - Square of the station heights
- Z - Terrain correction in mgal.
- GY - (Station height)² x Area.
- P - Assigned different values (see eqn. 2)
- SG - Specific gravity of the compartment
- Z_C = J x GY x Z_{BC} = Modified Bouguer correction due to difference between the specific gravity of compartment and specific gravity under station.
- Z_{BC} - Specific gravity difference between the station and the compartment.
- S_{GB} - Specific gravity of rocks under the station.

Integer Parameters:

- C, K, L, N Counting numbers
- A Number of numbers (number of blocks x 19)
- D₁ Station number
- V Number of stations
- W Number of blocks = A/19

Procedures of the program:

The seven procedures of the program are described here briefly.

- | Procedure Name | Function |
|----------------|--|
| Find G. | 1) Calculate the terrain effect at a station due to a square and store it in Z location. Summing the |

Procedure Name	Function
	contribution due to other squares to Z gives the terrain correction at station.
	2) Calculate the Bouguer modification due to the density differences between the compartments within the Bouguer slab.
B ₁₆	To square the difference of height between 1 Km square and a station and then call Find G procedure.
REJECT	To write REJECT and the co-ordinates of the square whose centre is less than 1 Km from the station.
Find R	Find out the distance between the station and the centre of the square (1 x 1, 2 x 2, or 4 x 4 Km ²)
A ₁	To square the height difference between station and the average height of a block of 16 sq. Kms. and to call Find G procedure
A ₄	To square the height difference between station and the average height of block of 4 Sq. Kms.
A ₁₆	To determine the co-ordinates of the centre of one square Km. and to call Find R for finding the distance between the centre of the square and the station.

Test: If the distance between the centre of square and the station is more than 0.99 Km then call B_{16} otherwise Reject.

ALCOMP41

```

'BEGIN' 'REAL' 'D,E,F,G,J,X1,X2,Y,P,Z,Z8,G2,GY,SG,ZC,ZBC,SGB;
'INTEGER' 'PROCEDURE' ININT;
'COMMENT' READS AN INTEGER FROM DEVICE 20. THE INTEGER MAY BE
DELIMITED BY ANY SYMBOL WHICH CANNOT FORM PART OF IT,
INCLUDING A BLANK OR END-OF-LINE;
'COMMENT' THIS PROCEDURE CALLS THE KDF9 PROCEDURE INBASIC TO READ
SYMBOLS. THE KDF9 CODES FOR RELEVANT NUMERIC SYMBOLS ARE -
DIGITS 0 - 9      DECIMAL POINT (.) 11      + 193      - 209;
'BEGIN' 'INTEGER' NUMBER, SYMBOL; 'BOOLEAN' NEG;
'FOR' SYMBOL = INBASI(20) 'WHILE' SYMBOL 'GT' 9 'AND' SYMBOL 'NE' 193
'AND' SYMBOL 'NE' 209 'DO';
'IF' SYMBOL 'EQ' 193 'THEN'
'BEGIN' NEG = 'FALSE';
NUMBER = 0
'END'
'ELSE' 'IF' SYMBOL 'EQ' 209 'THEN'
'BEGIN' NEG = 'TRUE';
NUMBER = 0
'END'
'ELSE'
'BEGIN' NEG = 'FALSE';
NUMBER = SYMBOL
'END';
'FOR' SYMBOL = INBASI(20) 'WHILE' SYMBOL 'LE' 9 'DO'
NUMBER = NUMBER * 10 + SYMBOL;
ININT = 'IF' NEG 'THEN' -NUMBER 'ELSE' NUMBER
'END' OF ININT;
'REAL' 'PROCEDURE' INREAL;
'COMMENT' READS AN OPTIONALLY SIGNED FRACTIONAL NUMBER FROM
DEVICE 20. THE NUMBER MAY BE DELIMITED BY ANY SYMBOL WHICH
CANNOT FORM PART OF IT, INCLUDING A BLANK OR END-OF-LINE;
'COMMENT' THIS PROCEDURE CALLS THE KDF9 PROCEDURE INBASI TO READ
SYMBOLS. THE KDF9 CODES FOR RELEVANT NUMERIC SYMBOLS ARE -
DIGITS 0 - 9      DECIMAL POINT (.) 11      + 193      - 209;
'BEGIN' 'REAL' NUMBER; 'INTEGER' DECS, SYMBOL; 'BOOLEAN' FRACT, NEG;
'FOR' SYMBOL = INBASI(20) 'WHILE' SYMBOL 'GT' 9 'AND' SYMBOL 'NE' 11
'AND' SYMBOL 'NE' 193 'AND' SYMBOL 'NE' 209 'DO';
'IF' SYMBOL 'EQ' 193 'THEN'
'BEGIN' NEG = 'FALSE';
SYMBOL = INBASI(20)
'END'
'ELSE' 'IF' SYMBOL 'EQ' 209 'THEN'
'BEGIN' NEG = 'TRUE';
SYMBOL = INBASI(20)
'END'
'ELSE' NEG = 'FALSE';
NUMBER = 0.0; DECS = 0; FRACT = 'FALSE';
L'..'IF' SYMBOL 'EQ' 11 'AND' 'NOT' FRACT 'THEN' FRACT = 'TRUE'
'ELSE' 'IF' SYMBOL 'LE' 9 'THEN'
'BEGIN' NUMBER = NUMBER * 10.0 + SYMBOL;
'IF' FRACT 'THEN' DECS = DECS + 1
'END'
'ELSE' 'GOTO' OUT;
SYMBOL = INBASI(20); 'GOTO' L;
OUT..'
INREAL = 'IF' NEG 'THEN' -NUMBER * 0.1 ** DECS 'ELSE' NUMBER * 0.1 ** DECS
'END' OF INREAL;
'BEGIN'
'INTEGER' A, C, K, L, H, V, W, D1, LAY1, LAY2, LAY3;
A = 10925;

```

```

LAY1=LAYOUT('('4S+HDDDDDDDDDD.D')');
LAY2=LAYOUT('('4S+HDDDDDDDD.D')');
LAYS=LAYOUT('('4S+D.DDDDD'E'+ND')');
'BEGIN''REAL''ARRAY'B(1,'A);
'PROCEDURE' FINDG;
'BEGIN' C=0;P=P*0.25; ZC=J-P;
J='IF' ZC 'GT' 0 'THEN' .3026/ZC/1'E'4'ELSE'0;
ZC=J*GY*ZBC;
'IF' P'LT' 0.25 'THEN' REJECT 'ELSE'
'BEGIN' Z=J*SG*Y+Z;
'IF' ABS(ZC) 'LT' 0.1 'THEN' ZB=ZC+ZB 'ELSE'
'BEGIN' C=1; REJECT;'END';
'END';
'END';
'PROCEDURE' B16;
'BEGIN' Y=(ABS((B(N+2+L+(K-1)*4))-G))**2; FINDG;
'END';
'PROCEDURE' REJECT;
'BEGIN' NEWLIN(70,1);
WRITE(70,LAY1,X1*10);
WRITEL(70,'('','')');
WRITE(70,LAY1,X2*10);
'IF' C 'EQ' 0 'THEN' WRITEL(70,'(='REJECT')')
'ELSE' WRITEL(70,'(='REJECT ZC')');
WRITE(70,LAYS,ZC);
WRITE(70,LAYS,ZBC);
'END';
'PROCEDURE' FINDR;
'BEGIN' J=SQRT((ABS(X1-E))**2+(ABS(X2-F))**2);P=J;J=J**3;
'END';
'PROCEDURE' A1;
'BEGIN' Y=(ABS((B(N+3)+B(N+4)+B(N+5)+B(N+6)+B(N+7)+B(N+8)+B(N+9)+
B(N+10)+B(N+11)+B(N+12)+B(N+13)+B(N+14)+B(N+15)+B(N+16)+
B(N+17)+B(N+18))/16-G))**2; Y=Y*16;P=P*16;GY=G2*16;FINDG;
'END';
'PROCEDURE' A4;
'BEGIN' Y=(ABS((B(N+3+(K-1)*4)+B(N+4+(K-1)*4)+B(N+5+(K-1)*4)+
B(N+6+(K-1)*4))/4-G))**2; Y=Y*4;P=P*4;FINDG;
'END';
'PROCEDURE' A16;
'BEGIN' L=L+1; X1=X1-0.5; X2=X2-0.5; FINDR;
B16;
L=L+1; X1=X1+1.0; FINDR;
B16;
L=L+1; X1=X1-1.0; X2=X2+1.0; FINDR;
B16;
L=L+1; X1=X1+1.0; FINDR;
B16; L=0;
X1=X1-0.5; X2=X2-0.5;
'END';
NEWLIN(70,1); WRITE(70,LAY2,A); NEWLIN(70,1);
Z=0;
'FOR' C=1 'STEP' 1 'UNTIL' A 'DO'
B(C)=INREAL;
'FOR' H=19 'STEP' 19 'UNTIL' 10925 'DO'
'BEGIN' WRITE(70,LAY2,B(N));
Z=Z+1;
'IF' Z'LT' 7 'THEN' 'GOTO' SK;
NEWLIN(70,1); Z=0;
SK''
'END';
V=ININT;
STARTB''D1=ININT; E=INREAL; F=INREAL; G=INREAL; SGB=INREAL;

```

```

W=A/19; L=0;
Z=0; N=0; E=E/10; F=F/10; G2=G*G;
ZB=.12774*SGB*G;
NEWLIN(70,1);
WRITE(70,LAY2,01);
STARTA',, X1=B(N+1)/10+2.0; X2=B(N+2)/10+2.0;
SG=B(N+19);
ZBC=SG-SGB;
'IF'X2'LT'133'THEN''BEGIN'X2=X2+530;
X1=X1+200;
'END'; FINDR;
'IF' P 'GT' 25 'THEN' 'GOTO' IGNORE;
'IF' P 'GT' 8 'THEN' A1 'ELSE'
'BEGIN' K=1; X1=X1-1.0; X2=X2-1.0; FINDR;
'IF' P 'GT' 4 'THEN' A4 'ELSE' A16;
K=2; X1=X1+2.0; FINDR;
'IF' P 'GT' 4 'THEN' A4 'ELSE' A16;
K=3; X1=X1-2.0; X2=X2+2.0; FINDR;
'IF' P 'GT' 4 'THEN' A4 'ELSE' A16;
K=4; X1=X1+2.0; FINDR;
'IF' P 'GT' 4 'THEN' A4 'ELSE' A16;
'END';
IGNORE',, N=N+19; W=W-1;
'IF' W'GT'0'THEN''GOTO'STARTA'ELSE'
'BEGIN' NEWLIN(70,1);
WRITE(70,LAY1,E*10);
WRITETEXT(70,'(,')');
WRITE(70,LAY1,F*10);
WRITE(70,LAY3,2);
WRITE(70,LAY3,G);
WRITE(70,LAY3,SGB);
WRITE(70,LAY3,ZB);
NEWLIN(70,1);
'END';
V=V-1;
'IF'V'GT'0'THEN''GOTO' STARTB;
'END';
'END';
'END'

```

Appendix 2

Program for the calculation of gravitational and/or magnetic potential fields.

This program has been written by Dr. Powell (personal communication) and the calculation of the potential fields (either gravity and/or magnetic) is based on equations (3a) and (7) (pp. 31, 35). The detailed mathematical basis and outline of the program is given in Sections 3.1, 3.2 and 3.3 (pp. 29-39). The arrangements of the input data are described briefly.

A graph-plotter, designed by Dr. Sharp (personal communication) has been used to draw anomaly along profiles and thickness of the model.

A description of the graph-plotter control follows that of the input arrangement of the main program.

Arrangements of the input data of the program:

The inputs to the program can be arranged in 10 separate sets identified by number of J but in fact 9 is the maximum number of sets of input - 9 and 10 are alternative to each other.

The following are the description of input data used in the program.

First the number of profiles and stations, station spacing and number of passes (which tells the program how many times it needs to go through different procedures) is arranged as input and the number of J followed by relevant parameters value are arranged in sequence according to program. For each value of J the program will look for a number of inputs or an input and will look for the

following input when

J = 1

Itern. = Number of iterations

Field = Indicate the nature of potential field to be
calculated.

and = 0 if magnetic potential

= 1 if gravity potential

Acc. = Accuracy of the calculation.

J = 2

Z_D = plane of observation

Top = depth to the top of the body

Base = depth to the bottom of the body

J = 3

Av. = Average - Residuals to be averaged when
estimating depths

J = 4

R₀ = density contrast for the case of gravity field
= Intensity of magnetisation x 10⁻⁵ cgs for the
case of Magnetic field and if magnetic field then

F_I = Field inclination

F_D = Field declination

M_I = Magnetic inclination

M_D = Magnetic declination

J = 5

PYC = Y-coordinates of the profiles

J = 6

NST = Number of strips

- LYC = Lower Y co-ordinates of the strips
- HYC = Higher Y co-ordinates of the strips
- J = 7 Sets the previous anomaly, if any, (carried out from previous pass), to zero.
- J = 8
- Datum = Average value of the observed anomaly used as a base value of the anomaly
- Anom. = Anomaly = 0 if no anomaly
= 1 if anomaly supplied
- J = 9 and 10 are alternative to each other and in the present case J = 10 has been used.
- J = 10
- Fix N = Number of times weighting factor W_A 's initially $0 < W_A < 1$ to be increased (limit = 1) if the residuals fails to reduce at a pre-defined rate.
- LXC = Lower co-ordinates of X-axis of the strip.
- HXC = Higher co-ordinates of X-axis of the strip.
- NS = Number of segments of the model element
- X_A = 1st X-coordinate of the segment
- Z_{TA} = Depth to the top of the model at X_A
- Z_{BA} = Depth to the bottom of the model at X_A
- W_A = Weight to be applied to the residuals for adjustments of depth at X_A and
- if $W_A = 0$ there is no adjustment
" = 1 there is adjustment
- P_A = 0 or 1 indicates whether the adjustment to be made on the bottom or top at X_A

X_B = 2nd X-coordinate of the segment
 Z_{TB} = Depth to the top of model at X_B
 Z_{BB} = Depth to the bottom of the model at X_B
 W_B = Weight to be applied to the residuals for
adjustments at X_B and
if $W_B = 0$ there is no adjustment
" = 1 there is adjustment
 P_B = 0 or 1 indicates whether the adjustment to be
made on the bottom or top respectively at X_B .

A set of input data are included here for reference.

5 - No. of profiles
67 - No. of station
2.0 - Space between station
2 - Pass
(1) 1 - No. of J.
0 or any
number up
to 17 - Intern.
0 or 1 - Field
1.0 - Acc.
(2) 2 - No. of J.
2.0 - Z_D
0.3 Km - Top
2.5 Km - Base
(3) 3 - No. of J.
1 - Av.

- (4) 4 No. of J
- if gravity field
then
- 0.10 Density
- 1.0 Amplitude
- if magnetic field
then
- 300 Polarisation contrast
- if North-South profile for 70° inclination
- 70.0 F_I
- 0.0 F_D
- 70.0 M_I
- 0.0 M_D
- (5) 5 No. of J.
- 2.0; 4.0; 8.0; Y-coordinates of the profile
- 10.0;
- (6) 6 No. of J.
- 5 NST
- 6.0; LYC
- 8.0 HYC
- (7) 7 No. of J.
- (8) 8 No. of J.
- 1 If anomaly is supplied
- 0 If anomaly is not supplied
- set of anomaly
value(for each
profile) at equal
station interval
to be supplied if 1

(9) or (10)

10	No. of J.
1	Fix N
23.0	LXC
46.0	HXC
NS	No. of Segment
10.0;	X_A (1st X-co-ordinate of Segment)
0.5	Z_{TA} (Depth to top)
2.5	Z_{BA} (Depth to bottom)
1	W_A
1	P_A
20.0;	X_B (2nd co-ordinate of segment)
0.6	Z_{TB} (Depth to top)
2.8	Z_{BB} (Depth to bottom)
1	W_B
1	P_B

All these data are separated by semicolon and can be punched either in all available (2 to 72) columns of a card or each data on separate cards.

Graph Plotter Control

Graphs may be produced on any or all passes and for all profiles being examined. For each profile, the variables plotted are GSHEET, DEPTH (i.e. top and bottom depths) and (optionally) GIN. Each profile constitutes a single frame of graphical output, which is split into two sections; the upper section contains the plots of GSHEET and GIN, while the lower section contains plots of top and bottom depths. Depths are plotted as negative numbers.

Points on the plots of GSHEET and GIN are joined by straight-line segments, whereas the depths are drawn in histogram form using straight-line segments parallel to the X-axis.

The range of the plots may be calculated by the program either for each individual profile, or as an overall value for all profiles in the pass, or may be supplied by the user.

Titles for each frame of output and annotations for each plot are supplied on cards by the user.

Graphs may be drawn for three cases

- 1) Using values appropriate to the first call of the procedure OUTPUT i.e. before the iteration section of the program.
- 2) Using values appropriate to the second call of the procedure OUTPUT i.e. after any required iteration.
- 3) A combination of (1) and (2) - in this case two frames are output for each profile, showing values before and after iteration.

Control For each pass plotter output is controlled by the input section 1 (i.e. $J = 1$). The amended format for this section is described below.

Parameter	Type	Value	Meaning (or Effect)
J	Integer	1	defines input section
ITERN	Integer	Arbitrary	max. allowed number of iterations
FIELD	Integer	\emptyset	magnetic case
		1	gravitational case
ACC	Real	arbitrary	accuracy criterion for the iteration
NPLOT	Integer	\emptyset	no graphs for this pass
		1	graphs for case (1) only
		2	graphs for case (2) only
		3	graphs for case (3)

If NPLOT = \emptyset go on to next input section

IRANGE	Integer	1	Range to be supplied by the user for each individual profile
		2	Range to be calculated by the program for each individual profile
		3	Overall range to be calculated by the program for all profiles in the sweep

If IRANGE \neq 1 go on to next part of graphical input

Parameter	Type	Value	Meaning (or Effect)
-----------	------	-------	---------------------

When IRANGE = 1, the following values must be supplied
for each profile

x1:x2	Real		Range of station - X $\left[\begin{array}{cc} x1 & \rightarrow & x2 \\ \text{min} & & \text{max} \end{array} \right]$
ya1:ya2	Real		Range of GSHEET (and GIN)
yd1:yd2	Real		Range of top and bottom depths $\left[\begin{array}{cc} yd1 & \rightarrow & yd2 \\ \text{min} & & \text{max} \end{array} \right] \text{: - given as } \underline{\text{-ve}}$ values)

[but note that for consistency yd1 will be
adjusted to be $\leq \emptyset.\emptyset$, and yd2 will be
adjusted to be $\geq \emptyset.\emptyset$]

NVAR	Integer	3	GIN is <u>not</u> to be plotted
		4	GIN <u>is</u> to be plotted

If NPLOT \neq 1 go to next part of graphical input

1) Supply two cards, giving two lines of heading for profiles. The same heading is used for each profile. Headings are punched as a string of characters, but only the first 50 columns of each card will be printed out.

N.B. both cards must be present, even if only one line of heading is required:- in this case the second card should be blank.

2) Supply a further two cards giving two lines of annotation for the profiles; the same annotation is

used for each profile. All 80 columns of each card may be used, and there must always be two such cards.

On each profile, the plots are numbered in the following way -

1 = GIN; 2 = GSHEET; 3 = top depth; 4 = bottom depth

The annotation should reflect this numbering.

Headings and annotation should be appropriate to the stage at which output is produced e.g. if NPLOT = 1, one could have

PLOT OF ANOMALIES AND DEPTHS

GRAVITATIONAL CASE

2 = CALCULATED ANOMALY

3 = CHANGED TOP DEPTH

4 = CHANGED BOTTOM DEPTH

If NPLOT \neq 2 go to next part of graphical input

Similar set of cards to case (1), but appropriate to case (2), i.e. appropriate to values output after iteration.

NPLOT = 3 : combination of cases (1) and (2)

Supply 8 cards; the first four of these are for graphs produced before iteration; the second four for graphs produced after iteration.

The above sequence of data is repeated for all passes where graphical output is required.

N.B. Because the routines used to produce this graphical output, the following card must be supplied as the first data card, whether or not graphical output is required on the run

Ø123456789, ABCDEFGHIJKLMNOPQRSTUVWXYZ., ; : ? ! + - * / = () _ < >
 ' " # £ & ∂ %

This is used to define the character set used in the graph annotations.

N.B. But in the present case the above mentioned annotations systems have been changed as shown on Figs. (cf. Figs. 13-17 etc.)

```

*BEGIN*
*COMMENT* RECTANGULAR AREA WITH PN PROFILES AT ANY Y-INTERVALS
(PYC ARRAY) EACH OF PS STATIONS AT REGULAR (KMS) X-SPACING
NST RECTANGULAR MODEL STRIPS OF ANY Y-EXTENTS (LYC AND HYC ARRAYS)
EACH DIVISIBLE INTO FROM 0 TO PS (LXC AND HXC ARRAYS)
THIN (KMS WIDE) SHEETS. MODEL CROSS-SECTION DEFINED BY THE TOP
AND BOTTOM DEPTHS OF EACH SHEETS.

*INTEGER* IPOINT,IRANGE,NPLOT,NVAR ;
*INTEGER* *ARRAY* CHARSET(/0:63/) ;
*BOOLEAN* GRAPHON ;
*REAL* X1,X2,YA1,YA2,YD1,YD2 ;
*INTEGER* PN,PS,PT,MM,NN,NO,NP,NPT,J,NL,NST,PST,K,NS,NPP,MO,CS,C,
PTS,LX,UX,
ITERN,DOME,SIGN,FITG,FIXN,LOOP,PASS,AV,FIELD,NK,SIG,OFF,ANOM ;
*REAL* KMS,DATUM,ACC,PO,TOP,BASE,MIN,CST,CINT,MCS,QF,GP,DTM,
G,GO,GS,GSM,XP,XX,RES,XA,LY,XB,ZD,AM,TEST,LIMIT,RMT,RMR,UY ;
*PROCEDURE* INITIALISE(CHARSET) ; *INTEGER* *ARRAY* CHARSET ;
*BEGIN* *INTEGER* I , FNDLINE ;
I .= 0 ; ENDFLINE .= CODE('('EL')) ;
*FOR* I.=I+1 *WHILE* NEXTCH *NOTEQUAL* ENDFLINE *DO* SKIPCH ;
SKIPCH ;
*FOR* I.=0 *STEP* 1 *UNTIL* 63 *DO* CHARSET(/I/).=READCH ;
*FOR* I.= I+1 *WHILE* NEXTCH *NOTEQUAL* ENDFLINE *DO* SKIPCH
*END* INITIALISE ;
*PROCEDURE* READCS(PHASE) ; *INTEGER* *ARRAY* PHASE ;
*BEGIN* *INTEGER* I,J,K,BLANK,ENDLINE ;
I .= 0 ; ENDFLINE .=CODE('('EL')) ; BLANK .= CODE('(%')) ;
*FOR* I.=I+1 *WHILE* NEXTCH *NOTEQUAL* ENDFLINE *DO* SKIPCH ; SKIPCH ;
*FOR* I.=1 *STEP* 1 *UNTIL* 80 *DO*
*BEGIN* K.=READCH ; PHASE(/I/) .= BLANK ;
*FOR* J.=0 *STEP* 1 *UNTIL* 63 *DO*
*IF* K=CHARSET(/J/) *THEN* *BEGIN* PHASE(/I/).=J ; *GOTO* ENDLLOOP *END*
;ENDLLOOP : *END*
*END* READCS ;
*PROCEDURE* TYPECA(PHASE,NC) ; *VALUE* NC ; *INTEGER* NC ;
*INTEGER* *ARRAY* PHASE ;
*BEGIN* *INTEGER* I ;
*FOR* I.= 1 *STEP* 1 *UNTIL* NC *DO* TYPENC(PHASE(/I/))
*END* TYPECA ;
INITIALISE(CHARSET) ;
PN.=READ;PS.=READ;KMS.=READ;PASS.=READ;
PT.=PN*PS;ITERN.=17;
MCS.=0.001;
X1.=X2.=YA1.=YA2.=YD1.=YD2.=0.0 ; GRAPHON.='FALSE' ;
*BEGIN*
*REAL* *ARRAY* GX,GSH1,GSH2,GSHIN,GDTP1,GDTP2,GDBOT1,GDBOT2
(/1:PT/) ;
*INTEGER* *ARRAY* HEAD11,HEAD12,HEAD21,HEAD22,ID11,ID12,ID21,ID22
(/1:80/) ;
*REAL* *ARRAY* PX1,PX2,PAY1,PAY2,PDY1,PDY2(/1:PN/) ;
*REAL* *ARRAY* GIN,GSHEET,GRESID(/1:PT/),
DEPTH,WT(/1:2,1:PT/),
FP,PYC,LYC,HYC(/1:PN+1/),TM(/1:5/),V(/1:12/),

```

```

RESM(/0:ITERN+4/)
'INTEGER' 'ARRAY' LXC,HXC,FPN(/1:PN+1/),A(/0:ITERN+3/)

'PROCEDURE' SHEETS:
'BEGIN' 'REAL' GP,GS,RA,RB,LA,LB,LY,UY,LYY,UY,Y,T,G
'REAL' 'ARRAY' ZZ,GG(/):2/);
'INTEGER' MP,MF,MS,MO,MPT,MN,R,I,NF,NS,NPL,NPP,LX,UX,J,K,L,NFX,
MC,MI,KK,S,NX,NXF,NXN,NO
WRITET('('('2C') SHEETS LOOP '));PRINT(NL,2,0);NEWLINE(1);
C.=0;CS.=PT*PS*NST*2;
KK.='IF'FIELD=0'THEN'5'ELSE'1;
MC.=MI.=0;
PST.=0;
'FOR'MM.=1'STEP'1'UNTIL'NST'DO'
'BEGIN'
MS.=LXC(/MM/);MF.=HXC(/MM/);
'IF'MF<MS'THEN'GOTO'NXR;
MP.=PS*(FPN(/MM/)-1);
'FOR'MO.=MS'STEP'1'UNTIL'MF'DO'
'BEGIN'
'COMMENT' SHEET COUNTER MPT

MPT.=MO+MP;
GP.=ZZ(/1/).=DEPTH(/1,MPT/);GO.=ZZ(/2/).=DEPTH(/2,MPT/);
K.=0;
'IF'NL=0'THEN''BEGIN'MN.=1;'IF'GO-GP<MCS
'THEN'GOTO'NXS'ELSE''GOTO'CAL'END';
Y.=WT(/1,MPT/);'IF'Y=0.0'THEN''GOTO'NXS;
R.='IF'MO-AV-OFF<1'THEN'MP+1'ELSE'MPT-AV-OFF;
L.='IF'MO+AV-OFF>PS'THEN'MP+PS'ELSE'MPT+AV-OFF;GP.=0.0;
'FOR'J.=R'STEP'1'UNTIL'L'DO'GP.=GP+GRESID(/J/);
GP.=GP*Y/(L-R+1);
('IF'ABS(GP)<RMT'THEN''BEGIN'MC.=MC+1;'GOTO'NXS'END';
G.=WT(/2,MPT/);GG(/1/).=GP*G;GG(/2/).=GG(/1/)-GP;
'FOR'K.=1,2'DO'
'BEGIN'GP.='IF'ABS(GG(/K/))<RMR'THEN'0.0'ELSE'
GG(/K/)*CINT;
'IF'KK=5'THEN'GP.=ZZ(/K/)*(1.0-EXP(-GP));
GG(/K/).=ZZ(/K/)-GP
'END'K;
'IF'GG(/1/)>GG(/2/)'THEN'GG(/1/).=GG(/2/).=
ZZ(/1/)+G*(ZZ(/2/)-ZZ(/1/));
'IF'GG(/1/)<TOP'THEN'GG(/1/).=TOP;
K.=1;
INK:
GP.=GG(/K/)-ZZ(/K/);
'IF'GP=0.0'THEN''GOTO'NXS;
PST.=PST+1;
DEPTH(/K,MPT/).=GG(/K/);
'IF'GP>0.0'THEN'
'BEGIN'MN.='IF'K=1'THEN'-1'ELSE'1;
GO.=GG(/K/);GP.=ZZ(/K/)'END'
'ELSE'
'BEGIN'MN.='IF'K=1'THEN'1'ELSE'-1;
GP.=GG(/K/);GO.=ZZ(/K/)'END';

```

```

CAL:
NFX.=IF'GP'NOTGREATER'0.01'THEN'101'ELSE'
1+2*(ENTIER(1.0/GP+0.5)'/2);
IF'NFX>1'THEN'BEGIN'
WRITFT('('C')'NFX=');PRINT(NFX,3,0);
WRITFT('FOR SHEET ');PRINT(MPT,3,0)'END';
GS.=G0*G0;G.=GP*GP;
UX.=PS-M0+1;
IF'M0>UX'THEN'BEGIN'I.=-1;NF.=1'END'ELSE'
BEGIN'I.=1;NF.=PS;UX.=M0;'END';
L.=1;NPL.=PN;NS.=FPN(/MM/);
INA:
FOR'NN.=NS'STEP'L'UNTIL'NPL'DO'
BEGIN'
NP.=PS*(NN-1);LY.=LYC(/MM/)-PYC(/NN/);
LX.=0;
UY.=HYC(/MM/)-PYC(/NN/);
Y.=UY*LY;R.=IF'Y<0.0'THEN'1'ELSE'-1;
NXN.=IF'Y>0.0'THEN'1'ELSE'NFX;
FOR'NO.=M0'STEP'I'UNTIL'NF'DO'
BEGIN'
COMMENT'STATION COUNTER NPT AND. SYMMETRICAL OFFSET FROM
SHEET MPT, NPP

NPT.=NP+NO;NPP.=NP-NO+2*M0;
XP.=M0-NO;NXF.=(NXN-1)/2;
CS.=CS+NXF;
LX.=LX+1;
FOR'NX.=0'STEP'1'UNTIL'NXF'DO'
BEGIN'FOR'J.=1,2,3,4,5'DO'TM(/J/).=0.0;
XP.=XP+NX/NXN;XX.=XP*XP;RB.=XX+GS;RA.=XX+G;
T.=LN(RB/RA);IF'T<MCS'THEN'BEGIN'MI.=MI+1;'GOTO'NXNN'END';
J.=0;Y.=UY;IF'R=-1'THEN'T.=0.0;
S.=-1;
INB:
C.=C+1;IF'C>CS'THEN'BEGIN'WRITET('('C SHEETS'))';'GOTO'FINISH'
END';
J.=J+1;
XA.=SQRT(RA+Y*Y);XB.=SQRT(RB+Y*Y);
IF'KK=1'THEN'BEGIN'Y.=ABS(Y);TM(/J/).=LN((Y+XB)/(Y+XA))'END'
ELSE'BEGIN'
S.=-1*S;
LA.=1.0/(XA+GP);LB.=1.0/(XB+G0);XA.=1.0/XA;XB.=1.0/XB;
LYY.=XA/RA;UYU.=XB/RB;
TM(/1/).=TM(/1/)+S*Y*((GP/XA-XX)*LYY*LA-(G0/XB-XX)*UYU*LB);
TM(/2/).=TM(/2/)-S*XP*(XA*LA-XB*LB);
TM(/3/).=TM(/3/)+S*Y*(GP*LYY-G0*UYU);
TM(/4/).=TM(/4/)+S*XP*Y*(LYY-UYU);
TM(/5/).=TM(/5/)-S*(XA-XB)'END';
IF'J=1'THEN'BEGIN'Y.=LY;'GOTO'INB'END';
IF'KK=1'THEN'TM(/1/).=T-R*ABS(TM(/1/)+R*TM(/2/));
S.=IF'NX=0'THEN'1'ELSE'2;
FOR'J.=1'STEP'S'UNTIL'KK'DO'
BEGIN'
TM(/J/).=TM(/J/)*V(/J/)*MN*S/NXN;

```


FIELD INCLINATION DOWN FRM NORTH 0 TO 360
 MAG. INCLINATION 0 TO 90 + OR -UP
 OFF = OFFSET OF PRINCIPAL PEAK FOR INFINITE SHEET AT DEPTH = TOP

```

WRITET('('('C')'MAGNETIC MODEL'('C4S')'FIELD      MAGNETIZATION
('C3S')'I      D      I      D('C')''))';
'FOR'I.=9,10,11,12'DO'
'BEGIN'V(/I/).=READ;PRINT(V(/I/),3,0);V(/I/).=V(/I/)*0.0174534;
V(/I-4/).=SIN(V(/I/));V(/I-8/).=COS(V(/I/))
'END'V5=SIN(IF),V6=SIN(DF),V7=SIN(IM),V8=SIN(OM),
V1=COS(IF),V2=COS(DF),V3=COS(IM),V4=COS(OM);
V(/9/).=V(/1/)*V(/6/);V(/10/).=V(/1/)*V(/2/);
V(/11/).=V(/3/)*V(/8/);V(/12/).=V(/3/)*V(/4/);
V(/1/).=V(/9/)*V(/11/)-V(/10/)*V(/12/);
V(/2/).=V(/10/)*V(/11/)+V(/9/)*V(/12/);
V(/3/).=V(/5/)*V(/7/)-V(/9/)*V(/11/);
V(/4/).=V(/10/)*V(/7/)+V(/5/)*V(/12/);
V(/5/).=V(/9/)*V(/7/)+V(/5/)*V(/11/);
QF.=V(/1/)+V(/3/);SIGN.='IF'QF'NOTLESS'0.0'THEN'1'ELSE'-1;
J.='IF'V(/4/)>0.0'THEN'1'ELSE''IF'V(/4/)=0.0'THEN'0'ELSE'-1;
J.=J*SIGN;
'IF'J=0'THEN'OFF.=0'ELSE''BEGIN'QF.=ARCTAN(QF/V(/4/));
QF.=ABS((1.0-ABS(SIN(QF)))/COS(QF));
OFF.=ENTIER(TOP*QF+0.5)*J'END';
CINT.=0.5*SIGN/RO;
WRITET('('('C3S')'CXX      CXZ      CZZ      CXZ      CZY      SIGN
QF      OFF('C')''))';
'FOR'I.=1,2,3,4,5'DO''BEGIN'PRINT(V(/I/),1,4);V(/I/).=V(/I/)*RO
'END';
PRINT(SIGN,1,0);PRINT(QF,1,3);PRINT(OFF,2,0);NEWLINE(2);
'END'MAGV

```

```

'PROCEDURE' OUTPUT(ICALL) ; 'VALUE' ICALL ; 'INTEGER' ICALL ;
'BEGIN'
'REAL'GO,GP,LY ;
'INTEGER'MO,NO,NN,NP,NS,NPP,J,LX,UX ;
IPOINT . = 0 ;
GO.=TOP*KMS;GP.=BASE*KMS;
NEWLINE(2);
WRITET('('AMPLITUDE  DATUM  ACCURACY  CONTRAST  TOP  BASE
DOME('C3S')''))';
'IF'FIELD=1'THEN'WRITET('('MGAL      MGAL      MGAL      G/CC')')
'ELSE'WRITET('('GAMMA      GAMMA      GAMMA      CGS*10E5')');
WRITET('('KMS      KMS('C')''))';
PRINT(AM,4,1);SPACE(1);PRINT(DATUM,4,1);SPACE(1);
PRINT(ACC,2,2);SPACE(1);PRINT(RO,4,2);
SPACE(1);PRINT(GO,2,3);SPACE(1);PRINT(GP,2,3);
NEWLINE(2);
'FOR'MO.=1'STEP'1'UNTIL'PN'DO'
'BEGIN'
NN.=0;LY.=PYC(/MO/);
'FOR'J.=NST+1'STEP'-1'UNTIL'1'DO'
'BEGIN''IF'LY>LYC(/J/)'THEN''BEGIN'NN.=J;'GOTO'NXL'END''END';
NXL:
'IF'NN=NST+1'THEN'NN.=0;

```

```

WRITET('('('('10S')'STRIP  PROFILE'('C11S')')));
PRINT(NN,2,0);SPACE(4);PRINT(MO,2,0);NEWLINE(2);
WRITET('('('('10S')'PROFILE-Y   STRIP-LY   STRIP-HY   BLOCK-LX
BLOCK-HXC'('C4S')')));
'FOR'J.=1,2,3,4,5'DO'WRITET('('('('9S')'KMS')));NEWLINE(1);
SPACE(10);PRINT((PYC(/MO/)-1.0)*KMS,3,2);
'IF'NN=0'THEN'WRITET('('('('10S')'PROFILE OUTSIDE MODEL'('2C')'))')
'ELSE''BEGIN'SPACE(3);
PRINT((LYC(/NN/)-1.0)*KMS,3,2);SPACE(3);
PRINT((HYC(/NN/)-1.0)*KMS,3,2);SPACE(3);
LX.=LXC(/NN/);UX.=HXC(/NN/);'IF'UX>LX'THEN'
'BEGIN'PRINT(KMS*(LX-1),3,2);SPACE(3);PRINT(KMS*(UX-1),3,2)
'END'
'ELSE''BEGIN'NN.=0;WRITET('('('('10S')'NO SHEETS'))') 'END' ;
NEWLINE(2);
'END';
WRITET('('(' STATION NUMBERS  CALC.      OBS.      RESIDUALS STATION-
X ZTOP      ZBASE  WT-1    WT-2'('C13S')')));
'FOR'J.=1,2,3'DO'
'BEGIN''IF'FIELD=1'THEN'WRITET('('          MGALS'))'ELSE'
WRITET('('          GAMMAS'))'END';
'FOR'J.=1,2,3'DO'WRITET('('          KMS')));
NEWLINE(1);
NO.=PS*(MO-1);'IF'NN>0'THEN'NS.=PS*(FPN(/NN/)-1);
'FOR'MM.=1'STEP'1'UNTIL'PS'DO'
'BEGIN'
'COMMENT'NP=STATION AND NPP=MODEL ELEMENT COUNT;
NPP.=NS+MM;
NP.=NO+MM;SPACE(2);PRINT(MM,3,0);SPACE(1);PRINT(NP,3,0);SPACE(1);
G.=GSHEET(/NP/);PRINT(G,4,2);
IPOINT .= IPOINT + 1 ;
'IF' ICALL=1 'THEN' GSH1(/IPOINT/).=GSHEET(/NP/)
'ELSE' 'IF' ICALL=2 'THEN' GSH2(/IPOINT/).=GSHEET(/NP/) ;
'IF'ITERN=0'THEN'SPACE(22)'ELSE'
'BEGIN'SPACE(1);GP.=GIN(/NP/);
GSHIN(/IPOINT/) .= GIN(/NP/);
PRINT(GP,4,2);SPACE(1);PRINT(GP-G,4,2)
'END';
SPACE(2);PRINT((MM-1)*KMS,2,2);
GX(/IPOINT/).=(MM-1)*KMS ;
'IF'NN=0'OR'MM<LX'OR'MM>UX'THEN''GOTO' NXP;
'FOR'J.=1,2'DO'
PRINT(DEPTH(/J,NPP/),3,3);
'IF' ICALL=1 'THEN'
'BEGIN' GDTOP1(/IPOINT/).=-DEPTH(/1,NPP/) ;GDBOT1(/IPOINT/).=
-DEPTH(/2,NPP/)
'END'
'ELSE' 'IF' ICALL=2 'THEN'
'BEGIN' GDTOP2(/IPOINT/).=-DEPTH(/1,NPP/) ;
GDBOT2(/IPOINT/) .= -DEPTH(/2,NPP/)
'END' ;
'IF'ITERN=0'THEN''GOTO'NXP;
'FOR'J.=1,2'DO'
PRINT(WT(/J,NPP/),1,3);
NXP:

```



```

NEWLINE(1);
'END'MM;
NEWLINE(2);
'END'MO;
'END'OUTPUT

'PROCEDURE' GRAPHS(NPLOT) ; 'VALUE' NPLOT ; 'INTEGER' NPLOT ;
  'BEGIN' 'INTEGER' I,J,JPOINT ;
'PROCEDURE' ANNOTATE(X1,X2, YA1,YA2, YD1,YD2, I1,I2, ITYPE) ;
'VALUE' X1,X2,YA1,YA2,YD1,YD2,I1,I2,ITYPE ;
'REAL' X1,X2,YA1,YA2,YD1,YD2 ;
'INTEGER' I1,I2,ITYPE ;
'BEGIN' 'REAL' XR,YAR,YDR ;
  'INTEGER' I ;
  XR .= X2 - X1 ; YAR .= YA2 - YA1 ; YDR .= YD2 - YD1 ;
  PSPACE(0.0,0.5,0.0,1.0) ;
  MAP(X1-0.2*XR,X2+0.1*XR,0.0,1.0) ;
  WINDOW(X1-0.2*XR,X2+0.1*XR,0.0,1.0) ;
  CSPACE(0.0,0.5, 0.0,1.0) ;
  CTRSET(1) ;
  BORDER ;
  POSITN(X1-0.1*XR, 0.5) ; JOIN(X2+0.1*XR , 0.5) ;
  'FOR' I.= I1 'STEP' 1 'UNTIL' I2 'DO'
    'BEGIN' POSITN(GX(/I/),0.49) ; JOIN(GX(/I/),0.51) 'END' ;
  POSITN(X2,0.5) ; JOIN(X2+0.1*XR , 0.5) ;
  'IF' ITYPE=1 'THEN' 'BEGIN'
  CTRMAG(15) ;
  POSITN(X1,0.98) ; TYPECA(HEAD11,20) ; TYPECS('(' ' PROFILE ')',10) ;
  TYPENI(J) ;
  POSITN(X1,0.96) ; TYPECA(HEAD12,20) ;
  CTRMAG(10) ;
  POSITN(X1,0.03) ; TYPECA(ID11,80) ; POSITN(X1,0.01) ; TYPECA(ID12,80) ;
  'END' ;
  'IF' ITYPE=2 'THEN' 'BEGIN'
  CTRMAG(15) ;
  POSITN(X1,0.98) ; TYPECA(HEAD21,20) ; TYPECS('(' ' PROFILE ')',10) ;
  TYPENI(J) ;
  POSITN(X1,0.96) ; TYPECA(HEAD22,20) ; TYPECS('(' ' ITERN ')',10) ;
  TYPENI(ITERN) ;
  CTRMAG(10) ;
  POSITN(X1,0.03) ; TYPECA(ID21,80) ; POSITN(X1,0.01) ; TYPECA(ID22,80) ;
  'END' ;
  PSPACE(0.0,0.5 , 0.5,1.0) ;
  MAP(X1-0.2*XR,X2+0.1*XR , YA1-0.1*YAR,YA2+0.1*YAR) ;
  WINDOW(X1,X2,YA1,YA2) ;
  CTRMAG(5) ;
  AXES ;
  CTRMAG(10) ;
  'FOR' I.= I1 'STEP' 1 'UNTIL' I2 'DO'
    PSPACE(0.0,0.5 , 0.0,0.5) ;
    MAP(X1-0.2*XR,X2+0.1*XR,YD1-0.1*YDR,YD2+0.1*YDR) ;
    WINDOW(X1,X2, YD1,YD2) ;
  CTRMAG(5) ;
  AXES ;
  CTRMAG(10) ;

```

```

'FOR' I.= I1 'STEP' 1 'UNTIL' I2 'DO'
'END' ANNOTATE :
'PROCEDURE' DPAW(GA,GD , I1,I2, X1,X2 , YA1,YA2 , YD1,YD2., IG1,IG2) ;
'VALUE' I1,I2,X1,X2,YA1,YA2,YD1,YD2,IG1,IG2 ;
'INTEGER' I1,I2,IG1,IG2 ;
'REAL' X1,X2,YA1,YA2,YD1,YD2 ;
'ARRAY' GA,GD ;
'BEGIN' 'INTEGER' I, IMID ;
'REAL' XR,YR,XMID,YNEW ;
IMID .=( I1+I2)'/2 ;
XR .=( X2 - X1 ) ; YR .=( YA2 - YA1 ) ;
CTRMAG(7) ;
  'IF' IG1=0 'THEN' 'GOTO' DEPTHS ;
  PSPACE(0.0,0.5 , 0.5,1.0) ;
  MAP(X1-0.2*XR,X2+0.1*XR , YA1 -0.1*YR,YA2+0.1*YR) ;
  WINDOW(X1-0.2*XR,X2+0.1*XR , YA1-0.1*YR,YA2+0.1*YR) ;
  POSITN(GX(/I/),GA(/I/)) ;
  'FOR' I.=I1+1 'STEP' 1 'UNTIL' I2 'DO' JOIN(GX(/I/),GA(/I/)) ;
  DENSTY(3) ;
PLOTNI(GX(/2/),GA(/2/),IG1) ;
DEPTHS :
  PSPACE(0.0,0.5 , 0.0,0.5) ;
  YR .=( YD2 - YD1 ) ;
  MAP(X1-0.2*XR,X2+0.1*XR, YD1-0.1*YR,YD2+0.1*YR) ;
  WINDOW(X1-0.2*XR,X2+0.1*XR, YD1-0.1*YR,YD2+0.1*YR) ;
  POSITN(GX(/I/),GD(/I/)) ;
  'FOR' I.= I1 + 1 'STEP' 1 'UNTIL' I2 'DO'
    'BEGIN' XMID.= 0.5*(GX(/I-1/)+GX(/I/)) ; YNEW.= GD(/I/ ) ;
    JOIN(XMID,GD(/I-1/)); JOIN(XMID,YNEW) ; JOIN(GX(/I/),YNEW) ;
    'END' ;
  PLOTNI(GX(/IMID/),GD(/IMID/), IG2) ;
  DENSTY(1) ; BLKPEN
'END' DRAW ;
'PROCEDURE' RANGE(G1,G2,G3, GD1,GD2,GD3,GD4, GX, NPLOT,NVAR,
  I1,I2, X1,X2, YA1,YA2, YD1,YD2) ;
'VALUE' I1,I2,NPLOT,NVAR ;
'INTEGER' I1,I2,NPLOT,NVAR ;
'REAL' X1,X2,YA1,YA2,YD1,YD2 ;
'ARRAY' G1,G2,G3,GD1,GD2,GD3,GD4,GX;
'BEGIN' 'INTEGER' I ;
'PROCEDURE' BIG(X,Y) ; 'VALUE' Y ; 'REAL' X,Y ;
  X .=( 'IF' X < Y 'THEN' Y 'ELSE' X ) ;
'PROCEDURE' SMALL(X,Y) ; 'VALUE' Y ; 'REAL' X,Y ;
  X .=( 'IF' X > Y 'THEN' Y 'ELSE' X ) ;
X1 .=( YA1 .=( YD1 .=( 1.0*10 ) ; X2 .=( YA2 .=( YD2 .=( -1.0*10 ) ;
'FOR' I.= I1 'STEP' 1 'UNTIL' I2 'DO'
'BEGIN' BIG(X2,GX(/I/)) ; SMALL(X1,GX(/I/)) ;
'IF' NVAR=4 'THEN' 'BEGIN' BIG(YA2,G1(/I/));SMALL(YA1,G1(/I/)) 'END';
'IF' NPLOT=1 'OR' NPLOT=3 'THEN' 'BEGIN' BIG(YA2,G2(/I/)) ;
  SMALL(YA1,G2(/I/));SMALL(YD1,GD1(/I/));SMALL(YD1,GD3(/I/))
  'END' ;
'IF' NPLOT=2 'OR' NPLOT=3 'THEN' 'BEGIN' BIG(YA2,G3(/I/)) ;
  SMALL(YA1,G3(/I/));SMALL(YD1,GD2(/I/));SMALL(YD1,GD4(/I/))
  'END'
'END' ;

```

```

'IF' YA1 > 0.0 'THEN' YA1 .= 0.0 ;
YD2 .= 0.0
'END' RANGE ;
JPOINT .= 1 ;
'IF' IRANGE=3 'THEN'
RANGE(GSHIN,GSH1,GSH2,GDTP1,GDTP2,GDBOT1,GDBOT2,GX,NPLOT,NVAR,
1,IPOINT,X1,X2,YA1,YA2,YD1,YD2) ;
'FOR' J .= 1 'STEP' 1 'UNTIL' PN 'DO'
'BEGIN' 'IF' IRANGE=2 'THEN'
RANGE(GSHIN,GSH1,GSH2,GDTP1,GDTP2,GDBOT1,GDBOT2,GX,NPLOT,NVAR,
JPOINT,JPOINT+PS-1,X1,X2,YA1,YA2,YD1,YD2)
'ELSE' 'IF' IRANGE=1 'THEN'
'BEGIN' X1.=PX1(/J/);X2.=PX2(/J/);YA1.=PAY1(/J/);YA2.=PAY2(/J/)
;YD1.=PDY1(/J/);YD2.=PDY2(/J/);
'IF' YA1 > 0.0 'THEN' YA1 .= 0.0 ;
'IF' YD2 < 0.0 'THEN' YD2 .= 0.0
'END' IRANGE=1 ;
'IF' NPLOT=1 'OR' NPLOT=3 'THEN' 'BEGIN'
ANNOTATE(X1,X2,YA1,YA2,YD1,YD2,JPOINT,JPOINT+PS-1, 1 ) ;
DRAW(GSHIN,GDTP1,JPOINT,JPOINT+PS-1,X1,X2,YA1,YA2,YD1,YD2,
'IF' NVAR=4 'THEN' 1 'ELSE' 0 , 3) ;
REDPEN ;
DRAW(GSH1,GDBOT1,JPOINT,JPOINT+PS-1,X1,X2,YA1,YA2,YD1,YD2,2,4) ;
FRAME
'END' ;
'IF' NPLOT=2 'OR' NPLOT=3 'THEN' 'BEGIN'
ANNOTATE(X1,X2,YA1,YA2,YD1,YD2,JPOINT,JPOINT+PS-1, 2 ) ;
DRAW(GSHIN,GDTP2,JPOINT,JPOINT+PS-1,X1,X2,YA1,YA2,YD1,YD2,
'IF' NVAR=4 'THEN' 1 'ELSE' 0 , 3) ;
REDPEN ;
DRAW(GSH2,GDBOT2,JPOINT,JPOINT+PS-1,X1,X2,YA1,YA2,YD1,YD2,2,4) ;
FRAME
'END' ;
JPOINT .= JPOINT + PS
'END' ;
'END' GRAPHS ;
DATUM.=0.0;DOME.=2;
FIXN.=0;
'FOR' NK.=1 'STEP' 1 'UNTIL' PASS 'DO'
'BEGIN'
'FOR' J.=1 'STEP' 1 'UNTIL' PT 'DO'
GX(/J/).=GSH1(/J/).=GSH2(/J/).=GSHIN(/J/).=GDTP1(/J/).=GDTP2(/J/).=
GDBOT1(/J/).=GDBOT2(/J/).=0.0 ;
NEWLINE(5);
WRITET('('('C10S')'INPUT SECTIONS IN PASS ')');PRINT(NK,2,0);
PST.=0;
INPUT:
NEWLINE(1);
J.=READ;'IF' J>0 'THEN' PRINT(J,3,0) 'ELSE' 'GOTO' ON;
SPACE(3);
PST.=PST+1;
'IF' PST>12 'THEN' 'BEGIN' WRITET('('PST')'); 'GOTO' FINISH 'END'

'IF' J=1 'THEN' 'BEGIN'
ITERN.=READ;FIELD.=READ;ACC.=READ;

```

```

NPLOT .= READ ;
'IF' NPLOT > 0 'THEN' 'BEGIN'
  'IF' 'NOT' GRAPHON 'THEN' 'BEGIN' PAPER(1) ; GRAPHON.='TRUE' 'END';
IRANGE .= READ ;
'IF' IRANGE=1 'THEN' 'FOR' K.=1 'STEP' 1 'UNTIL' PM 'DO'
  'BEGIN' PX1(/K/).=READ;PX2(/K/).=READ;PAY1(/K/).=READ;
  PAY2(/K/).=READ;PDY1(/K/).=READ;PDY2(/K/).=READ;
  'END' ;
NVAR .= READ ;
'IF' NPLOT=1 'OR' NPLOT=3 'THEN' 'BEGIN' READCS(HEAD11);READCS(HEAD12);
  READCS(ID11) ; READCS(ID12) 'END' ;
'IF' NPLOT=2 'OR' NPLOT=3 'THEN' 'BEGIN' READCS(HEAD21) ; READCS(HEAD22
) ; READCS(ID21) ; READCS(ID22) 'END'
  'END' ;
  'GOTO' INPUT 'END'

  'IF' J=2 'THEN' 'BEGIN'
  'INTFGR' LX,UX
  ZD.=READ/KMS; 'IF' ZD=0.0 'THEN' 'BEGIN'
  TOP.=READ/KMS;BASE.=READ/KMS 'END' 'ELSE'
  'BEGIN' 'FOR' MM.=1 'STEP' 1 'UNTIL' NST 'DO'
  'BEGIN' NP.=PS*(FPN(/NM/)-1);
  LX.=LXC(/MM/); UX.=HXC(/MM/);
  'IF' UX<LX 'THEN' 'GOTO' NXA;
  'FOR' NN.=LX 'STEP' 1 'UNTIL' UX 'DO'
  'BEGIN'
  NPT.=NP+NN;
  DEPTH(/1,NPT/).=DEPTH(/1,NPT/)+ZD;
  DEPTH(/2,NPT/).=DEPTH(/2,NPT/)+ZD;
  'END' NN;
  NXA:
  'END' MM;
  TOP.=TOP+ZD;BASE.=BASE+ZD;
  'END' ZD NOTEQUAL 0.0;
  'GOTO' INPUT 'END'

  'IF' J=3 'THEN' 'BEGIN'
  'COMMENT' 2*A(LOOP)+1 RESIDUALS WILL BE AVERAGED WHEN ESTIMATING
  DEPTHS. THIS SMOOTHING IS REDUCED IF THE RESIDUAL SUMS FAIL TO
  REDUCE > TEST
  AV.=A(/0/).=READ;
  'FOR' MM.=1 'STEP' 1 'UNTIL' ITERN 'DO'
  A(/MM/).='IF' AV<PS 'THEN' AV 'ELSE' READ;
  'GOTO' INPUT 'END'

  'IF' J=4 'THEN' 'BEGIN'
  RO.=READ;AM.='IF' RO=1.0 'THEN' READ 'ELSE' 0.0;
  'IF' FIELD=1 'THEN' 'BEGIN' OFF.=0;
  SIGN.=READ;RO.=RO*SIGN;
  CST.=V(/1/).=RO*KMS*6.6681;
  CINT.=1.0/CST/3.1416 ;
  'END'
  'ELSE' MAGV; 'GOTO' INPUT 'END'

  'IF' J=5 'THEN' 'BEGIN'

```

```

*FOR*MM.=1*STEP*1*UNTIL*PN*DO*PYC(/MM/).=READ;
*GOTO*INPUT*END*
;
*IF*J=6*THEN**BEGIN*
NST.=READ;*IF*NST>PN*THEN**BEGIN*WRITET('('NST')');*GOTO*FINISH
*END*;
*FOR*MM.=1*STEP*1*UNTIL*NST*DO*
*BEGIN*
*COMMENT* VALUES IN Y-ARRAYS IN INCREASING ORDER

LY.=LYC(/MM/).=READ;UY.=HYC(/MM/).=READ;
LY.=LY+UY;
*FOR*NN.=1*STEP*1*UNTIL*PN*DO*
*BEGIN*NO.=NN-1;
FP(/NN/).=ABS(LY-2.0*PYC(/NN/));
*IF*NN=1*THEN*FPN(/MM/).=1*ELSE*
*IF*FP(/NN/)>FP(/NO/)*THEN**GOTO*NXM;
NO.=NN
*END*NN;
NXM:
FPN(/MM/).=NO;
WRITET('('C')*FPN ');*PRINT(MM,2,0);WRITET('('=)');
*PRINT(FPN(/MM/),2,0);NEWLINE(1);
*END*MM;
LYC(/NST+1/).=HYC(/NST/);
*GOTO*INPUT*END*

*IF*J=7*THEN**BEGIN*
*FOR*MM.=1*STEP*1*UNTIL*PT*DO*
GIN(/MM/).=GRESID(/MM/).=0.0;
*GOTO*INPUT*END*

*IF*J=8*THEN*
*BEGIN*
DATUM.=READ;ANOM.=READ;
WRITET('('C')*DATUM=');*PRINT(DATUM,4,1);NEWLINE(1);
G.=XX.=GS.=GSM.=0.0;
K.=12;
*FOR*MM.=1*STEP*1*UNTIL*PN*DO**FOR*NN.=1*STEP*1*UNTIL*PS*DO*
*BEGIN*
*IF*NN=1*THEN*NEWLINE(2);
NO.=(MM-1)*PS+NN;
*IF*ANOM=0*THEN*GP.=0.0*ELSE*GP.=*IF*ANOM=1*THEN*
READ*ELSE*GSHEET(/NO/);
XP.=GIN(/NO/).=GRESID(/NO/).=GIN(/NO/)-DATUM+GP;
K.=K-1;*IF*K=0*THEN**BEGIN*NEWLINE(1);K.=12*END*;
*PRINT(XP,4,1);
*IF*G<XP*THEN**BEGIN*G.=XP;NL.=MM*END*;
*IF*XP<XX*THEN**BEGIN*XX.=XP;NS.=MM*END*;
*IF*XP>0.0*THEN*GS.=GS+XP*ELSE*GSM.=GSM+XP;
*END*;
*IF*ABS(XX)>ABS(G)*THEN**BEGIN*NL.=NS;G.=XX;GO.=GSM;GSM.=GS;
GS.=GO;SIG.=-1*END**ELSE*SIG.=1;
WRITET('('C3S')*PROFILE PEAK NEGATIVE POSITIVE SIGN('C
)')));

```

```

SPACF(3);
PRINT(NL,2,0);PRINT(G,5,1);PRINT(GSM,6,1);PRINT(GS,6,1);
PRINT(SIG,1,0);NEWLINE(1);
'IF'G=0.0'THEN''GOTO'FINISH;
'GOTO'INPUT'END'

'IF'J=9'THEN'
'BEGIN'
FITG.=READ;DOME.=PEAD;
XP.='IF'DOME=1'THEN'BASE'ELSE'TOP;
'FOR'MM.=1'STEP'1'UNTIL'PT'DO'
'BEGIN'
'IF'FITG=1'THEN'DEPTH(/1,MM/).=DEPTH(/2,MM/)
'ELSE'DEPTH(/1,MM/).=DEPTH(/2,MM/).=XP;
WT(/1,MM/).=1;
WT(/2,MM/).=DOME;
'END'MM;
'GOTO'INPUT'END'
;
'IF'J=10'THEN''BEGIN'
'REAL'X,XA,XB,ZTA,ZTB,ZT,ZBA,ZBB,ZB,W,WA,WB,P,PA,PB,Y,Z;
'COMMENT'LOOP OVER STRIP READ X BOUNDS AND NS SEGMENTS
IF NS NOT EQUAL 0 READ X,Z AND WEIGHTING OF CORNERS TO
SEGMENTS (COMMON TO TOP AND BOTTOM SURFACE)
DEFINING MODEL CROSS SECTION.
WA IS PROPORTION OF RESIDUAL TO BE USED IN
ADJUSMENTS PA IS PROPORTION OF IT APPLIED TO TOP
SURFACE ADJUSTMENTS;
PTS.=0;
FIXN.=READ;
'FOR'MM.=1'STEP'1'UNTIL'NST'DO'
'BEGIN'NP.=PS*(FPN(/MM/)-1);
LXC(/MM/).=READ;HXC(/MM/).=READ;
SEG:NS.=READ;'IF'NS=0'THEN''GOTO'NXR;
'FOR'MO.=1'STEP'1'UNTIL'NS'DO'
'BEGIN''IF'MO=1'THEN''BEGIN'
XA.=READ;ZTA.=READ/KMS;ZBA.=READ/KMS;WA.=READ;
PA.=READ
'END'
'ELSE''BEGIN'XA.=XB;ZTA.=ZTB;ZBA.=ZBB;WA.=WB;PA.=PB'END';
XB.=READ;ZTB.=READ/KMS;ZBB.=READ/KMS;WB.=READ;PB.=READ;
NL.=NP+XA;X.=XB-XA;ZT.=ZTB-ZTA;
ZB.=ZBB-ZBA;
W.=WB-WA;P.=PB-PA;PTS.=PTS+X;
'FOR'NN.=0'STEP'1'UNTIL'X'DO'
'BEGIN'NPT.=NL+NN;Y.=NN/X;
DEPTH(/1,NPT/).=ZTA+ZT*Y;
DEPTH(/2,NPT/).=ZBA+ZB*Y;
WT(/1,NPT/).=WA+W*Y;
WT(/2,NPT/).=PA+P*Y
'END'NN;
'END'MO;
PTS.=PTS+1;
'GOTO'SEG;
NXR:

```

```

'END'MM;
'GOTO'INPUT'END' J=10

ON:
WRITET('('INPUT COMPLETE')');
NEWLINE(5);
'FOR'MM.=1'STEP'1'UNTIL'PT'DO'GSHEET(/MM/).=0.0;
NL.=LOOP.=0;
'IF'ITERN=0'THEN'DATUM.=0.0;
SHEETS:
'IF'AM>0.0'THEN'
'BEGIN'
XX.=XP.=0.0;
'FOR'MM.=1'STEP'1'UNTIL'PT'DO'
'BEGIN'
G.=GSHEET(/MM/);
'IF'G>XP'THEN'XP.=G;
'IF'G<XX'THEN'XX.=G;
'END'MM;
RO.=AM/ABS(XP-XX);
'FOR'MM.=1'STEP'1'UNTIL'PT'DO'
GSHEET(/MM/).=GSHEET(/MM/)*RO;
'END'AM>0.0;
WRITET('('('C')'INITIAL MODEL'('C')')');
OUTPUT(1); 'IF' NPLOTT=1 'THEN' GRAPHS(NPLOT);
'IF'ITERN > 0'THEN'
'BEGIN'
'IF'SIGN*SIG<1'THEN''BEGIN'WRITET('('SIGN')');'GOTO'FINISH'END';
RESIDUALS;
NO.=MO.=0;
'FOR'LOOP.=1'STEP'1'UNTIL'ITERN'DO'
'BEGIN'
NL.=LOOP:AV.=A(/NL/);SHEETS;RESIDUALS;
XP.=RESM(/NL-1/)-RES;
'IF'NL=1'THEN'TEST.=XP/5.0;
'IF'XP<TEST'THEN'
'BEGIN'
WRITET('('('C')'XP<TEST'('C')')');
'IF'XP<0.0'THEN'
'BEGIN'
WRITET('('XP<0.0')');
CINT.=CINT*0.5;
'END'XP<0'ELSE'
'BEGIN'
WRITET('('('C')'TEST>XP>0.0')');
'IF'RES>ACC*PTS'THEN'
'BEGIN'
WRITET('('RES>ACC*PTS')');
'IF'A(/NL/)=0'THEN''BEGIN'
'IF'FIXN>0'THEN''BEGIN'
FIXN.=FIXN-1;
'FOR'MM.=1'STEP'1'UNTIL'NST'DO'
'BEGIN'
LX.=LXC(/MM/);UX.=HXC(/MM/);
'IF'UX<LX'THEN''GOTO'NXX;

```

```

NP.=PS*(FPN(/MM/)-1);
  FOR NN.=LX STEP 1 UNTIL UX DO
  BEGIN
  NPT.=NP+NM;
  LY.=WT(/1,NPT/);
  WT(/1,NPT/).=2.0*LY/(1+LY*LY)
  END NN;
NXX:
  END MM;
  END FIXM>0;
  END A(NL)=0 ELSE
  FOR MM.=NL+1 STEP 1 UNTIL ITERN DO
  A(/MM/).=IF A(/MM/)>0 THEN A(/MM/)-1 ELSE 0
  END RES>ACC*PTS ELSE GOTO OUT END TEST>XP>0 END XP<TEST;
  END LOOP;
OUT:
NEWLINE(1);
RES.=G.=GO.=0.0;NL.=NL+1;
A(/NL/).=A(/NL-1/);
  FOR MM.=1 STEP 1 UNTIL PT DO
  BEGIN
  XP.=GSHEET(/MM/);
  IF XP>0.0 THEN GO.=GO+XP ELSE G.=G+XP;
  RES.=RES+ABS(GIN(/MM/)-XP)
  END MM;
RESM(/NL/).=RES;
  IF G/SIGN>GO/SIGN THEN BEGIN XX.=GO;GO.=G;G.=XX END;
  FOR J.=1,2 DO WRITET('(' OBS. SUM CALC. SUM')));
WRITET('('('11S') INPUT R0 RATIO COL.1/2('C8S'))');
PRINT(GS,0.5);SPACE(1);PRINT(GO,0.5);SPACE(5);PRINT(GSM,0.5);
SPACE(1);PRINT(G,0.5);SPACE(5);PRINT(R0,0.3);GO.=GS/GO;
PRINT(GO,0.5);NEWLINE(2);
RES.=0.0;
  FOR MM.=1 STEP 1 UNTIL PT DO
  BEGIN
  G.=GIN(/MM/)-GO*GSHEET(/MM/);
  RES.=RES+ABS(G)
  END;
RESM(/NL+1/).=RES;
  IF RESM(/NL+1/)<RESM(/NL/) THEN
  BEGIN R0.=R0*GO;FOR MM.=1 STEP 1 UNTIL PT DO
  BEGIN
  GSHEET(/MM/).=XX.=GSHEET(/MM/)*GO;
  GRESID(/MM/).=GIN(/MM/)-XX
  END REVISED WITH BEST R0;
WRITET('(' REVISED R0 APPLIED('C'))');
  END;
WRITET('('('C') ADJUSTED MODEL('C'))');
OUTPUT(2);IF NPLOT=2 OR NPLOT=3 THEN GRAPHS(NPLOT);
WRITET('('('2C10S') ITERATION RESIDUAL SUM POINTS MEAN AV
('C'))');
  FOR NN.=0 STEP 1 UNTIL NL+1 DO
  BEGIN
  SPACE(11);IF NN>NL-1 THEN PRINT(NL-1,2,0) ELSE
  PRINT(NN,2,0);

```



```
SPACE(5):PRINT(RESM(/NN/),4,2);SPACE(4);
MO.=IF'NN>NL-1'THEN'PT'ELSE'PTS;PRINT(MO,3,0);
PRINT(RESM(/NN/)/MO,3,2);
IF'NN>NL'THEN'WRITET('WITH REVISED CONTRAST'('C')(''))
ELSE'PRINT(A(/NN/)*2+1,3,0);
NEWLINE(1);
END'NN;END'ITERN>0;
END'PASS;
FINISH:
IF'GRAPHON'THEN'GREND
END'END'
```